Techno-Economic Evaluation of Refuse Derived Fuel Torrefaction

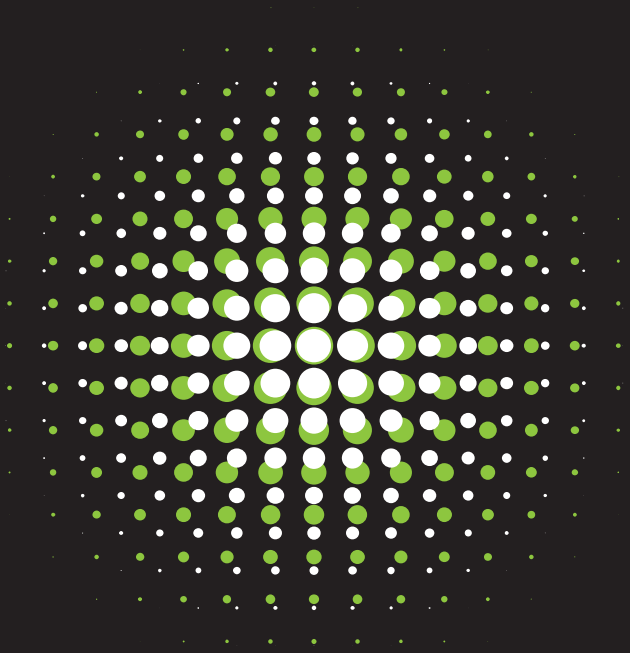

TU Delft

Sridar Sandeep

Techno-Economic Evaluation of Refuse Derived Fuel Torrefaction

A study on the modelling and economics associated with torrefaction of refuse derived fuel

A thesis submitted to the Delft University of Technology in partial fulfilment of the requirements for the degree of

Master of Science in Sustainable Energy Technology
To be publicly defended on Tuesday 30th November, 2021 at 10:15 AM CET by

Sridar Sandeep
November 2021

Student number	5060079			
Project duration	30th January 2020 - 30 November 2021			
Thesis committee :	Prof. dr. ir. W. de Jong	TU Delft	-	Supervisor
	Dr. Luis Cutz	TU Delft	-	Co-supervisor
	Dr. Lorenzo Botto	TU Delft	-	Committee chairman
	Prof. dr. ir. Earl Goetheer	TU Delft	-	Committee member

Delft University of Technology

Preface

This report was written in partial fulfilment of the requirement for the degree of MSc in Sustainable Energy Technology at Technical University of Delft. This project titled "Techno-Economic Evaluation of Refuse Derived Fuel Torrefaction" was performed from January 2021 till November 2021.

Delft, 24 November 2021
Sridar Sandeep

Acknowledgements

First of all, I thank the Lord Almighty for His grace and wisdom which has guided me through out my thesis. In my moments of despair I felt His comforting presence inspiring and enlightening me, He can never be praised or thanked enough.

My deepest gratitude to my parents for their unconditional love, support and inspiration. I dedicate this thesis to you, for all your hard work and sacrifice in helping me to achieve my dreams.

The completion of my thesis would not have been possible without the help of my mentors, Luis Cutz and Prof.Wiebren de Jong. I would like to express my sincere thanks and gratitude for their critical comments, guidance and support. Special thanks to Prof.de Jong who introduced me to the field of biomass and thermochemical conversion technologies in my second quarter.

I would also like to thank my friends, Lee, Charu, Mahesh, Govind and Meenakshi for their constant support, encouragement as well as happy distractions outside of my research. I am also grateful to Pradeep for helping me in the successful completion of my report.

The past two years at TU Delft has been a wonderful experience, one which I shall always fondly remember. During this time I was able to grow personally and professionally. This thesis represents the culmination of my efforts in the completion of my master's degree.

Sridar Sandeep
November, 2021

Abstract

The last decade has seen an increase in the world wide energy demand, it was recorded as the highest spike encountered in the energy demand over a decade. On analysing the main sources which were able to satisfy this overwhelming demand it was found that the majority was still from non-renewable sources or fossil fuels such as coal, oil and natural gas[41]. The aftermath of the continued use of these fossil fuels are already well known, one can argue that there has still not been a serious attempt to phase out these non-renewable sources even though the concerns regarding the harmful emissions being released with their continued use are subject of numerous discussions and studies. It is paramount that the share of renewable energy technologies in the overall energy mix needs to be increased,various options must be explored such that it is possible to substitute these renewable energy sources in place of fossil fuels particularly in energy and emission intensive industries without a comprise in meeting their energy demand.

Refuse derived fuel (RDF), which is the combustible fraction that has been separated from municipal solid waste (MSW) has gained attention due to it being seen as an alternative to convectional fossil fuels as well as a method of sustainable waste management and disposal. The reason for their use as an alternative fuel is mainly attributed to their physical and chemical characteristic such as their low moisture content, high grindability and calorific value. However, the challenges faced in their application as a substitute fuel or feedstock is attributed mainly to the high variability in the properties of the RDF material that is being supplied to the relevant industries. Therefore a standardization in its properties needs to be carried out particularly with regards to their moisture content and calorific value in order to promote their application.

Torrefaction, also referred to as mild pyrolysis is a thermal treatment method that usually is carried out in temperature ranges of 200-300°C and residence times of 30-60 min in the absence of oxygen. The material that is being subject to this treatment method partly decomposes to release volatiles,and the left over solid product has been reported to undergone a modification its physical and chemical characteristics when compared to the initial solid material. From a chemical point of view the final solid product is reported to have an increase in the carbon content and decrease in the hydrogen and oxygen content which leads to a higher calorific value than the original material. Several experimental studies have been conducted for the torrefaction of RDF with aim of improving and standardizing the calorific value and have yielded promising results. However there has not yet been a work that has focused on the torrefaction of RDF on large scale, that takes into account the process design and economics associated with their production.

The aim of this thesis was to carry out a techno-economic evaluation into the torrefaction of refuse derived fuel. An initial composition of raw RDF was selected from literature which has a high moisture content and low calorific value. The raw material is then subject to several process such as drying, torrefaction, grinding and pellitization with the aim producing torrefied RDF pellets. These process were simulated and optimized through Aspen Plus in order to obtain a better understanding of the influence of process parameters such as moisture content, drying temperature, torrefaction temperature and residence time on the final product as well as to select the optimum route for their production. Economic evaluation was also carried out to determine if the implementation of such a project is feasible. This was done on the basis of certain economic or profitability indicators. Results from simulations show that the optimum torrefaction conditions were 250°C and residence time of 30 min,which resulted in the final torrefied RDF having an increased calorific value. The economic analysis provides positive results particularly when moving towards a higher processing capacity of initial raw RDF. Finally, the effect of substitution of the torrefied RDF in a cement plant was also evaluated and has shown that significant savings can be achieved through the reduction in fossil fuel consumption and carbon dioxide emissions.

Acronyms

S.No	Abbreviation	Expansion
1	MSW	Municipal Solid Waste
2	RDF	Refuse Derived Fuel
3	w.b	Wet Basis
4	d.b	Dry Basis
5	NDR	Normalized Drying Rate
6	NMC	Normalized Moisture Content
7	NPV	Net Present Value
8	CAPEX	Capital Expenditures
9	OPEX	Operational Expenditures
10	RMSE	Root Mean Square Error
11	V1	Volatiles 1
12	V2	Volatiles 2
13	PBP	Payback Period
14	MR	Moisture Ratio
15	LV	Latent Heat for Vaporization
16	MM$	Million dollars

Nomenclature

β	Inclination angle
β	Instantaneous product yield
χ	Film thickness (mm)
η	Fill percentage (%)
γ	Instantaneous product yield
μ	Viscosity (cP)
ϕ	Porosity (-)
ϕ_{O}	Half central angle
ρ	Density (kg/m^3
θ	Dynamic angle of repose
ε	Fill grade (-)
ϑ	Instantaneous product yield
ξ	Instantaneous product yield
A	Area (m^2)
A	Pre-exponential factor
c_{p}	Specific heat capacity (kJ/kg.K)
D	Diffusion coefficient(m^2/s)
D_{e}	Equivalent diameter
E	Energy (kJ/kg)
E_{a}	Activation Energy (s^{-1})
f	Filling degree
Fr	Froude number
G	Mass velocity(kg/m$_2$/hr
H	Bed depth (m)
h	Heat transfer coefficient (W/m^2.K)
HHV	Higher heating value (MJ/kg)
k	Rate constant (s^{-1})
L	Length of drum (m)

l_{p}	Characteristic particle length (m)
m	Mass flow (kg/hr)
n	Rotational speed (rad/s)
N_{t}	Area (m^2)
Pr	Prandtl number
Q	Heat loss (kW)
R	Radius of drum (m)
Re	Reynolds number
Re_{w}	Rotational Reynolds number
Sc	Schmidt number
T_{W}	Wet bulb temperature (K)
T	Temperature difference (°C)
t	Time (min)
u	Velocity (m/s)
U_{a}	Overall heat transfer coefficient ($\mathrm{W/m}^2$.K)
Y_{s}	Total solids yield
Y_{v}	Total volatile yield

List of Figures

1.1 Total primary energy demand. . . . 1

2.1 Volume of waste generated (MT) across the globe . . . 6
2.2 Steps involved in sourcing RDF from MSW. . . . 6
2.3 Fractional composition of RDF sourced from MSW. . . . 7
2.4 Drying Methods for Refuse Derived Fuel. . . . 8
2.5 Schematic diagram of a solar drying set up for RDF. . . . 9
2.6 Schematic of a Belt dryer. . . . 11
2.7 Schematic of a rotary dryer. . . . 11
2.8 Schematic of an indirect steam tube dryer. . . . 12
2.9 Schematic of a fluidized bed dryer. . . . 13
2.10 Dryer selection criteria . . . 14
2.11 Different stages in torrefaction . . . 15
2.12 Typical mass and energy balance of the torrefaction process. . . . 15
2.13 Torrefaction reactor classification based on Ref.[31]. . . . 16
2.14 Schematic representation of the auger type reactor. . . . 17
2.15 The Torspyd^{TM} column,example of a moving bed torrefaction reactor design. . . . 18
2.16 Schematic representation of a rotary drum reactor. . . . 18
2.17 Schematic representation of Torbed reactor. . . . 19
2.18 Reactor selection criteria. . . . 20

3.1 Process flow diagram . . . 21
3.2 Typical drying rate curve. . . . 22
3.3 Experimental drying data for RDF (10 mm). . . . 23
3.4 Drying curves fitted to Lewis model. . . . 24
3.5 Drying curves fitted to Henderson-Pabis model. . . . 25
3.6 Variation of constant A with temperature. . . . 26
3.7 Variation of rate constant (k) with temperature. . . . 26
3.8 Effect of drying temperature on residence. . . . 26
3.9 Influence of particle size on residence time. . . . 27
3.10 Normalized drying rate vs normalized moisture content. . . . 28
3.11 Material flow in and out of dryer. . . . 29
3.12 Dryer simulation methodology. . . . 31
3.13 1-step mechanism. . . . 32
3.14 2-step mechanism. . . . 32
3.15 3-step mechanism. . . . 32
3.16 Experimental weight loss data for bio waste(kitchen and yard waste). . . . 33
3.17 Fitted weight loss curves . . . 34
3.18 Curve fitting algorithm . . . 34
3.19 Influence of temperature on rate constants. . . . 35
3.20 Influence of temperature on mass and volatile yields (t = 30 mins). . . . 36
3.21 Influence of torrefaction temperature and residence time on total volatile yields(V_1+V_2). . . . 36
3.22 Influence of torrefaction temperature on mass fraction of gaseous species in V1 (t = 30 min). . . . 39
3.23 Influence of torrefaction temperature on mass fraction of gaseous species in V2 (t = 30 min). . . . 39

3.24 Design elements of reactor . . . 40
3.25 Motion of solids within the drum . . . 41
3.26 Operational parameters for different solids motion . . . 41
3.27 Hardgrove Grindability Index for the torrefied biomass at different temperatures . . . 43
3.28 Aspen Plus simulation flowsheet. . . . 45
3.29 Economic evaluation methodology . . . 46
3.30 Costs considered within CAPEX. . . . 46
3.31 Costs considered within OPEX . . . 48

4.1 Moisture content profile along dryer length . . . 51
4.2 Temperature profile along dryer length . . . 51
4.3 Variation in mass concentration with residence time for temperatures (a) 250°C (b) 270 °C and 300 °(C). . . . 52
4.4 Effect of torrefaction temperature on mass yield (t = 30mins). . . . 53
4.5 Instantaneous product yields . . . 53
4.6 Change in elemental compositions with torrefaction temperature for solid B (j = C,H,O). . . . 54
4.7 Change in elemental compositions with torrefaction temperature for solid C (j = C,H,O). . . . 54
4.8 Position of torrefied RDF on the Van Krevelen diagram . . . 55
4.9 Surface plot for HHV estimation . . . 56
4.10 Torrefaction mass and energy yields for different temperatures with residence time of 30 mins. . 56
4.11 Unresolved hot and cold stream connections . . . 57
4.12 Resolved hot and cold stream connections . . . 58
4.13 Composite curve . . . 58
4.14 Grand composite curve . . . 58
4.15 CAPEX variation for selected plant capacities. . . . 59
4.16 Energy consumption of different unit operations with varying capacity. . . . 60
4.17 OPEX variation for selected plant capacities. . . . 61
4.18 NPV of low capacity plant. . . . 62
4.19 NPV of base capacity plant. . . . 62
4.20 NPV of high capacity plant . . . 62
4.21 Payback for the different RDF torrefaction plants. . . . 63

List of Tables

2.1 Classification system for RDF[63]. . . . 5
2.2 Ultimate and proximate analysis of RDF. . . . 7

3.1 Properties of studied RDF. . . . 23
3.2 Mathematical models to predict drying behavior . . . 24
3.3 Curve fitting results of Lewis model. . . . 25
3.4 Curve fitting results of Henderson-Pabis Model. . . . 25
3.5 Rate equation parameters. . . . 35
3.6 Volatile species evolved during torrefaction of RDF. . . . 38
3.7 General equations for volatiles concentration variation with torrefaction temperature (T, °C). . 40
3.8 Main inputs for convective dryer block. . . . 44
3.9 Main inputs to RPlug reactors. . . . 45
3.10 Scale factor for process equipment. . . . 47
3.11 CAPEX cost percentages. . . . 47
3.12 Utility prices. . . . 48
3.13 Cost associated with OPEX. . . . 48
3.14 Costs associated with OPEX . . . 49

4.1 Dryer output variables . . . 50
4.2 Estimated higher heating values from Boie correlation . . . 55
4.3 Processing capacities selected for economic analysis . . . 59
4.4 CAPEX of RDF torrefaction plants . . . 59
4.5 OPEX of RDF torrefaction plants . . . 61
4.6 Minimum selling price needed for different plant capacities . . . 62
4.7 Data sourced for economic model . . . 64
4.8 Model summary for the use and savings associated with RDF and petcoke . . . 66

Contents

List of Figures vii

List of Tables ix

1 Introduction 1
- 1.1 Thesis Objective . . . 3
- 1.2 Thesis Structure . . . 4

2 Literature review 5
- 2.1 Refuse derived fuel . . . 5
  - 2.1.1 Production and characteristics . . . 5
  - 2.1.2 Applications of refuse derived fuel . . . 7
- 2.2 Drying methods . . . 8
  - 2.2.1 Bio-drying . . . 9
  - 2.2.2 Solar drying . . . 9
  - 2.2.3 Thermal drying . . . 9
- 2.3 Industrial Dryers . . . 10
  - 2.3.1 Belt dryer . . . 10
  - 2.3.2 Rotary drum dryer . . . 11
  - 2.3.3 Indirect steam tube dryer . . . 11
  - 2.3.4 Fluidized bed dryer . . . 12
  - 2.3.5 Dryer selection . . . 13
- 2.4 Torrefaction . . . 14
  - 2.4.1 Significance of RDF Torrefaction . . . 15
- 2.5 Torrefaction Reactors . . . 16
  - 2.5.1 Auger Reactors . . . 17
  - 2.5.2 Moving Bed Reactor . . . 17
  - 2.5.3 Rotary Drum Reactor . . . 18
  - 2.5.4 Fluidized Bed Reactor . . . 19
  - 2.5.5 Reactor selection . . . 19

3 Methodology 21
- 3.1 Process overview . . . 21
- 3.2 Dryer modelling and simulation . . . 22
  - 3.2.1 Drying kinetics of RDF . . . 22
  - 3.2.2 Dryer design . . . 28
- 3.3 Torrefaction of refuse derived fuel . . . 32
  - 3.3.1 Weight loss kinetics . . . 32
  - 3.3.2 Volatile modelling . . . 37
  - 3.3.3 Reactor design . . . 40
- 3.4 Grinding and pelletization . . . 43
- 3.5 Aspen Plus simulation model . . . 43
  - 3.5.1 Dryer . . . 43
  - 3.5.2 Torrefaction . . . 44
  - 3.5.3 Grinding and pellitization . . . 45

3.6 Economic Evaluation . . . 46
3.6.1 Capital expenditure (CAPEX) . . . 46
3.6.2 Operational expenditure (OPEX) . . . 47
3.6.3 Economic Indicators . . . 49

4 Results and Discussion 50
4.1 Dryer Profiles . . . 50
4.2 Torrefaction . . . 52
4.2.1 Heat integration . . . 57
4.3 Economic Analysis . . . 58
4.3.1 CAPEX . . . 59
4.3.2 OPEX . . . 60
4.3.3 Net present value (NPV) . . . 61
4.3.4 Payback Period . . . 63
4.4 RDF substitution . . . 63

5 Conclusion and recommendations 67
5.1 Conclusion . . . 67
5.2 Recommendations . . . 68

Bibliography 69

Appendices 75

A Dryer 76
A.1 MATLAB Code . . . 76
A.2 CALCULATOR BLOCK . . . 80

B Torrefaction 82
B.1 Two-step mechanism derivation . . . 82
B.2 Database for HHV estimation . . . 88

Chapter 1

Introduction

The world today is still very much dependent on fossil fuels, even though concerns regarding their gradual depletion and harmful emissions are constantly raised, there is still yet to be a complete transition to renewable sources. Ever since the beginning of the age of industrialization, the consumption and generation of energy has increased more rapidly than the population of the world. Along with this increased energy generation through the use of finite natural resources, there resulted a large amount of CO_2 emissions, which has negatively impacted the health of the populations and the environment. In a report published by the International Energy Agency (IEA), the current worldwide energy demand has increased by about 2.3% when compared to the last decade which is being reported as the highest increase recorded over a decade[41]. Out of the all the energy sources, the share of non-renewable technologies (fossil fuels) are still found to be the highest. This can be explained by some numbers in order to get a better picture, 583 Exajoules is the current total annual energy demand, out of which 80% is being provided through the use of fossil fuels such as coal, oil and natural gas[2]. The share of different energy sources in the total energy consumption reported for the year of 2020 is shown in figure 1.1.

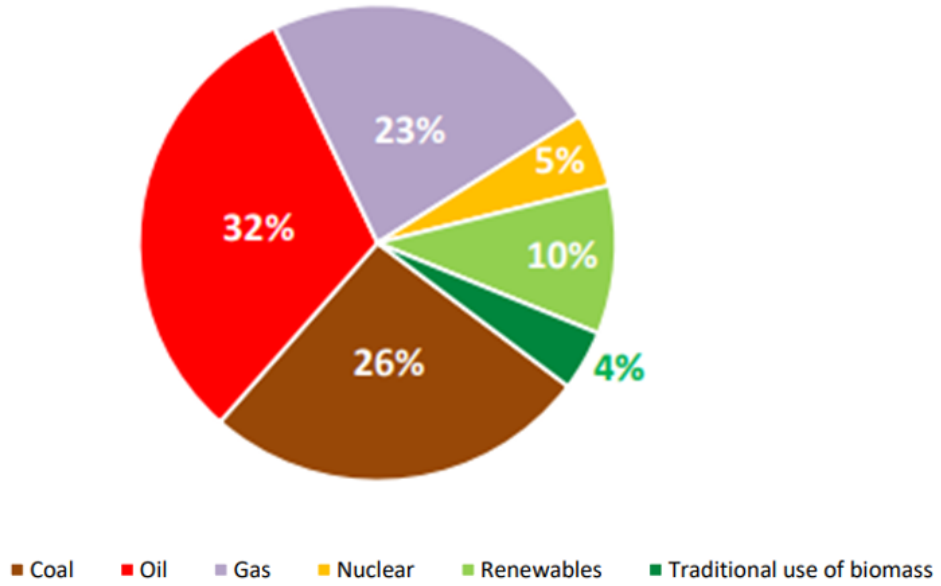

Figure 1.1: Total primary energy demand [41].

The aftermath of the increased dependency on fossil fuels is the rise in the global emissions, as of 2019 it is about 33 giga tones (Gt) of CO_2 annually and is expected to rise further [41]. In order to combat these rising emissions and reduce the dependency on the depleting fossil fuels for energy requirement it is necessary to promote renewable energy technologies and investigate alternative fuels.

Renewable energy technologies can be classified into two categories, mainstream and emerging technologies. Biomass energy is classified as a mainstream technology and plays a large and growing role in the global energy system[72]. According to the European Energy Directive, biomass is defined as follows[28]:

'biomass' means the biodegradable fraction of products, waste and residues from biological origin from agriculture (including vegetable and animal substances), forestry and related industries including fisheries and aquaculture, as well as the biodegradable fraction of industrial and municipal waste.

Municipal solid waste (MSW) and its derivatives such as refuse derived fuel (RDF) can therefore in the broad sense be considered as a biomass feedstock. Regarding their subsequent conversion for energy, can be considered as renewable, biomass and waste are the largest sources of renewable energy in Europe amounting to 63.1% of the total share of renewable energy sources[73]. Over the last decade there has been an alarming increase in the amount of waste of generated, according to the World Bank the global annual MSW generation was 2 billion tons in 2018 up from 1.3 billion tons in 2012 and this number is further expected to rise up to 2.59 billion tons by 2030[56][47]. Various factors have been identified in contributing to this increase such as economic growth, population increase, industrial development, urbanization and rural to urban migration etc[56][47][57]. Along with the increase in waste volumes, their composition is becoming more heterogeneous, which poses difficulty in their sustainable disposal leading to economic losses as well as negative impact on health and environment[35]. Coming back to fossil fuels, we see that the power generation and transportation sector are the top two most energy intensive sectors and whose energy needs are mostly fulfilled by the use of these fossil fuels. But as mentioned above, the continued combustion of these fossil fuel adds to the further deterioration of the environment. Considering the above challenge towards the sustainable disposal of waste and the substitution of fossil fuels in processes, waste to energy (WtE) technologies can serve as potential solution. The term WtE refers to the treatment of waste for energy recovery in the form of heat and electricity or other alternative fuels in gaseous, liquid and solid forms[35]. They can be classified into three categories based on the conversion pathways,viz.,thermochemical, biochemical, and physicochemical. The key arguments in favour of WtE is that through the diversion of waste from landfills, prevention of methane emissions can be accomplished along with the reduction in volume of the waste. In addition it can also be an attractive source of energy as it is possible to make the process carbon neutral[49]. However, currently the skepticism towards WtE mainly lies in its disruption of recycling in the waste hierarchy, as with an increase in WtE capacity recycling will be jeopardised[53]. But in recent studies carried out by Malinauskaite et al.[53] has shown that this is not always the case, as some countries such as Sweden, Denmark and the Netherlands have the most number of WtE facilities and the highest recycling rates in the EU. Based on the aforementioned advantages and findings it can be concluded that WtE technologies can aid immensely towards a carbon neutral and circular economy.

Refuse derived fuel (RDF) is a broad designation that is used to specify the fuel obtained through the processing of MSW, regular industrial waste (RIW), construction and demolition waste (CDW) with the aim of improving its calorific value[63]. In order to produce RDF, the feedstock in this case waste obtained from the above mentioned sources is initially shredded and then carefully sorted to remove all non-combustible material such as glass, metal and plastics (allowing the reuse/recycling of these materials)[59], these operations are usually carried out at mechanical and biological treatment plants (MBT) for MSW processing or mechanical treatment facilities for RIW or CDW processing [63]. Since the shredding and separation are carried out through a series of mechanical processes which are quite energy intensive, there are still certain advantages of RDF over mixed MSW, with regards to the quality and uniformity of its physical and chemical characteristics along with the increase in the Higher Heating Value(LHV). This homogeneity in its physical and chemical characteristics leads to lower pollutant emissions, reduced excess air requirements during combustion, easier storage, handling and transportation [19][29][75][24]. Refuse derived fuels mainly finds their applications in energy recovery purposes through thermochemical conversion in WtE plants mostly through incineration or co-incineration. Currently the major end users for RDF are the energy intensive industries such as cement and lime production, who are facing several economic and environmental challenges. The different types of fuels used within in these industries mentioned are natural gas, coal and petroleum oil which are not renewable and are being consumed rapidly, moreover their price volatility also needs to be considered[38][55]. In regards to their carbon dioxide (CO_2) emissions, it has been reported than 40% of total CO_2 emitted from the cement manufacturing plant are from the burning of fuels and 5-7% of generated CO_2 emissions are produced by the cement industry globally[38][[10]. Recent studies have shown that there is a

great deal of promise in lowering the emissions associated with the combustion process and reducing fossil fuel consumption within these industries through the substitution of RDF as an alternative fuel without decreasing the quality of the final product[10]. Initially an upper limit of 20% RDF substitution with the total fuel consumption was placed in order to keep in check the emission levels air pollutant such as acid gases, dioxins, furans etc[62]. However, over the past decade with the development of more efficient gas cleaning systems several countries such as Austria, Germany and The Netherlands have managed to increase their substitution rates to about 60-80%[10]. In order to facilitate the further increase in substitution percentages for co-firing, a characterization of the physical and chemical properties as well as the thermal behavior RDF is required. The RDF that is being produced from MSW generally has a large range proximate composition and calorific value due its high heterogeneous composition, which depends on the source, day-to-day and seasonal variability[63]. Their direct use could lead to operational problems or toxic emissions, particularly through the formation of HCl leading to the production of dibenzodioxins(PCDD) and dibenzofurans(PCDF) which are highly hazardous substances[32]. The high chlorine and ash content can also lead to slagging and fouling in boilers and gasifiers[79]. Due to the presence of these negative characteristics of RDF certain pretreatment technologies such as torrefaction or carbonization is carried out and have proven to improve the fuel properties, thereby reducing the operational and environmental impacts associated with their application as a feedstock or fuel[63].

Torrefaction also termed as roasting or low temperature pyrolysis is a thermal treatment that takes place at temperatures in the range of 200-300 °C in the absence of oxygen[71]. The process phases that can be distinguished are pre-heat, pre-drying and transient heating, torrefaction and cooling of the product[15]. Torrefaction yields two products; bio-char and torrefaction gas also referred to as tor gas, with a mass balance of 70-80% for the left over solid product and 23-30% for the volatiles released[15]. It has been found that through torrefaction there is a great improvement in the physical, chemical and energy characteristics of of waste derived fuels, contributing to their homogenization, improved grindabilty and gross calorific value along with reduction in volume [63]. The experimental studies carried out by Bialowiec et al.[16] on the torrefaction of RDF at different temperatures indicated that the process could bring about a decrease in the moisture content and subsequently increase the higher heating value.

To summarise, we have seen that refused derived fuels (RDF) can be viewed as a solution to aid in sustainable waste management and decrease the dependency on fossil fuels in energy intensive processes by co-firing. However, their thermal applications are conditioned by the physical and chemical properties such as the heterogeneity, high moisture, chlorine and ash content present in the waste material. Torrefaction has shown to be an adequate process to upgrade these solid fuels, the chars obtained are found to have higher homogeneity, reduced chlorine content and increased heating value among other things. These improved properties could help to remove the environmental and operational problems associated with RDF, but this thermal treatment has not been implemented on a large or commercial scale and is still in its initial phases particularly for waste derived fuels.

1.1 Thesis Objective

This thesis aims to analyse and evaluate the operation of a torrefaction plant for refuse derived fuel in order to determine its feasibility from a technical and economic perspective. Through this study it would possible to identify key factors that could aid in increasing the attractiveness of waste derived fuels through their thermal treatment. The goals of this work are:

- To develop a process system and simulate the the torrefaction of RDF considering the unit operations of drying, torrefaction reactor, combuster, grinder and pelletizer through the use of MATLAB and ASPEN Plus.
- To investigate the influence of various parameters(e.g moisture content, temperature, residence time) on the overall process through sensitivity analysis to determine the optimum process parameters.
- To carry out an economic evaluation of the process plant by means of economic indicators such as Net Present Value (NPV) and Payback Period (PBP).

- To evaluate the effect of substitution of torrefied RDF within a typical cement plant based on certain parameters such as CO_2 and cost savings .

The increased knowledge would aid in defining the directions of future studies for the implementation and improvement of the discussed process, thereby making it economically agreeable to be applied.

1.2 Thesis Structure

The report is divided into four chapters:Literature Review, Methodology, Results & Discussion, Conclusion & Recommendations. The first chapter, Literature review aims to provide information regarding refuse derived fuel (RDF), its definition, production characteristics and applications along with brief descriptions on the equipment used in the unit operations involved and its selection procedure.

The second chapter, Methodology provides insights into the process modelling and simulation carried out through Aspen Plus in addition to the method followed for an economic analysis. The unit operations of drying, torrefaction, grinding and pellitization modelled on the basis of literature data and a brief description of the Aspen Plus model integrating these unit operations are discussed. The economic indicators that were chosen for the profitability evaluation of the process plant is also discussed. Within the third chapter, Results & Discussion all the simulation results obtained from the Aspen Plus model is presented and discussed for the selection of the optimum operating conditions. The results from the economic evaluation along with a study into the effect of RDF substitution in a typical cement plant is provided. The final chapter, Conclusion & Recommendations outlines the main findings obtained from the current work and provides certain recommendations that could be implemented in order to adress the limitations of the current project.

Chapter 2

Literature review

The aim of this chapter contains an overview into the material, processes and its necessary equipment which are being considered within the current work. The first section provides information regarding refuse derived fuel(RDF), its sourcing, composition, characteristics and current applications. This is followed by a review into the various drying methods employed for the removal moisture from the raw RDF and its associated equipment. The last section introduces the process of torrefaction, its significance with respect to RDF and an evaluation of the various reactors through which the process is achieved.

2.1 Refuse derived fuel

This section aims to provide the reader with general information into what is refuse derived fuel, its characteristics, significance in the current energy systems and applications for energy production. The term Refuse Derived Fuels (RDF) in the general sense is used to classify the combustible matter or fuels that are extracted from wastes which are not under any specific technical standards and is more often than not extended to fuels with low quality[60]. Due to the urgency in transitioning from the use of fossil fuels to sustainable energy production methods from renewable feedstock and solutions to sustainable waste management RDF has been gaining an increased attention in the recent years, offering to be a solution to these main challenges that are being faced by the world. The first step in evaluating the application of refuse derived fuel in energy production was identified to be its standardization, which was done by the European Standardization Commission (ECN). The specification standards that were drawn up was based on the fuel's calorific value, moisture, ash and chlorine content. The general classification system used for RDF is show in in table 2.1 below.

Table 2.1: Classification system for RDF[63].

Parameter	Statistical Measure	Units	Class				
			1	2	3	4	5
Higher Heating Value (HHV)	Average	MJ.kg-1 (a.r)	≥ 25	≥ 20	≥ 15	≥ 10	≥ 3
Chlorine Content (Cl)	Average	% (d.b)	≤ 0.2	≤ 0.6	≤ 1.0	≤ 1.5	≤ 3

2.1.1 Production and characteristics

The main waste streams from which RDF can be sourced are MSW, industrial waste, construction and demolition waste (CDW)[69]. All the current works on the analysis of RDF focuses on the sourcing from MSW mainly owing to the fact the technology used within MSW treatment is a well known and mature, which results in an increased efficiency of separation of the combustible fractions which can be used as a fuel. The sustainable management and disposal of MSW has been growing in concern over the past decade, due to the rising levels in waste being generated and lack of landfill area to compensate for its disposal due to the competition with urbanization. It was estimated that a the generation of MSW will reach numbers about 1.24 kg/capita/day by 2025 and will be close to 2.6 billion metric tones by 2030[40][5]. An approximate estimate of the volume of MSW generated across the globe is shown in figure 2.1 below, where the United States, China and India are largest producers of MSW[4]. These numbers are only further expected to grow which reiterates

that their sustainable management and disposal are the need of the hour to reduce the risk to the environment and human health. This is where RDF comes into the picture, by recovering the combustible fractions present within the MSW and their subsequent application in WtE technologies a circular energy recovery can be established and the amount of wastes being sent to the landfills can be substantially reduced[88].

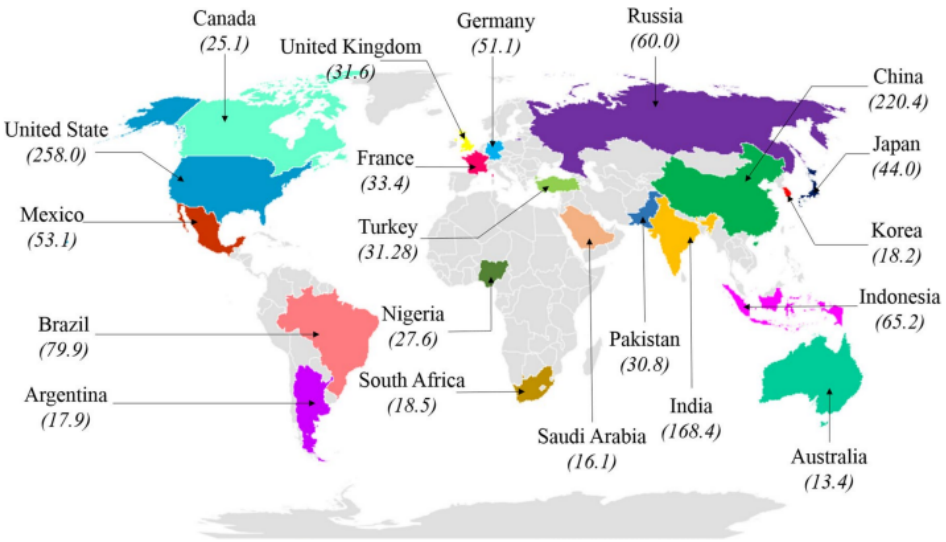

Figure 2.1: Volume of waste generated (MT) across the globe[4].

The treatment of the raw MSW to obtain RDF is carried out in mechanical treatment (MT) or mechanical biological treatment plants (MBT), the methods of treatment the waste is being subjected to is detailed by the figure 2.2 given below.

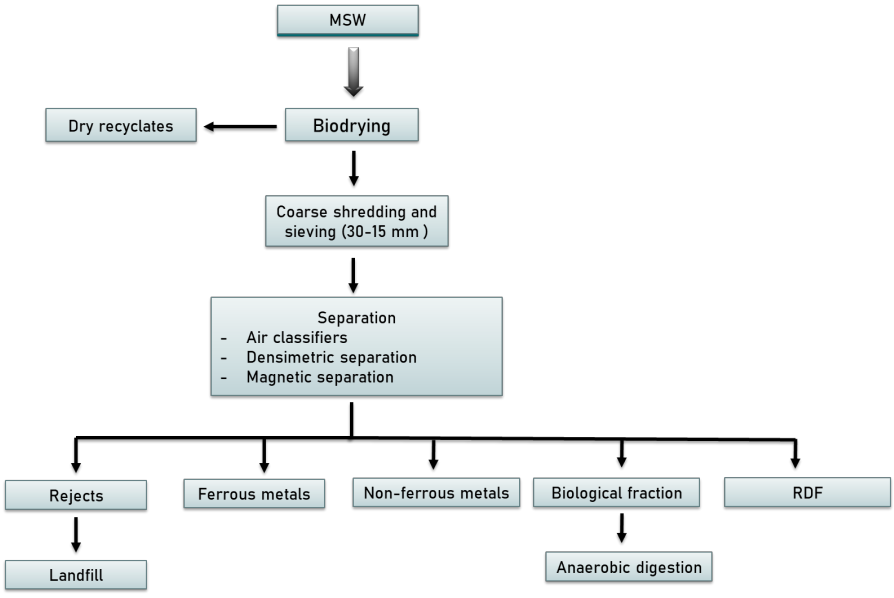

Figure 2.2: Steps involved in sourcing RDF from MSW[26][30].

These treatment plants create additonal opportunities to recover resources,however their complexity increases resulting in additional loses and energy consumption[26]. The ferrous materials are sent to foundries where they are smelted and recycled, while the non-ferrous materials more often than not end up with in the landfills due to the challenges in their recyclability. It is essential that well established waste separation and treatment facilities are present in order to effectively separate the combustible RDF fractions. As mentioned

within the above section the United States has the highest generation of MSW and at the same time well established mechanical treatment facilities, based on these considerations the US is proposed as a suitable location for setting up the plant.

To understand the various fractional compositions of RDF, a more in depth literature review needs to be conducted into the daily, monthly and seasonal variation of the waste generation patters within the region. To avoid this complexity the typical compositional fractions present within RDF sourced from MSW is shown in figure 2.3. It is evident from the figure that the organics which consists of food as well yard wastes among constitutes the majority fraction and this is in line with the waste generation patterns of developed countries[76]. The corresponding proximate and ultimate analysis of the waste is shown in table 2.2. It can be observed that raw RDF has a high moisture content and low calorific or heating value (HHV), which hinders its application for energy conversion and must be subject to treatment methods for the improvement of its properties.

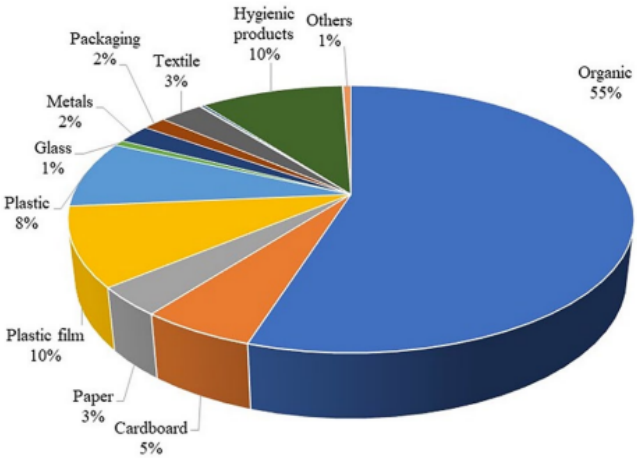

Figure 2.3: Fractional composition of RDF sourced from MSW[76].

Table 2.2: Ultimate and proximate analysis of RDF[76].

	Units	Value
Ultimate Analysis		
C	TS%	35.1
H	TS%	4.7
N	TS%	1.5
S	TS%	0.2
O	TS%	16.1
Proximate Analysis		
Moisture [a]	wt.%	45.8
Volatiles	TS%	51.1
Fixed carbon	TS%	6.3
Ash content	TS%	42.6
Measure HHV	MJ kg-1 dry mass	15.4

[a] Moisture content presented on wet mass basis

2.1.2 Applications of refuse derived fuel

Refuse derived fuel (RDF) has recently been gaining attention for applications within thermochemical conversion processes primarily due to the fact that these technologies are also essential to waste management and energy recovery from the materials which cannot be recycled. It has been found that the existing technologies of combustion or co-combustion, gasification and pyrolysis could be extended to

RDF valorization[63]. However, there are certain challenges posed by RDF with regards to its heterogeneity and low calorific value as each technology has specific requirements and a standardization of its properties is essential. The application of RDF within power plants via its incineration for producing electricity or combined heat and power have been investigated. Previously, before the introduction of the standardization limits it was found that their incineration lead to high concentrations of dangerous emissions due to the chlorine and mercury content[60]. The experimental work carried out by Hernandez-Atonal et al.[39] reported that by the reduction in the chlorine content of RDF used the combustion efficiency of the system had vastly improved along with reduction in NOx emissions. Another area where RDF finds its application is in cement industries as an alternative fuel. Currently this is been as the most suitable option for RDF co-combustion. It has been reported that the greenhouse gas (GHG) emissions from these plants could be reduced through substitution of RDF with traditional fuels, also the high temperatures achieved within the cement kilns facilitate the destruction of residuals[51][63].

Gasification and pyrolysis of RDF is still being investigated,thou they have yielded promising results they have not been employed on a large scale. An experimental study on single-stage plasma gasification of RDF by Agon et al.[9], reported the production of syngas with medium calorific value, LHV close to 10.9 $MJ.Nm^{-3}$ and a cold gas efficiency of 56%. The pyrolysis of RDF was studied by Efika et al.[33] within a tubular horizontal reactor by varying parameters such as heating rate and pyrolysis temperature. It was reported that under conditions of 800°C and long residence time, the product gas had a calorific value of 25 $MJ.m^{-3}$.

2.2 Drying methods

The most important pre-treatment method before the application of thermochemical conversion techniques of biomass or waste feed stocks is drying. The high and variable moisture content on an average of 50% (wet basis) present within the RDF that is being obtained from various sources makes this step a necessity in order to have a uniformity in its moisture content by reducing it to an acceptable level of 10 % (dry basis) in order improve energy efficiency,energy of final product and reduce emissions during the thermochemical energy conversion[64]. The work carried out by Brammer et al.[20], further stresses the importance of the drying step,wherein high levels of moisture present within the biomass used as a feedstock for small-to-medium scale gasification plants for producing power and heat caused an overall decrease in the performance of the plants along with deteriorated quality of the product gas[36]. The additional purpose of carrying out the drying of feed, specific to torrefaction is to restrict the evolution of wet torgas, as the volatiles released during torrefaction of a material rich in moisture makes the them undesirable for recovering heat for the process through combustion due to lowering of the flammability and adiabatic flame temperature[54]. The advantages of this pre-treatment method however, comes at a cost, as drying is highly intensive in terms of its energy and capital requirement. One way of reducing the energy cost is through the integration of low-grade waste within the process[36]. Thermal drying through the use of hot air or steam as the drying medium either by direct or indirect mode of contact is the mostly commonly used approach for moisture removal in biomass, the same can also be extended to the case of wastes however, in addition to thermal drying there are two other methods that are specific to refuse derived fuel namely bio-drying and solar drying. These methods are further reviewed in the subsequent sections to determine the feasibility and relevance for their application within the current work.

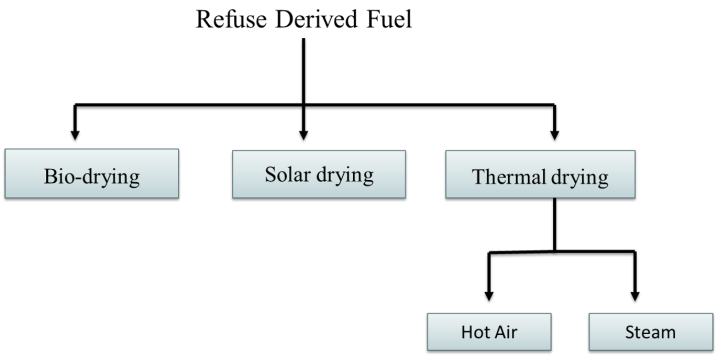

Figure 2.4: Drying Methods for Refuse Derived Fuel.

2.2.1 Bio-drying

Bio-drying method can be classified as an aerobic conversion process that applies either natural or forced aeration with aim of utilizing the heat from the internal exothermic reactions taking place due to decomposition for conversion of moisture of within the waste material. The product obtained is the bio-dried material from which RDF can be recovered through the separation of the inert and inorganic fractions [69]. The addition of certain microorganism such as bacteria,fungi and cellulose degraders lowers the drying residence time required to about 7-15 days with drying temperatures between 40 and 70 °C[85]. This method is economically attractive and environmentally friendly, it has slowly been gaining attention and several works have been carried out from a lab to a partly industial scale in order to investigate its integration with WtE and thermochemical conversion technologies for waste feeds. A greenhouse dryer is a combination of the principles of bio-drying and solar drying, by allowing solar-energy to be incident directly on the waste placed inside, heat is generated within the greenhouse increasing the air temperature and promoting microbial action for subsequent moisture removal and volume reduction[74].

2.2.2 Solar drying

As the name implies,this method makes use of solar energy in order to carry out the drying operation. This method offers the benefits of making use of a renewable energy source as well reduced emissions, however they are usually accompanied with high capital and operation investments[85]. The application of this drying technique can vary to a large extent and increasing in complexity of the systems installed. In principle the incident light is made to pass through a transparent sheet and the solar absorber plate converts this incident light to heat which is retained within the drying chamber, with temperatures reaching to about 30-60 °C[86]. Through the use of natural (passive system) or forced convection (active system) of this thermal energy along the drying chamber, the moisture removal is achieved. Several studies have been carried out to determine whether this method could be extended to the drying of waste, a design of a system consisting of a solar absorber plate with additional electrical heating coils was put forward by Pawale et al.[65] for MSW and refuse derived fuel. Another potential design of a solar integrated conveyer-belt dryer was proposed by Shirinbaksha et al.[77] for applications in large WtE facilities. However one important drawback of this mode of drying that has been reported in all of these studies is the long drying times that are required to achieve significant moisture reduction, usually in the range of one to two days, owing to the low operational temperature and intermittency of energy source. A schematic of a solar drying system for refuse derived is shown in the figure 2.5.

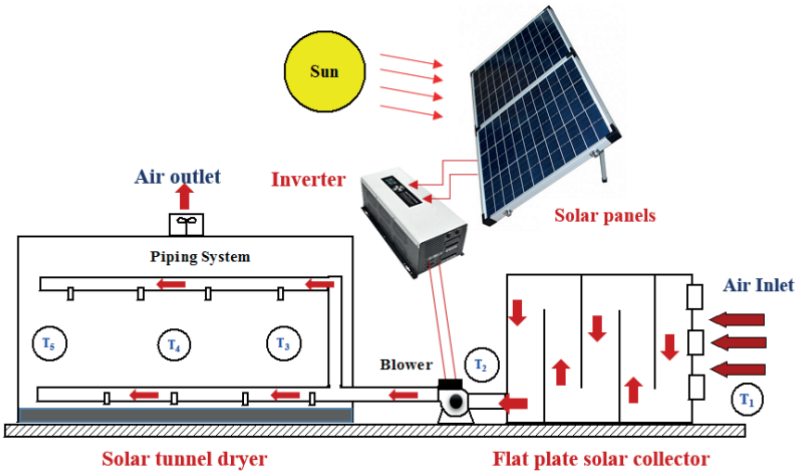

Figure 2.5: Schematic diagram of a solar drying set up for RDF[43].

2.2.3 Thermal drying

The term thermal drying is used when an external source or heating medium is used for in the reduction of moisture content of the solids. The thermal energy present within the hot stream is transferred to the wet feed for evaporating the moisture present, in addition to a rise in the temperature of the solid and remaining

water present. The thermal energy sources are usually hot air or super heated steam and the operational configuration of such drying systems can classified into two modes based on the type of contact between the heating medium and wet solids, which are :

- **Directly heated:** As the name implies, the thermal energy is transferred via direct contact between the heating medium and wet solid, while the evaporated moisture is carried away by the hot gas. This method can also be termed as convective drying, since the dominant mode of heat transfer is convection. The characteristics of this mode operation are that the efficiency of the drying system can be enhanced by increasing the temperature of the inlet gas, gas cleaning needs to be done due to dust entrainment as there is direct contact with the solids and significant reduction in moisture content is achievable but with high energy consumption[11]
- **Indirectly heated :** In this configuration, the heating medium flows around the outside of the drying chamber and heat transfer occurs through the wall or hot surface. Steam is the most commonly used heating medium in this type of dryers and it does not serve as medium for moisture to be carried away. The characteristics of this system are that, they can be applied when dealing with easily combustible materials in order to avoid risk of oxidation or explosion and the absence of solid entrainment makes the the ideal choice when dealing with dusty materials [37]

Several studies have been conducted to determine the feasibility of thermal drying for MSW and refuse derived fuel, by analysing the effect of drying temperatures on the moisture reduction and residence time. Bukhmirov et al.[21] carried out experimental studies on the convective drying process by hot air for MSW and reported that close to 100% reduction in moisture was achievable at drying temperatures of 106-170°C and residence times of 60-170 min. The research carried out by Asadi[11], has found that the direct and indirect modes by using hot air or steam can be employed in the drying of refuse derived fuel to be used for co-incineration or WtE technologies. Based on the results from these studies it is evident that thermal drying is the most optimum method which can be employed for refuse derived fuel torrefaction to have a continuous operation and steady product outflow. In order to select the optimum drying equipment employing the direct or indirect mode, the most commonly used industrial dryers are reviewed in the subsequent section.

2.3 Industrial Dryers

This section reviews the different dryers that are most commonly used within the process industries that makes use of either direct or indirect operational mode in order to determine the most optimum equipment to be used for the drying of refuse derived fuel.

2.3.1 Belt dryer

This a type of dryer that employs hot air as the drying agent, which is blown over the thin layer of solid bed roughly about 2-15 cm, being transported continuously via a conveyor belt[37]. The flow of the hot gas could be in counter-current, co-current or cross flow, hot flue gas may also be used as the drying medium apart from air[34]. The drying operation can be carried at a constant temperature through the use of additional heating coils and re-circulation fans. The dried solid product is discharged at the end through the use of a discharge screw.The design and operation of belt dryers are quite simple, they are also quite flexible towards different air flows and temperatures. However due to the lack of adequate heat and mass transfer they are significantly large systems[34]. A schematic representation of a belt dryer is shown in the figure 2.6

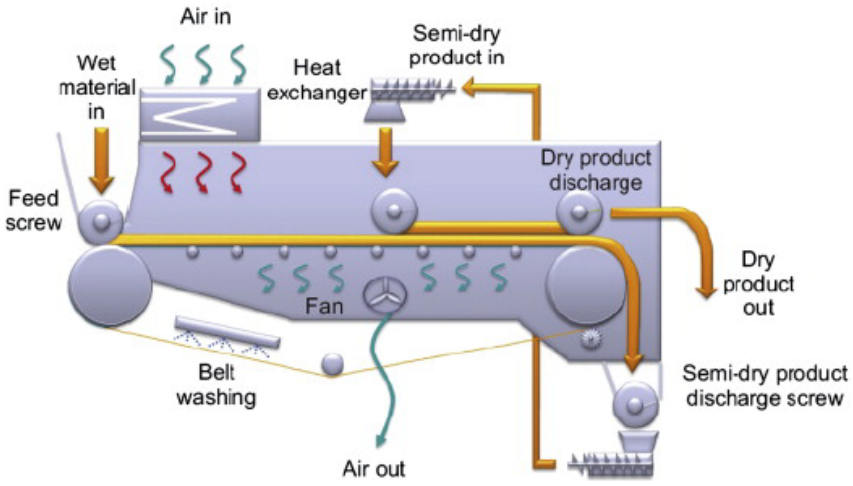

Figure 2.6: Schematic of a Belt dryer[34].

2.3.2 Rotary drum dryer

This type of dryer consists of a cylindrical drum that rotates along the horizontal axis that allows for the movement of solids in the forward direction, and ensuring good heat and mass transfer. The hot gas that is in direct contact with the solids, having a temperature usually in the range of 120-400 °C can be made to flow along the cylinder in counter-current or co-current configuration [34]. A co-current flow is usually preferred in the case of refuse derived fuel due the presence heat sensitive combustible fractions that may be present[11]. The final dried solid product is separated at the end, while the drying gas is sent through a series of cyclones and filters to remove the fines or dust that may be entrained in it. The direct rotary drum dryers are cost-effective and have a simple design, with better heat and mass transfer rates when compared to belt dryers [34]. A schemactic representation of a direct rotary drum dryer is shown in the figure 2.7 below.

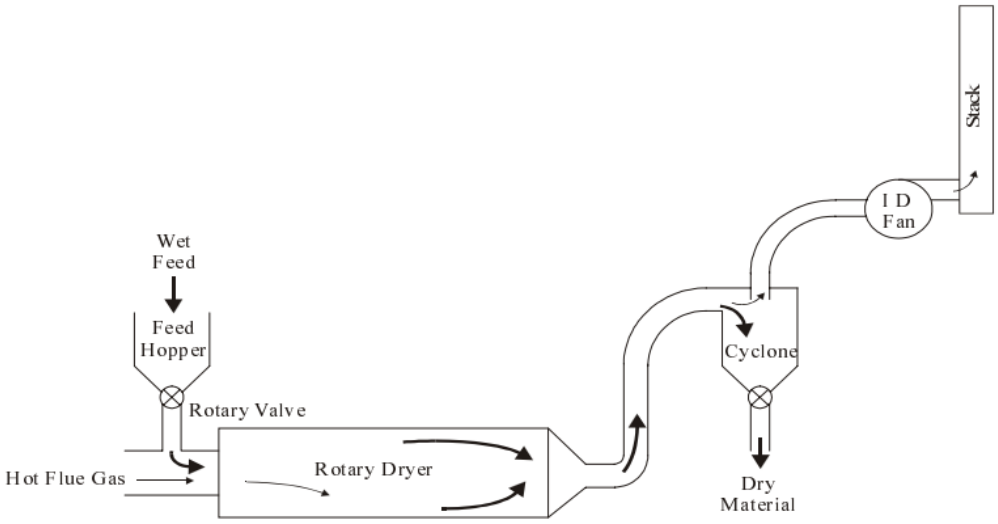

Figure 2.7: Schematic of a rotary dryer [34].

2.3.3 Indirect steam tube dryer

These are rotary dryers that make use of the indirect contact operational mode through application of super heated steam as the drying agent.A schematic representation of an indirect steam tube dryer is shown

in the figure 2.8. The steam is made to pass through tubes that are installed along the drum length, there may one or several rows of these tubes[11]. The drying takes place through the heat transfer mechanisms of conduction and radiation,when the solids that enter the dryer through a screw conveyor are in contact steam tubes. An advantage of this system is that several design and operation parameters can be controlled such as temperature and pressure of the steam inside the tubes, number of tubes, the solids residence time as well the installation of flights inside the dryer for improved mixing in order in order to ensure an efficient drying operation[11]. However with increase in control parameters their design complexity increases which leads to large capital and operation investment along with additional costs incurred through the handling of large volumes of steam[11][34].

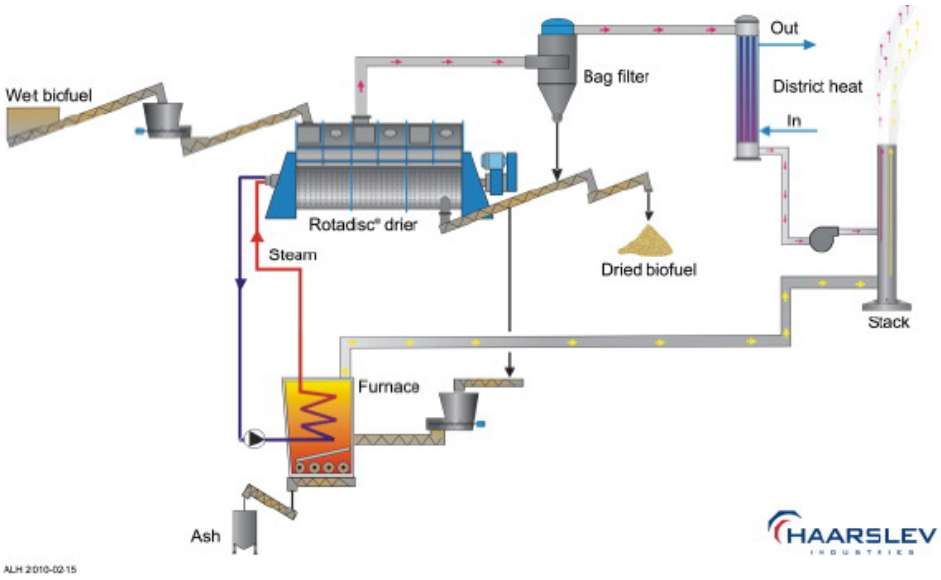

Figure 2.8: Schematic of an indirect steam tube dryer[34].

2.3.4 Fluidized bed dryer

These type of dryers are quite commonly used within the industry due their operational conditions and vast applications. As the name implies the system consists of a cylindrical column within which a fluidized bed of solid particles in contact with the incoming gas phase is maintained[11]. They can operate within the temperature ranges of 100 to 400°C when using superheated steam as the drying agent. Other advantages offered by these dryers are that they promote solid mixing, improved mass and heat transfer and homogeneity of dried solid, which aids in decreasing the size of the dryer. However, despite these advantageous certain restrictions limit their applicability such as a high power consumption, particle entrainment and the small size of solid feed (1-5 mm) required for fluidization[34]. A schematic representation of a fluidized bed dryer is shown in figure 2.9.

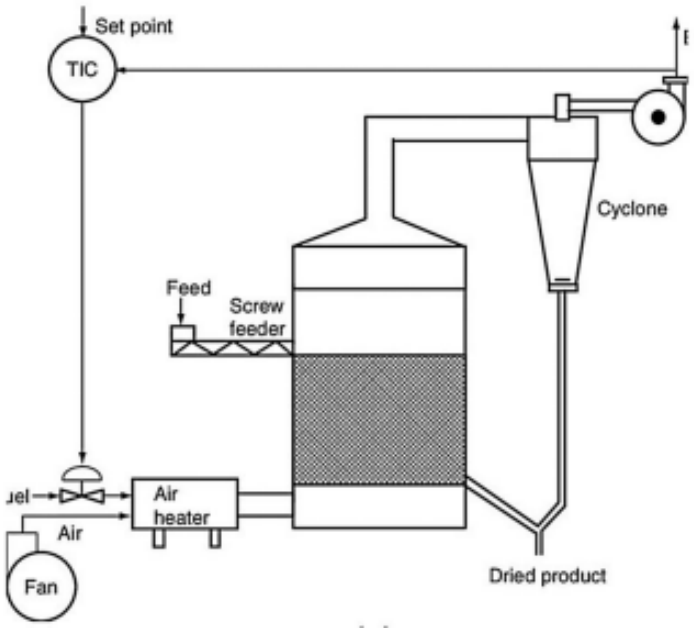

Figure 2.9: Schematic of a fluidized bed dryer [58].

2.3.5 Dryer selection

To summarise, the different methods such as bio-drying, solar drying and thermal drying employed for drying of refuse derived fuel have been reviewed. Based on the results and discussions obtained from the studies conducted on these methods available in literature, we can come to the conclusion that bio-drying cannot be integrated into a continuous operation of a WtE or thermochemical conversion facility due the long drying periods involved, inclusion of additional material and treatment. Solar drying proves to be an attractive option due to it being based on an renewable energy source and having reduced emissions, however the long drying periods due to the intermittency of the energy source and capital investments again hinder their applicability in a continuous operation, but they could be integrated into a batch operation. Thermal drying is the best option available, as it is a proven and well known technology along with having a continuous operational capability. Moderate to high temperatures can be achieved through thermal drying which significantly shortens the residence times and improves moisture removal, hence it has been selected within the current work.

The criteria that were considered while selecting the optimum drying equipment are shown in the figure 2.10 below. The belt dryer offers flexibility in handling heterogeneous materials along with the use of hot air as a drying medium, makes it a suitable option. However due to its very large size and lack of efficient heat and mass transfer it has not been considered. The indirect steam tube offers to be good alternative, however the studies conducted by Asadi.[11] shows that capital and operational costs incurred through the handling of large volumes of steam make this option unfeasible particularly in this study since the aim is produce torrefied refuse derived fuel pellets that could be as competitive as coal prices if not lower. The fluidized bed dryer is also not considered due the really low particle size required to maintain the fluidized phase. There is also a possibility of product loss, low flexibility for wet feed, entrainment of fines and a high energy consumption to maintain the fluidized phase. The best option available is the directed heated rotary drum dryer, it is a cost-effective and proven technology involving the use of hot air as the drying medium, it offers good flexibility in handling heterogeneous materials and a uniform product can be obtained owing to proper mixing within the drum as reported by Pinacho et al [67]. Hence the direct heated rotary drum dryer has been selected to be modelled and simulated for the drying of refuse derive fuel for its pre-treatment before torrefaction.

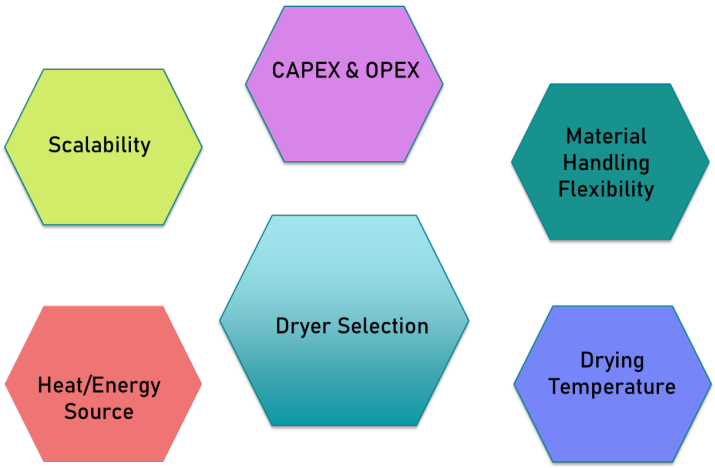

Figure 2.10: Dryer selection criteria.

2.4 Torrefaction

Torrefaction, also referred to as mild- pyrolysis is a thermal upgrading method or treatment which is carried out in temperature ranges of 200-300°C, residence of time of 30-60 min and in the absence of oxygen[15]. When the process is carried out, the material partly decomposes, giving rise to volatiles and the left-over solid product is referred to as char. Through this process the material undergoes a modification in its physical and chemical characteristics particularly an improvement to its energy density, calorific value, grindability and hydrophobicity[63]. The torrefaction process can be split up into five distinct stages as represented in figure 2.11 and they are discussed briefly below :

1. **Initial Heating** - This period marks the start of torrefaction.The biomass is heated up gradually from ambient temperature to the desired temperature at which the drying of the biomass starts and the moisture starts to evaporate towards the end of this stage.

2. **Pre-Drying** - During this stage, the unbound moisture present within material is being removed at a constant rate. Until the critical moisture content of the material is reached the temperature remains fairly constant,below which the rate of drying decreases

3. **Post drying and Intermediate heating** - The biomass is again subject to further increase in its temperature to about 200°C, where all the bound moisture is released. Beyond this stage the material is completely free of moisture, some amount of mass is also expected to be lost due to evaporation light organics.

4. **Torrefaction** - This stage is when the material is being torrefied.The torrefaction period starts immediately after the temperature exceeds 200°C and ends once the it drops below 200°C.Within this stage there is a heating, cooling and period of constant temperature. The peak or constant temperature range is referred to as the torrefaction temperature. The mass loss (devolatilisation) initially occurs during the period of heating, resumes across the torrefaction temperature and subsides after the cooling period.

5. **Solids Cooling** - After the end of the cooling period from the previous stage the final temperature of the solids is close 200°C. During this stage, the temperature of the torrefied material is brought down further to the required temperature and no mass loss can be observed.

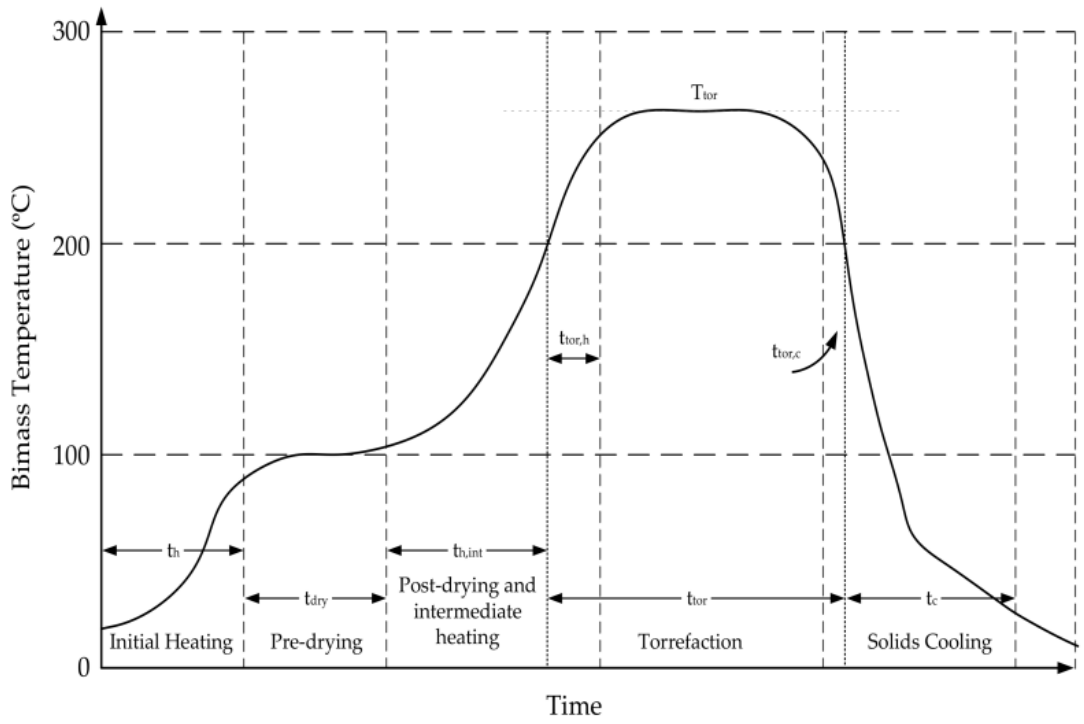

Figure 2.11: Different stages in torrefaction.Explanation: t_h = time for heating to drying temperature,t_{dry} = time required for drying, $t_{h,int}$ = intermediate time for heating from drying to torrefaction temperature, $t_{tor,h}$ = time for heating from 200 °C to desired torrefaction temperature, T_{torr} = residence time for torrefaction, $t_{tor,c}$ = time for cooling from T_{torr} to 200°C . t_c = cooling time till ambient temperature.[15].

Figure 2.12 shows the mass and energy of a typical torrefaction process. The final solid product retains close to 70% of the initial mass, and 90% of the initial energy present within the raw material. The remaining 30% of mass from the initial raw material gets evolved to volatiles or torrefaction gas, with an energy content of 10%. It can be observed that an energy densification is achieved by a factor of 1.3 on mass basis [15].

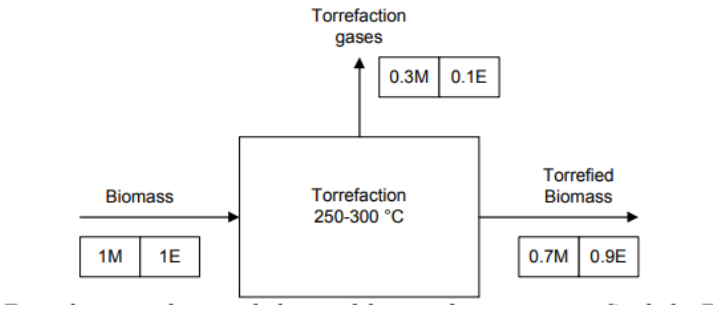

Figure 2.12: Typical mass and energy balance of the torrefaction process[15].

2.4.1 Significance of RDF Torrefaction

As mentioned in the previous sections, production of RDF from MSW and its subsequent application in WtE technologies is an effective route for energy recovery particularly to aid in sustainable waste management, reduction in landfill deposits and fossil consumption by co-incineration in cement plants[63]. However RDF faces certain challenges in their application as a feedstock due to the large variability in the initial MSW which results in the sourced RDF having a heterogeneous nature, high moisture content, low calorific value, low grindability and presence of high chlorine and ash contents[32][63]. Another factor that presents an issue is that there are certain quality requirements that are to be met by the produced RDF which is put forward by the European Committee for Standardization (CEN). There are two classes of RDF namely RDF

and RDF_Q, distinguished by their calorific value (>15 and 20 MJ/kg,respectively), moisture content (<25% and 18%, respectively) and ash content(<20% and 15%,respectively)[69][16]. Apart from these standards set by CEN, each individual cement plant has certain fuel quality specifications that need to be met by the RDF for co-incineration, mostly it should have a higher heating value (HHV) above 15 MJ/kg with a moisture content less than 15%(d.b) and more often than not these requirements are not being met by the suppliers which results in RDF being less attractive to the cement industry to meet their energy demands [16]. This is where the torrefaction technology has an important role to play, the alteration of physical and chemical characteristics accompanied with the torrefaction process improves the calorific value of RDF and standardizes its properties. Several studies have been conducted to analyse the effect of torrefaction and its parameters on refuse derived fuel.

Experimental studies on RDF torrefaction within the temperature range of 200-300 °C with residence time of 1 h were conducted by Bialowiec et al[16]. A mass of loss of 21% due to removal of moisture and evolution of volatiles were observed. The final torrefied RDF was reported to have shown an increased homogeneity and HHV of 25.3 MJ/kg when compared to the original RDF having HHV of 19.6 MJ/kg. Another research carried out by Edo et al.[32] focused on the torrefaction of RDF and MSW. The authors observed that the final torrefied product had lower chlorine content when compared to the raw material. This partial removal of chlorine lowers the possibilities of hazardous chlorinated compounds to originate from the char.

Based on the results reported in these works, we can conclude that torrefaction does indeed have a positive impact in improving the physical and chemical characteristics of RDF. However all these works were performed on an laboratory scale and in depth study into the continuous operation of RDF torrefaction has not yet been conducted. The current work aims to bridge this gap, by exploring the process design and economics of such a plant producing torrefied RDF pellets.

2.5 Torrefaction Reactors

This section deals with the evaluation of different reactor technology available for RDF torrefaction.The reactors can be classified on the basis of its heating mode either as direct or indirectly heated. The various types of available reactors based on this distinction is represented in the figure 2.13 below. The well-known and commonly used reactor types will be further briefly discussed in order to select the optimum.

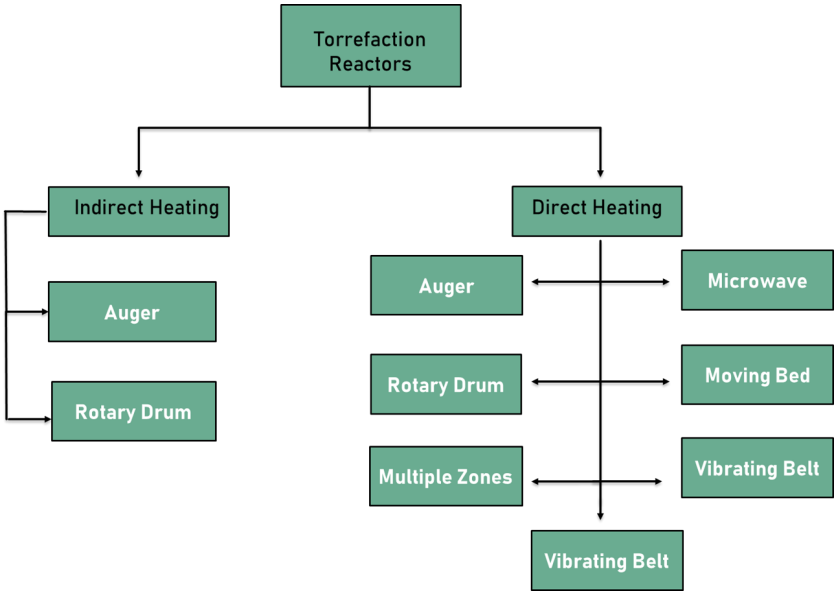

Figure 2.13: Torrefaction reactor classification based on Ref.[31].

2.5.1 Auger Reactors

The screw conveyor or auger reactors are considered to be proven reactor technology and have a continuous mode of operation,where the feed is transported through the reactor with help of screw conveyors. The reactor maybe placed vertically, horizontally or at an angle with the ground. As the material is being transported, it is heated either indirectly by a heating medium such as hot sand or directly through heating elements placed along the reactor wall. The advantages offered by this reactor system are their relatively low price and low demand of inert gas. However, it has many drawbacks with regards to uneven heat distribution due to limited mixing of material, formation of char in hot zones and limited scalabilty [48]. A schematic representation of the auger type reactor is shown in figure below 2.14.

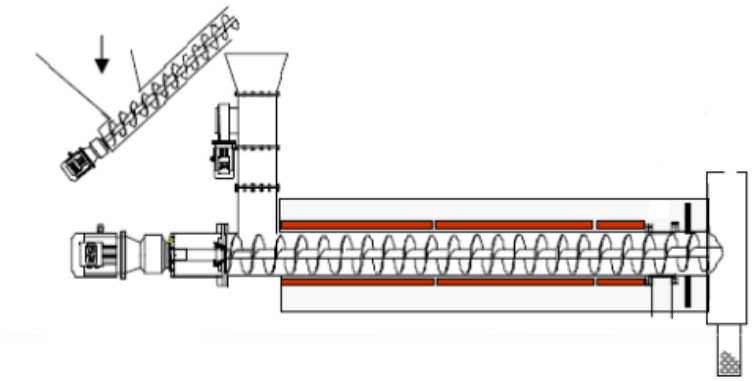

Figure 2.14: Schematic representation of the auger type reactor[48].

2.5.2 Moving Bed Reactor

In these types of reactors, the solids enter the reactor from the top into a closed process chamber.The solids move down freely with the help of gravity and there no special mechanism or moving parts involved in solids transport. The heating medium/gas enters the reactor from the bed, heats up the solids and the leaves the reactor along with the torgas through the outlet port located on top of reactor, the torrefied solid product is collected at the bottom of the reactor. The duration of a single operation is in the range 30-40 min and can handle temperatures up to 300 °C[48]. The advantages offered by these type of reactors are that they have a simple design, good heat transfer and increased bed density. However, these reactors pose difficulty in maintaining temperature control and pressure of the heating gas, resulting in a non-uniform solids conversion[61]. A schematic representation of a moving bed reactor is shown in the 2.15 below.

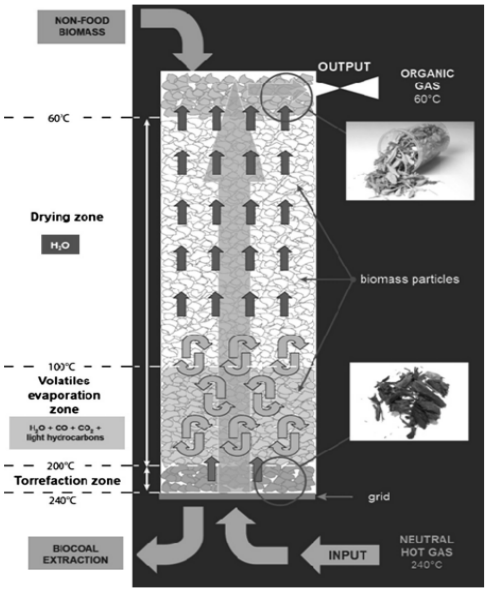

Figure 2.15: The Torspyd^{TM} example of a moving bed torrefaction reactor design Ref.[70].

2.5.3 Rotary Drum Reactor

Rotating reactors facilitate a continuous torrefaction operation.The heating medium can be supplied either directly or indirectly to the reactor. The torrefaction process can be controlled by several parameters such as the rotating speed,length and drum inclination angle [80]. A schematic representation of a rotary drum reactor is shown in figure 2.16.

In the case of directly heated rotary drum,the flue gas resulting from the torrefaction process could be used as the heating medium by recycling it back to the reactor and with heat exchange between the excess torgas. The solids are in direct contact with the heating gas,heat transfer takes place via gas-particle convection with the drum serving as as mixing medium[31]. An important factor to be considered during the operation is that the heating gas should be made to be free from oxygen. In the case of indirectly heated rotary drum reactors, the main difference is that there is no direct contact between the solids and the heating gas, the walls of the drum serve as the heat transfer medium through the mechanism of wall-particle conduction.The advantages offered by these type of reactors is that, a uniform heat distribution is possible due to efficient substrate mixing ensuring a uniform torrefaction, the heating gas does not need to be completely oxygen free and dilution of the volatile released does not occur which allows them to combusted to provide the heat load to the reactor[31]. A disadvantage of rotary drum reactors in general is their large footprint and relatively high capital costs[14].

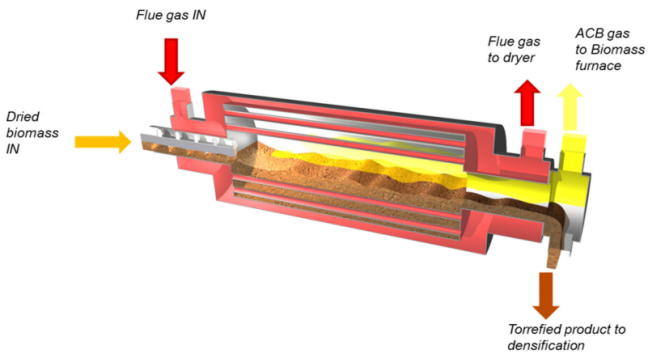

Figure 2.16: Schematic representation of a rotary drum reactor[78].

2.5.4 Fluidized Bed Reactor

This is a proven reactor technology and finds its application in various industries.For the application in torrefaction, the bubbling fluidized bed and toroid or torbed confgurations are used, the basic operation remains the same. Considering the torbed reactor,the heating medium enters from the bottom of reactor with really high velocities of 50 to 80 m/s, this causes the material to be torrefied within the rector to move about vertically or horizontal causing a toroidal swirl[48]. This movement results in rapid heating of the particles, causing torrefaction and is accompanied by low residence times in the range of seconds. The advantages offered by this reactor technology as mentioned are its uniform heat transfer rates, short residence times, accurate product control. But their application particularly for waste torrefaction is hindered by the restriction of on feedstock particle size, along with risk of tar formation and limited production capacities A schematic representation of a torbed reactor is shown in the figure 2.17.

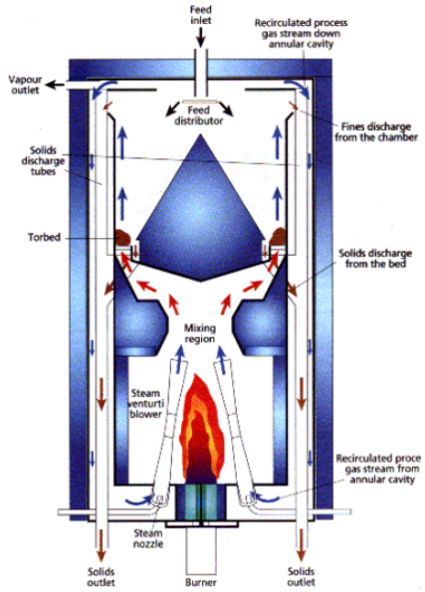

Figure 2.17: Schematic representation of Torbed reactor[48].

2.5.5 Reactor selection

The selection criteria in order to determine the optimum reactor for the torrefaction of RDF is represented in figure 2.18. The Auger reactor was rejected due its incapability in achieving uniform mixing of material,inefficient heating and limited scalabilty particularly for the screw conveyor within the rector. In the case of moving bed reactors, though they offer high capacity, good heat transfer rates and simple design. Their applicability is limited in the case of RDF torrefaction mainly due to the low particle sizes required and difficulty in scalabilty. The same drawback can be extended to the Torbed reactor along with high loss of volatiles due the high temperatures reached.

The indirect heated rotary drum reactor has relatively more advantages than the other options in terms of its flexibility in handling material with a heterogeneous particle size, efficient mixing leading to uniform heat transfer and more variables such as the angle, length and rotational speed among others to control the torrefaction operation. Due to these factors this reactor technology was therefore selected as the optimum to be used for refuse derived fuel torrefaction.

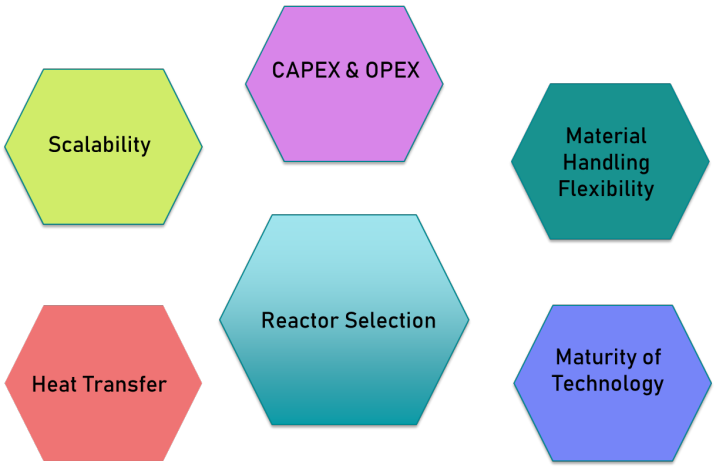

Figure 2.18: Reactor selection criteria.

Chapter 3

Methodology

This chapter presents the methodology that was followed for modelling and simulating the the main unit operations of drying,torrefaction grinding and pellitization in Aspen Plus. Firstly, a brief description of the overall process that is being carried out is provided. Secondly, the approach that was followed for carrying out the modelling and simulation of drying,torrefaction, grinding and pelletisation operations is detailed. Thirdly, an overall description of the developed Aspen Plus model that integrates the above processes is provided. Finally the method that was followed for evaluating the economic feasibility of the project is outlined.

3.1 Process overview

The aim of the current work is to carry out torrefaction of RDF, in order to improve its fuel properties by reducing the moisture content and increasing the calorific value. The process starts from the sourcing of the raw RDF that is being sent from the mechanical treatment plant, having a high moisture content of 45.6% (w.b) and particle size of 15 mm. The raw RDF is then dried in order to reduce its moisture content to an acceptable level of 10%(d.b) for its subsequent thermal-treatment via torrefaction. The dried RDF enters the torrefaction reactor where it undergoes conversion to form the solid char through the loss of mass which results in release of volatiles. The released volatiles are then combusted to provide the heating requirements for the drying medium and thermal fluid used within the dryer and torrefaction rector respectively. The solid char exiting the reactor is then cooled to room temperature and is further subject to grinding, followed by a pelletisation process in order to improve its physical properties for transportation and storage.A basic process flow is shown in below in figure 3.1

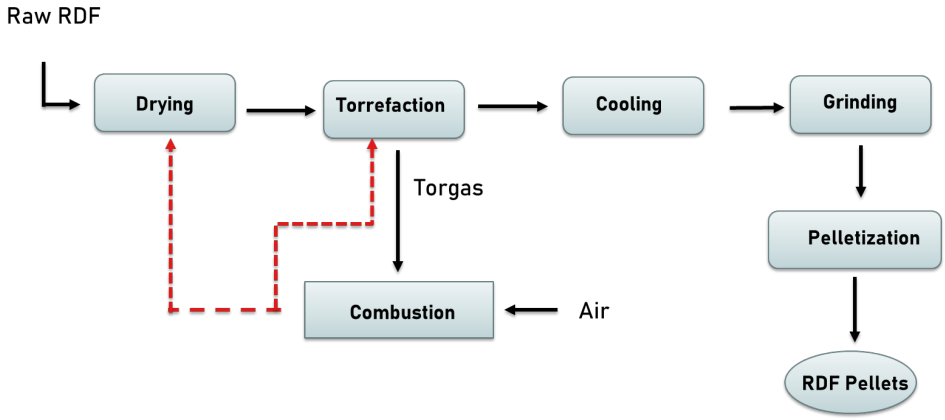

Figure 3.1: Process flow diagram.

3.2 Dryer modelling and simulation

In order to carry out the simulation of a convective dryer model in Aspen Plus the parameters associated with the dryer being designed need to be specified by the user such as the cross-sectional area, length, residence time, critical moisture content, equilibrium moisture content, normalized drying data and dimensionless numbers associated to heat and mass transfer among other things. The first part of this section focus on the drying kinetics of RDF in order to obtain the critical moisture content, equilibrium moisture content, drying rate and expected residence time. The second part deals with the sizing of the dryer based on the equations of mass and energy balance.

3.2.1 Drying kinetics of RDF

For accurately predicting the behaviour of the solids within the dryer and the performance of the dryer itself it is essential to obtain an understanding of the drying kinetics associated with the material.T his section focus on understanding and extracting the critical and equilibrium moisture content, along with the development of a mathematical model to best represent the drying behaviour of RDF in order to analyse the effect of temperature and particle size on the residence times of RDF within the dryer.

Figure 3.2 represents a typical drying rate curve, where the x-axis represents the moisture content usually denoted by X, within the material being dried and the y-axis represents the drying rate i.e the amount of moisture evaporated with respect to time, denoted by N. Following the initial transient period, evaporation starts and there is a reduction in the moisture content of the material which is varying linearly with time. This period from B to C is known as the constant rate period and is usually denoted by N_C. During this period all the amount free water present on the surface is evaporated and the rate of evaporation depends on only the external heat and mass transfer[12]. After all the unbound moisture has been evaporated,the solids reach the critical moisture content X_C, beyond which the drying rate begins to decrease with further reduction in X. This is because the moisture cannot move up to the surface of solid as quickly as in the N_C period due to internal transport limitations[12]. Reaching the equilibrium moisture X_e, marks the end of the drying operation. The duration of the initial transient period can be considered to be insignificant if the drying times are long.

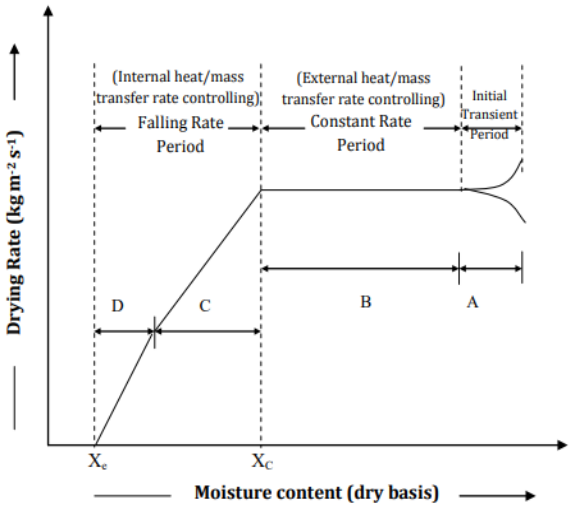

Figure 3.2: Typical drying rate curve[12].

Drying Equations

In order to carry out the mathematical modelling of RDF drying behaviour, experimental data showing the variation of moisture ratio (M.R) given by equation 3.2.1 with time based on experimental studies conducted by Słomka-Polonis et al.[81] was extracted and is shown in the figure 3.3 below.

$$Moisture\ Ratio(M.R) = \frac{M - M_e}{M_o - M_e} \tag{3.2.1}$$

where M, M_o, M_e are the moisture content at any time, initial moisture content and equilibrium moisture content respectively.

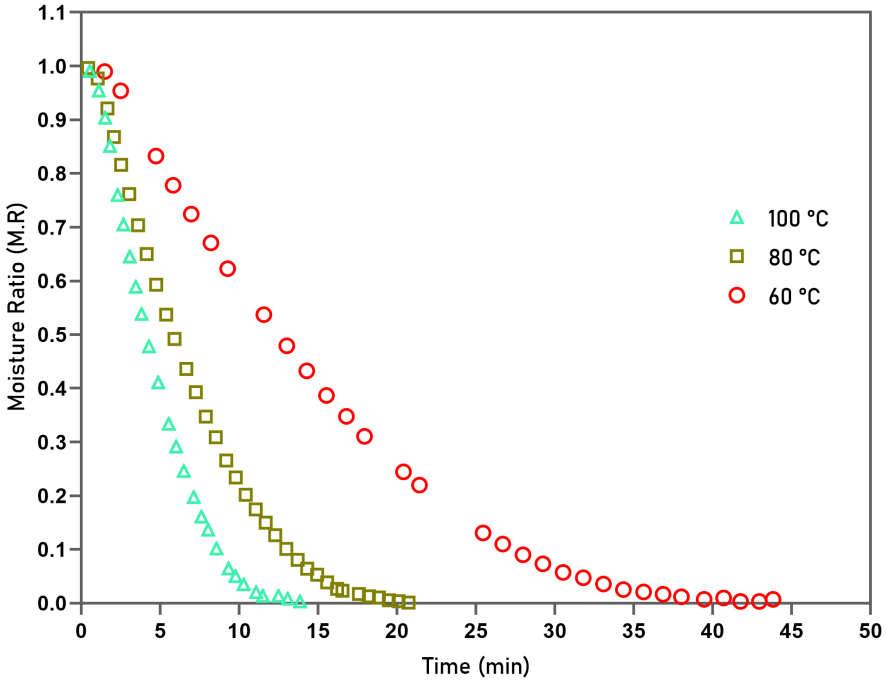

Figure 3.3: Experimental drying data for RDF (10 mm)[81].

The characteristics of the RDF samples studied such as the particle diameter(mm), initial moisture content (X_i) along with the equilibrium moisture(X_e) and critical moisture (X_C) that were extracted is shown in the table 3.1.

Table 3.1: Properties of studied RDF.

Parameter	Value
Length (mm)	10
X_i	40%
X_C	18%
X_e	3%

To carry out the mathematical modelling, the different drying equations that were commonly used were determined from literature and are shown in table 3.2. Out of these equations, the Lewis model and Henderson-Pabis model are mostly employed for predicting the drying behaviour of MSW, RDF and agricultural residues. Hence these were chosen to be modelled in the current study.

Table 3.2: Mathematical models to predict drying behavior[42]

S/N	Model name	Model equation
1	Newton/Lewis	MR = exp(-kt)
2	Page	MR = $\exp(-kt^n)$
3	Modified Page	MR = $\exp[(-kt)^n]$
4	Modified Page II	MR = $\exp[-k(t/L^2)^n]$
5	Modified Page III	MR = $k.\exp(-t/d^2)^n$
6	Henderson and Pabis	MR = A.exp(-kt)

Curve fitting of the experimental data to the selected models were carried out in order to obtain a more specific formulae, describing the drying behaviour of RDF which is dependent on the temperature and time. The developed equations are then used to determine the residence time of RDF within a dryer. The results obtained from the curve fitting carried out through the Curve Fitting Toolbox in MATLAB environment are discussed below.

Lewis Model

The general equation of the Lewis model is shown below.

$$MR(t) = e^{-k.t} \tag{3.2.2}$$

The results obtained from the curve fitting of the above equation to the experimental data carried out in MATLAB is shown in figure 3.4 and table 3.3

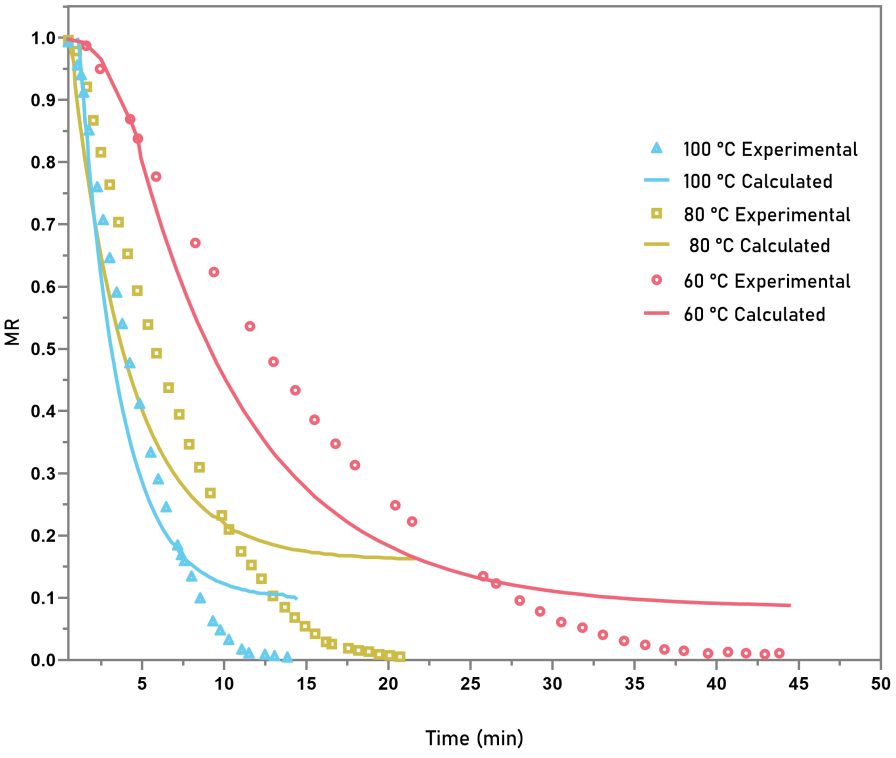

Figure 3.4: Drying curves fitted to Lewis model.

Table 3.3: Curve fitting results of Lewis model.

Temperature (°C)	Rate constant, k (s^{-1})	R^2	RMSE
60	0.0022	0.9044	0.0936
80	0.0047	0.8501	0.1279
100	0.0070	0.906	0.1056

Henderson-Pabis Model

The general equation of the Henderson-Pabis model given by equation 3.2.3 is shown below.

$$MR(t) = A.e^{-k.t} \tag{3.2.3}$$

The results obtained from the curve fitting of the above equation to the experimental data carried out in MATLAB is shown in figure 3.5 and the values are given in table 3.4

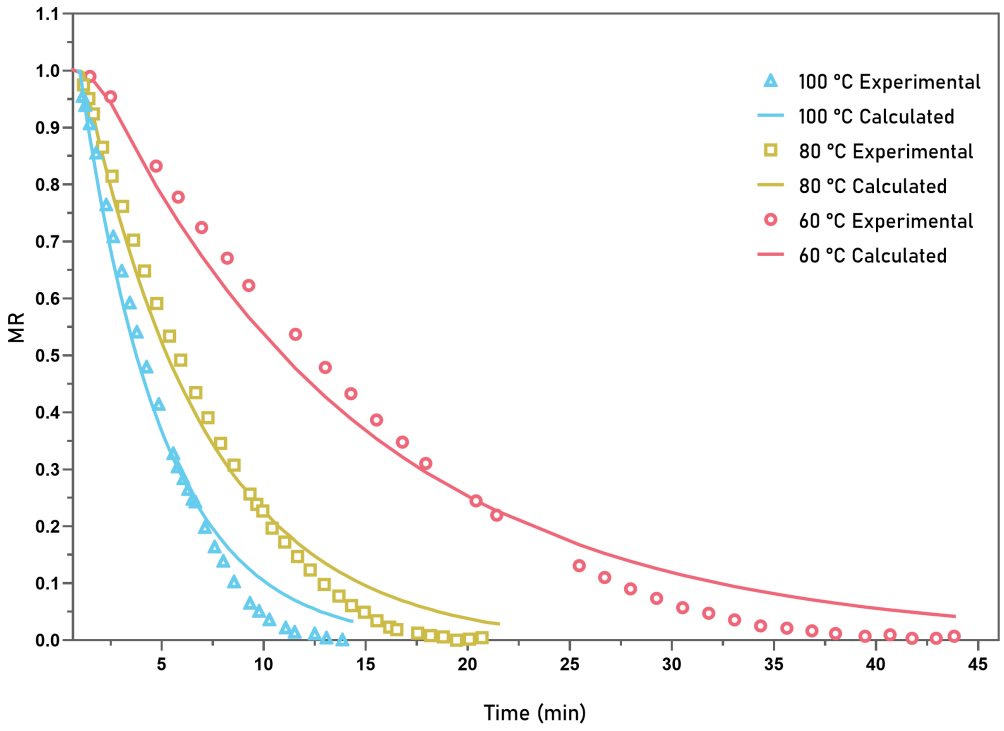

Figure 3.5: Drying curves fitted to Henderson-Pabis model.

Table 3.4: Curve fitting results of Henderson-Pabis Model.

Temperature (°C)	A	Rate constant, k (s^{-1})	R^2	RMSE
60	1.267	0.00133	0.9828	0.0434
80	1.199	0.002761	0.9789	0.0501
100	1.385	0.004174	0.9819	0.0430

Based on the results of curve fitting visualised in figures 3.4 and 3.5, it is evident that the Lewis model is not accurate in predicting the drying behavior of RDF, while the Henderson-Pabis(HP) model shows a very good fit with the experimental drying curve of RDF. This conclusion is further reinforced by the results shown in table 3.3 and 3.4, where a comparison of the R^2 and RMSE values for both models shows that Henderson-Pabis is a better fit than the Lewis model and hence was selected within the current work.

The next step was to analyse the variation of residence time for a range of drying temperatures, this was carried out by developing temperature dependent expressions for pre-factor(A) and rate constant(k). The equations (3.2.4 & 3.2.5) were developed through curve fitting for A and k values within the temperatures selected and their variation is shown in figures 3.6 and 3.7. The effect of drying temperature on residence time is shown in figure 3.8.

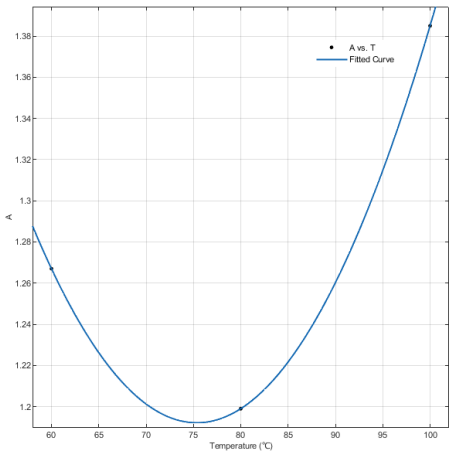

Figure 3.6: Variation of constant A with temperature.

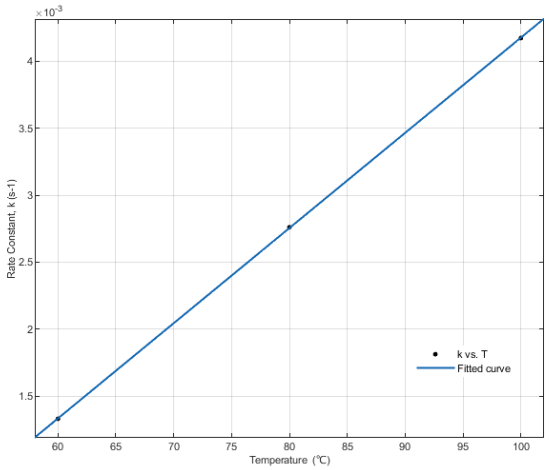

Figure 3.7: Variation of rate constant (k) with temperature.

$$A = 0.000115T^2 - 0.01665T + 1.795 \tag{3.2.4}$$

$$k = -2.25 \times 10^{-08}T + 7.47 \times 10^{-05}T - 0.003071 \tag{3.2.5}$$

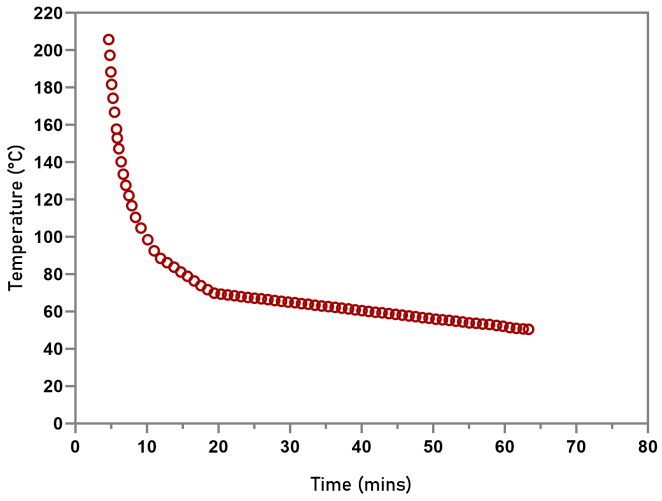

Figure 3.8: Effect of drying temperature on residence.

Effect of particle size

As seen from table 3.1, the size of the particle for which the drying data was reported is around 10 mm. But in a continuous industrial operation of sourcing RDF from MSW , after the screening and shredding process the size of the RDF obtained shows a large variability and is in the range of 15 to 30 mm. The particle size also influence the drying times which cane be seen from equation 3.2.6, and is commonly reported that smaller

the particle lower the residence times during drying. In order to include the effect of particle size on the residence times, the equation of the rate constant is modified and is shown below.

$$MR(t,D,L) = \frac{8}{\pi^2} e^{\frac{D \cdot t}{4 \cdot L^2}} \tag{3.2.6}$$

The inclusion of the length of particle within the rate constant was done using equation 3.2.7. L_{old} is the particle size of the sample studied and k_{old} is given by equation 3.2.5. The effect of temperature and particle size on the residence time is shown in figure 3.9.

$$k_{new} = (\frac{L_{old}}{L_{new}})^2 \cdot k_{old} \tag{3.2.7}$$

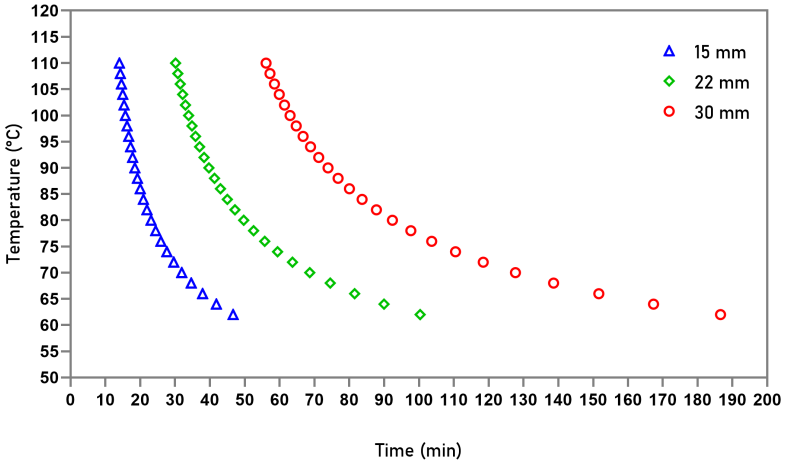

Figure 3.9: Influence of particle size on residence time.

Based on the developed equations 3.2.4, 3.2.5 and 3.2.7 a general model to describe the drying behavior of RDF with variation in temperature, residence time and particle size is formulated and is shown by equation 3.2.8.

$$MR = (0.000115 \times T^2 - 0.01665 \times T + 1.795) e^{((-2.25\times10^{-08}\times T + 7.725\times10^{-05}\times T - 0.003308)\cdot(\frac{L_{old}}{L_{new}})^2 \cdot t)} \tag{3.2.8}$$

As mentioned previously, in order to simulate the convective dryer in Aspen Plus two more additional inputs need to be specified based on the drying behavior of RDF which are the normalized moisture content (NMC) and normalized drying rate (NDR). Their corresponding equations are given below,where X, X_e, X_C are the moisture content, equilibrium moisture and critical moisture content respectively. The NMC and NMR values for drying temperature of 110°C is shown in figure 3.10.

$$NMC = \frac{X - X_e}{X_C - X_e} \tag{3.2.9}$$

$$NDR = \frac{Current\ drying\ rate}{Drying\ rate\ in\ first\ period} \tag{3.2.10}$$

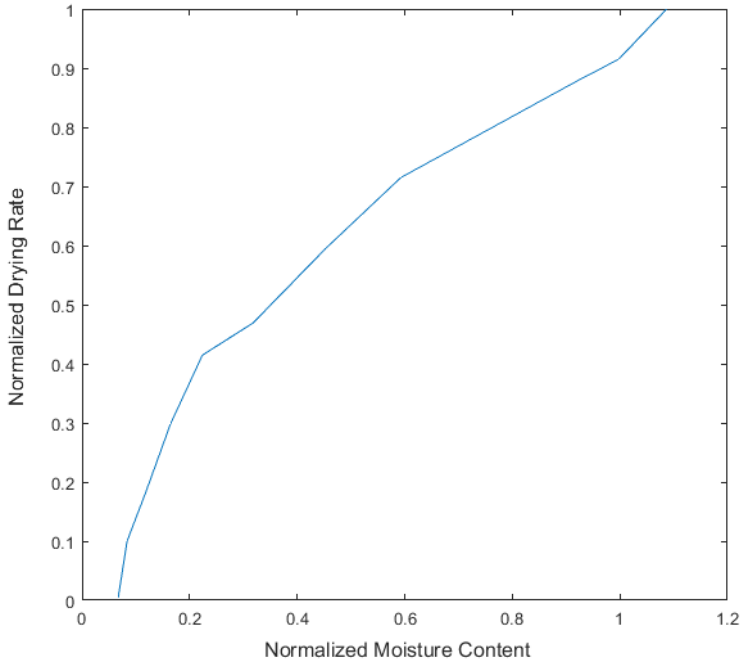

Figure 3.10: Normalized drying rate vs normalized moisture content.

3.2.2 Dryer design

The kinetic analysis of RDF drying is able to provide the essential information in designing the convective dryer.From equation 3.2.8, we are able to determine the necessary residence time of RDF of a particular size needed to to achieve a certain target moisture content, when a desired drying temperature is selected. Based on literature reviewed, the target moisture content required by RDF before its application in energy recovery processes is around 10% (d.b) and the same has been selected within the current work[11].

Energy balance

A schematic representation of the dryer,outlining the material flows is shown in figure 3.11. The RDF to be dried enters dryer at an ambient temperature of 25°C with a moisture content of 45.6% (w.b) as shown in section 2.1. The drying medium (hot air) enters the dryer at a temperature of 110 C, in previous works drying medium temperatures in the rang 110-250 °C were used. However due to the unavailability of drying curves reported in literature to carry out kinetic analysis and since the maximum temperature analysed within the current study is 100 °C, a nominal temperature of 110 °C was selected to avoid large uncertainties in the expected residence times.The mass flow rate of hot air m_{air}(kg/hr), required to achieve the required drying operation is determined through an option within Aspen Plus called design spec. The function of this option is to return the optimum design specification in this case mass of air, by varying it to determine the value at which the required target is achieved. The final moisture content of 10% including a tolerance of 0.1 is the target specified, while the mass of air required is the variable .The specific heat of RDF, c_{pR} (kJ/kg.K) was selected as 1.255 as reported by Asadi[11].

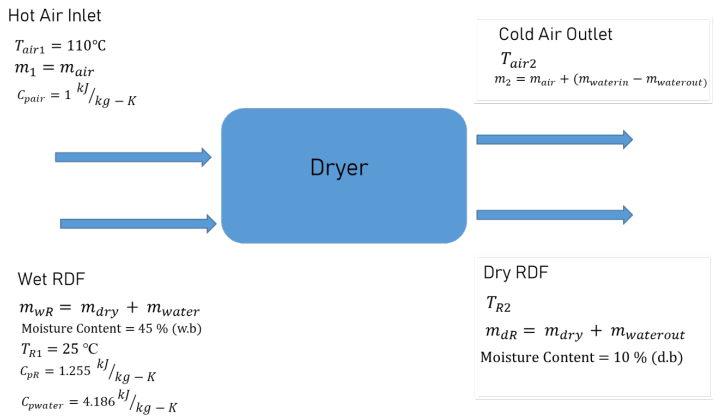

Figure 3.11: Material flow in and out of dryer.

The energy balance with in the dryer is shown by equations 3.1 and 3.2 below.

$$\Delta E_{RDF} = -\Delta E_{Air} \tag{3.2.11}$$

$$\Delta E_{RDF} = (m_{wR} \cdot c_{pR} + m_{waterin} \cdot c_{pwater}) \cdot \Delta T_{RDF} + (m_{waterin - m_{waterout}} \cdot LV) \tag{3.2.12}$$

$$\Delta E_{Air} = \Delta T_{Air} \cdot m_{air} \cdot c_{p,air} \tag{3.2.13}$$

Where E_{RDF} is the energy required by the RDF for the reduction of moisture from 45% (w.b) to 10%(d.b) which is to be supplied by the drying medium in kJ/hr which, E_{Air} is the energy that is carried by the hot air used as the drying medium in kJ/hr, m is the mass flow rate(kg/hr), LV the latent heat of vaporization for water (J/kg), ΔT_{RDF} is the temperature difference between the wet and dry RDF, similarly ΔT_{Air} is the change in temperature between the hot and cold air. The outlet temperatures and the corresponding profiles along the length of the dryer are obtained from Aspen Plus discussed in chapter 4

Dryer sizing

The sizing of the dryer was done on the basis of the design steps provided within Perry's Chemical Engineering Handbook, the main variables affecting the size of the dryer are the material flow and duty[37]. The design equations used to determine the diameter and length of the dryer are given below.

$$Area = \frac{m_{air}}{G} \tag{3.2.14}$$

$$D = \sqrt{\frac{4 \cdot Area}{\pi}} \tag{3.2.15}$$

$$U_a = \frac{k \cdot G^n}{D} \tag{3.2.16}$$

$$N_t = \ln(\frac{T_{a1} - T_w}{T_{a2} - T_w}) \tag{3.2.17}$$

$$\Delta T_{ln} = \frac{(T_{a1} - T_w) - (T_{a2} - Tw)}{\ln(\frac{T_{a1} - T_w}{T_{a2} - T_w})} \tag{3.2.18}$$

$$L = \frac{\Delta E_{RDF}}{A \cdot U_A \cdot \Delta T_{LN}} \tag{3.2.19}$$

Where G is mass velocity of air ($kg/m^2/hr$), U_a is the overall heat transfer co-efficient ($W/m^2.K$), N_t is the number of transfer units, T_W is the wet bulb temperature(K), T_{a1} and T_{a2} are the inlet and outlet temperature

of the hot air respectively, k and n are constants associated with industrially operated dryers specified within Perry's Chemical Engineering Handbook[37] and are taken as to 5.25 and 0.67 respectively.

The Sherwood number was calculated on the basis of the following equations extracted from Manoucherinejad et al [54].

$$Sh = \sqrt{Sh_{laminar}^2 + Sh_{turbulent}^2} \tag{3.2.20}$$

$$Sh_{laminar} = 0.664 \cdot \sqrt{Re} \cdot Sc^{\frac{1}{3}} \tag{3.2.21}$$

$$Sh_{turbulent} = \frac{0.664 \cdot Re^{0.8} \cdot Pr}{1 + 2.433 \cdot Re^{-0.1} \cdot (Pr^{2/3} - 1)} \tag{3.2.22}$$

The Reynolds (Re), Prandtl(Pr) and Schmidt (Sc) numbers are determined from the following equations.

$$Re = \frac{u_G \cdot \rho_g \cdot d_p}{\mu_g} \tag{3.2.23}$$

$$Pr = \frac{\mu_g \cdot c_{pg}}{k_G} \tag{3.2.24}$$

$$Sc = \frac{\mu_g}{\rho_r \cdot D} \tag{3.2.25}$$

where u_G is velocity of gas (m/s), μ_g is the dynamic viscosity of gas (kg/m.s), c_{pG} is specific heat capacity (J/kg.K), k_G is thermal conductivity (W/m.K), ρ_g is density of gas (Kg/m^3) and D is the mass diffusivity (m^2/s). The heat loss along the length of the dryer was estimated by considering the temperature difference between the surrounding air and drying temperature, along with the heat transfer co-efficient of air (W/m^2.K) along the surface are of the dryer (m^2) similar which was done by Manoucherinejad et al [54].

$$h_{conv} = 1.32 \times (\frac{\Delta T}{D})^{0.25} \tag{3.2.26}$$

$$Q_{loss} = h_{conv} \times Area \times \Delta T \tag{3.2.27}$$

The estimated parameters that have been discussed above have been have been implemented into the calculator block in Aspen Plus and can been seen in Appendix A. The results obtained from the simulation of the dryer are discussed in chapter 4. A flowsheet representing the steps involved in simulating of the dryer is shown in the figure 3.12 below.

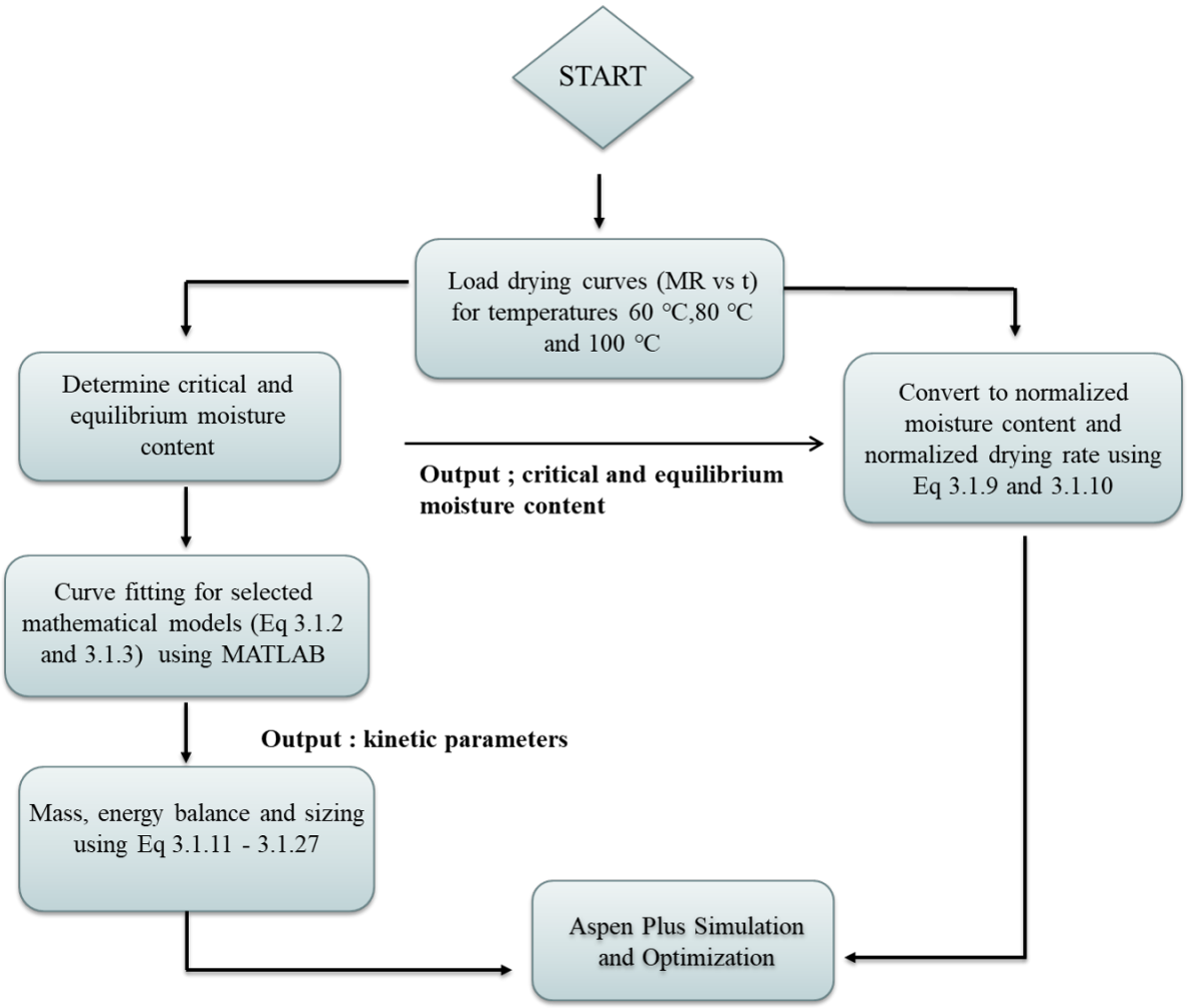

Figure 3.12: Dryer simulation methodology.

3.3 Torrefaction of refuse derived fuel

This section deals with the analysis of torrefaction of refuse derived fuel.Firstly the kinetics of the torrefaction mechanism of refuse derived fuel is determined through the modelling of weight loss from experimental data, then the volatiles that are expected to be evolved are characterised along with development of expressions to view their variation in mass fractions with change in torrefaction temperatures. Based on these information obtained the reactor selected for torrefaction as discussed in section 2.5 is designed and simulated through Aspen Plus.

3.3.1 Weight loss kinetics

In order to visualise the influence of torrefaction parameters on the final yield of RDF, it is essential to understand the kinetic mechanisms involved during process. There are three main models as show in figures 3.13 to 3.15 that are usually used to describe torrefaction namely 1-step mechanism, 2-step mechanism and 3-step mechanism with each increasing in the their degree of complexity.

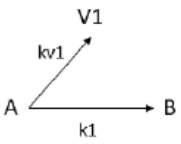

Figure 3.13: 1-step mechanism[3].

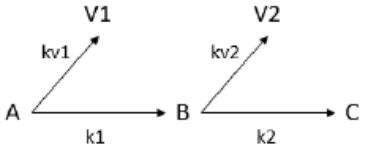

Figure 3.14: 2-step mechanism[3].

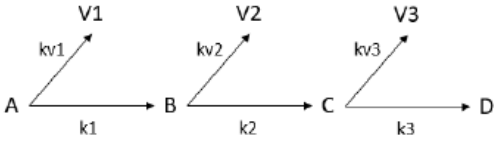

Figure 3.15: 3-step mechanism[3].

Within the 1-step mechanism, the initial solid A gets converted to the torrefied product B, with mass lost as volatiles V_1. It is the same principle within the 2-step mechanism, however the the solid B is an intermediate product which undergoes conversion to final solid C with evolution of volatile V_2. Similarly for the 3-step, with the solid C being the intermediate with evolution of volatiles V_3 and the final solid product being D. Among the various torrefaction modelling studies conducted,the 2-step mechanism which involves first order rate equations developed by Di Blasi et al[17], have been the most widely used, mainly based on the results that they have obtained which shows the short comings of the 1-step model[54][68]. The 3-step mechanism has not been extensively studied due to the complexity and further research into their implementation needs to be done. Considering these factors, the 2-step mechanism has been chosen to model torrefaction kinetics within this study.

The data required to model the kinetics of torrefaction is the weight loss over time for different temperatures carried out through experiments. At this point an assumption had to be made in order to continue the modelling due to kinetic limitations, that is the refuse derived fuel would consists majorly of organic wastes or bio-waste which is a combination of kitchen and garden waste fractions. This assumption had to be made as there is no data available in literature that reports the experimental weight loss data specifically for refuse derived fuel having different material compositions that is being subject to torrefaction and their influences on the final yield. The selected weight loss data for torrefaction temperatures of 250°C, 270 °C and 300°C with residence times up to 30 mins to determine the kinetic parameters is shown in figure 3.16.

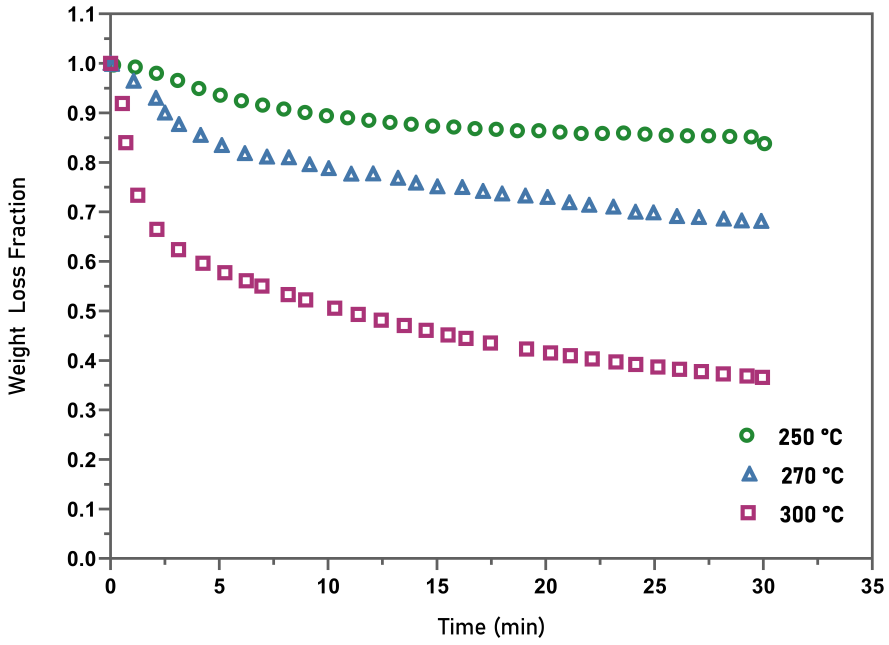

Figure 3.16: Experimental weight loss data bio waste (kitchen and yard waste)[44].

The analytical solution of the two-step mechanism shown in figure 3.15, for the four different components A, B, C, V_1 and V_2 are given below. The detailed solution to the model is show in Appendix B.

$$A = e^{-K_1 \cdot t} \tag{3.3.1}$$

$$B = \frac{k_b}{K_1 - K_2}(e^{-K_2 \cdot t} - e^{-K_2 \cdot t}) \tag{3.3.2}$$

$$C = \frac{k_b \cdot k_c}{(K_1 - K_2) \cdot K_2 \cdot K_1}(K_1 - K_2 - K_1 \cdot e^{-K_1 \cdot t} + K_2 \cdot e^{-K_2 \cdot t}) \tag{3.3.3}$$

$$V_1 = \frac{k_{v1}}{K_1} \cdot (1 - e^{K_1 \cdot t}) \tag{3.3.4}$$

$$V_2 = \frac{k_{v2} - k_b}{K_1 - K_2} \cdot (K_1 - K_2 - K_1 \cdot e^{-K_2 \cdot t} + K_2 \cdot e^{-K_1 \cdot t}) \tag{3.3.5}$$

Where $K_1 = k_b + k_{v1}$ and $K_2 = k_c + k_{v2}$. On combing the individual equations of the solids A, B and C the, the total mass yield (Y_s) can be obtained and is represented by equation 3.3.6. Similarly on combining the equations of V_1 and V_2, the total volatile yield (Y_v) can be obtained and is given by equation 3.3.7

$$Y_s = (1 + [\frac{k_1 \cdot k_2 + k_1 \cdot k_2}{K_1(K_2 - K_2)}] \cdot e^{-K_1 \cdot t} + [\frac{-k_1 \cdot K_2 + k_1 \cdot k_2}{K_2(K_2 - K_1)}] + \frac{k_1 k_2}{K_1 K_2}) \tag{3.3.6}$$

$$Y_v = (\frac{k_1 \cdot k_{v1}}{K_1(K_2 - K_1)} - \frac{k_{v1}}{K_1})e^{-K_1 \cdot t} - \frac{k_1 \cdot k_{v2}}{K_2(K_1 - K_2)} + \frac{k_{v1}}{K_1} + \frac{k_1 \cdot k_{v2}}{K_1 K_2}) \tag{3.3.7}$$

The rate constants k_b, k_c, k_{v1} and k_{v2} are obtained by means of curve fitting to the experimental weight loss data. This is done by the Non-linear Curve Fitting option in MATLAB along with the Niedler-Mead optimization technique to obtain the minimum value and an additional specified constraint. The results of the curve fitting obtained and the algorithm implemented in MATLAB are shown in figures 3.17 and 3.18 respectively.

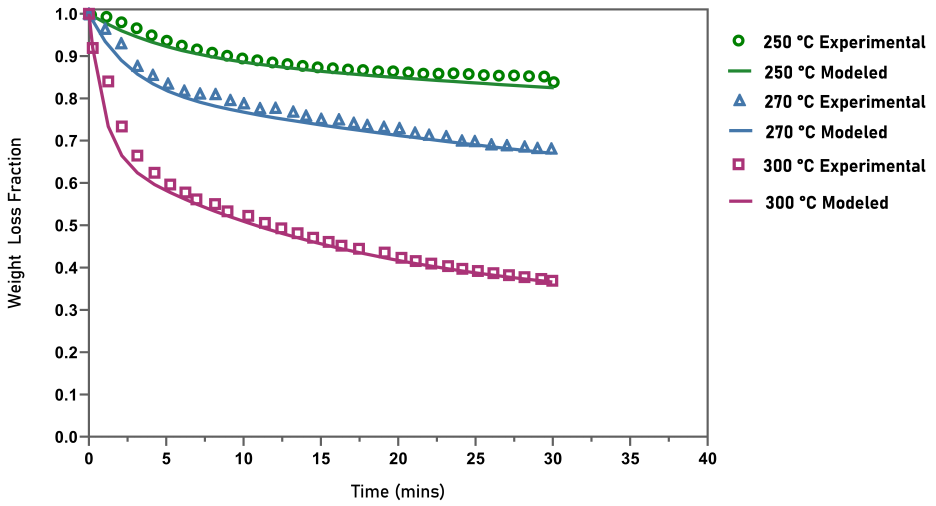

Figure 3.17: Fitted weight loss curves.

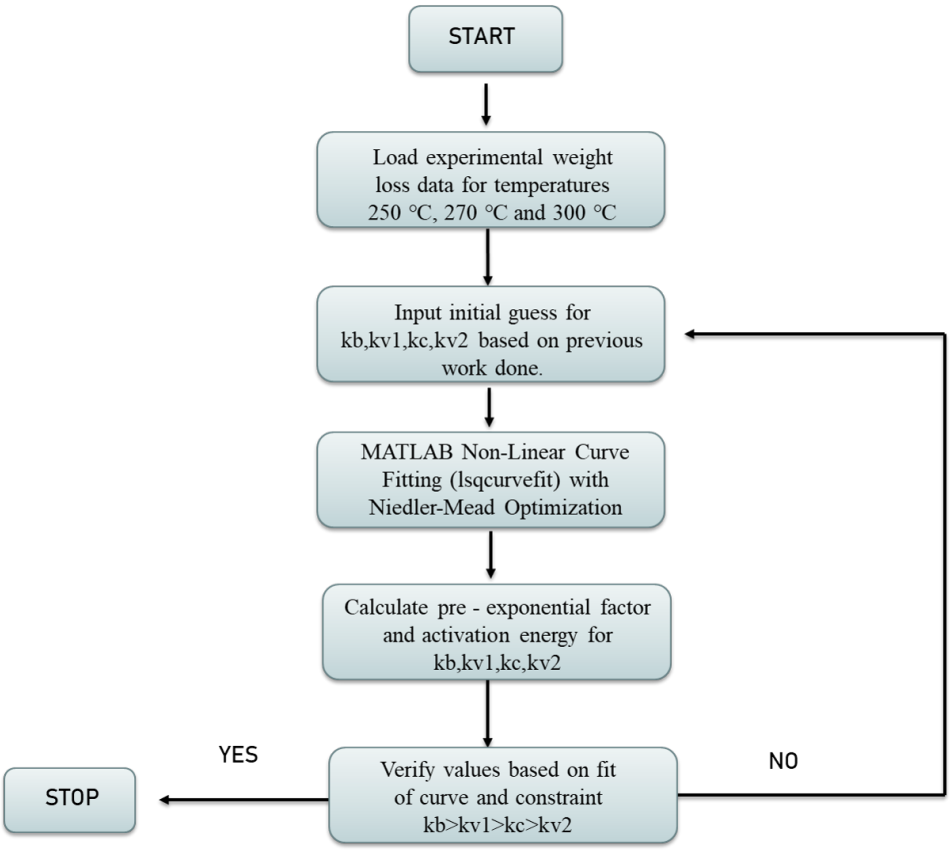

Figure 3.18: Curve fitting algorithm.

Based on the results of the curve fitting carried out, the rate constants determined is shown in table 3.5 and their variation with temperature can be seen in figure 3.19.Equation 3.3.8 represents a first order rate equation which shows the relation between the rate constants and torrefaction temperature.

Table 3.5: Rate equation parameters.

Rate Constant (s^{-1})	Pre-Exponential Factor(s^{-1})	Activation Energy (J/mol)
k_b	3.50×10^{04}	71×10^{03}
kv_1	3.20×10^{10}	14.1×1^{04}
k_c	4.34×10^{03}	7.7×10^{04}
kv_2	3.56×10^{07}	1.20×10^{05}

$$k_i = A.e^{\frac{-E_a}{RT}} \tag{3.3.8}$$

Where k_i (i = b, v1, c, v2) is the rate constant (s^{-1}), A is the pre-exponential factor, E_a is the activation energy (J/mol), R is the universal gas constant and T is temperature in Kelvin. From figure 3.19 we can observe that the rate constants obtained for various temperatures are in line with the findings in Di Blasi et al.[17], where the first step ie, conversion from A to B is much faster than B to C

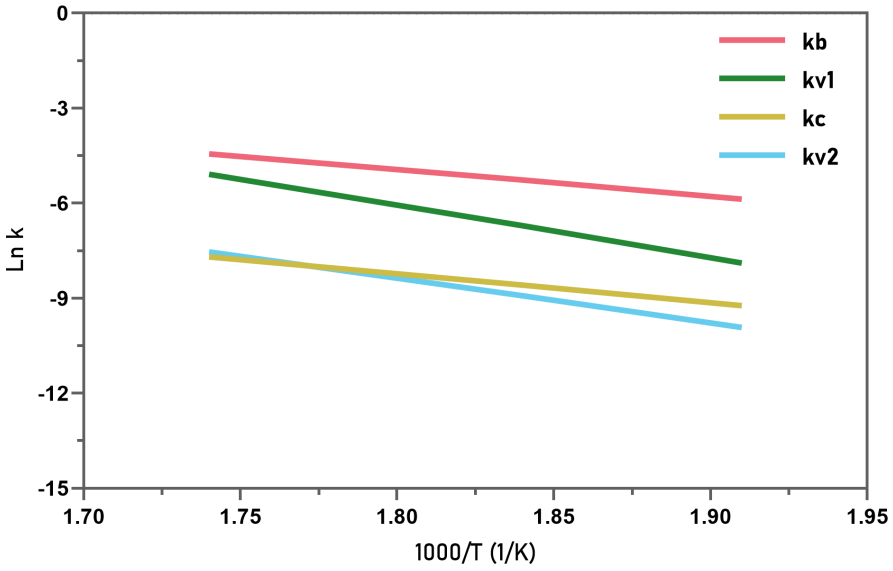

Figure 3.19: Influence of temperature on rate constants.

The determination of the rate constants helps to understand the effect of torrefaction temperature and residence times on the mass and volatile yields expected during the when carrying out the process. On substituting the parameters obtained in table 3.5 into the equations (3.2.4) to (3.2.6) we can obtain the expected yields of the products during torrefaction at the selected temperatures.The mass and volatile yields expected with variation in temperature and residence time of 30 min along with the comparison of the experimental yield of the solid as shown in figures 3.20 and 3.21.

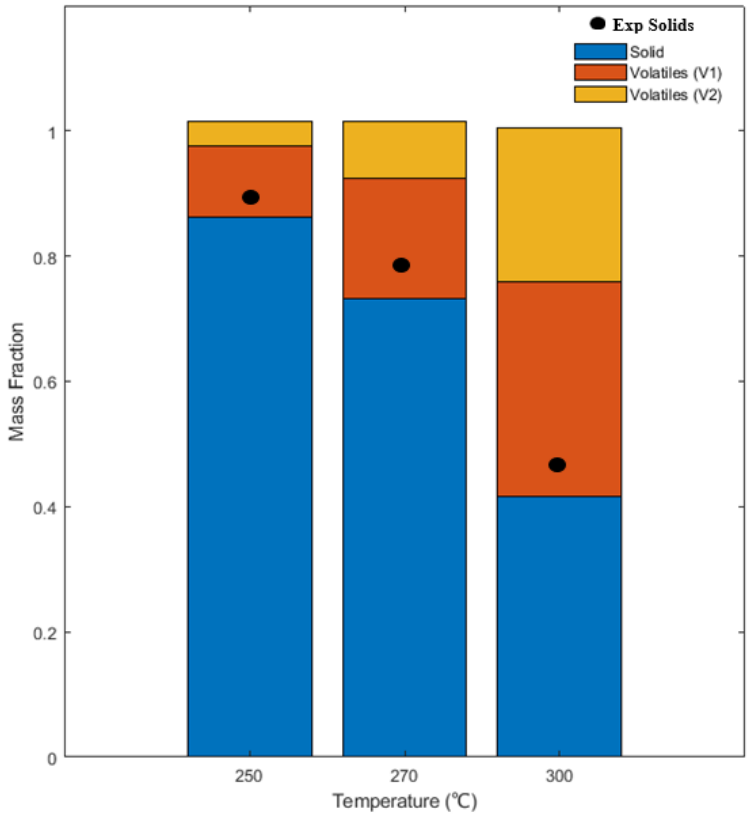

Figure 3.20: Influence of temperature on mass and volatile yields (t = 30 mins).

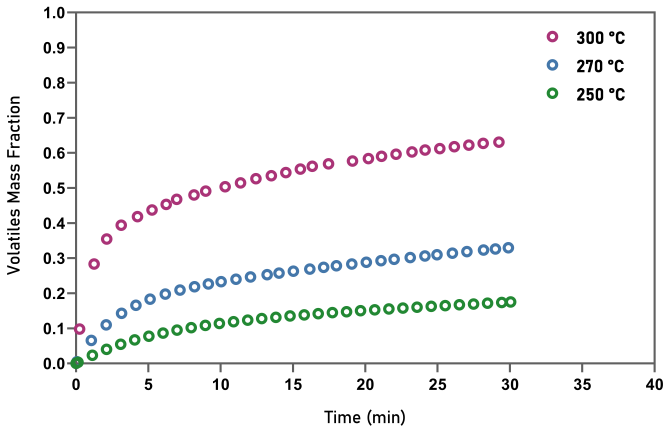

Figure 3.21: Influence of torrefaction temperature and residence time on total volatile yields(V_1+V_2).

From the above figures we can observe that while increasing the temperature of torrefaction and residence there is a decrease in the mas yield of the final production and an increased volatile yield due to the devolatilizaiton of the products.

To determine the energy content within the final product an additonal set of equations relating the instantaneous fractional yields to the variation in elemental compositions needs to be evaluated, this is done on the basis of the work carried out by Bates et al[13]. The instantaneous fractional yields are obtained based on the formation rate of products and decomposition rate of reactant, which are shown by equations 3.3.9 to 3.3.14

$$A \rightarrow \beta B + \vartheta V_1 \tag{3.3.9}$$

$$B \rightarrow \gamma C + \xi V_2 \tag{3.3.10}$$

$$\beta = \frac{k_b}{k_b + k\upsilon_1} \tag{3.3.11}$$

$$\vartheta = \frac{k\upsilon_1}{k_b + k\upsilon_1} \tag{3.3.12}$$

$$\gamma = \frac{kc}{k_c + k\upsilon_2} \tag{3.3.13}$$

$$\xi = \frac{k\upsilon_2}{k_c + k\upsilon_2} \tag{3.3.14}$$

Where the instantaneous fractional yields are given by β, ϑ, γ, ξ.It can be understood that that for each amount of A reacting at any temperature T, β amounts of B and ϑ amount of V_1 are formed, the same can be said for the amount of B reacting to C and V_2. Based on this definition, the sum of β and ϑ and sum of γ,ξ should be equal to 1.
The variation in the elemental composition of the products B and C with respect to the torrefaction temperature can be determined on the basis of equations 3.3.15 and 3.3.16

$$Y_{j,B} = \frac{(Y_{j,A} - \vartheta Y_{j,\upsilon_1})}{\beta} \tag{3.3.15}$$

$$Y_{j,C} = \frac{(Y_{j,B} - \xi Y_{j,\upsilon_2})}{\gamma} \tag{3.3.16}$$

Where $Y_{j,X}$ are the mas fractions of the components A, B, C, V_1 and V_2 composed of elements (j = C,H,O,N,Ash).

Apart from these parameters, the evaluation of the torrefaction process depends three additonal variables which are the mass yield and energy yield and efficiency shown in equations 3.3.17 and 3.3.18

$$Mass\,Yield = (\frac{m_{torr}}{m_{raw}}) \tag{3.3.17}$$

$$Energy\,Yield = Mass\,Yield \times (\frac{HHV_{torr}}{HHV_{raw}}) \tag{3.3.18}$$

As the aim of the current work is the production of torrefied RDF pellets, it is necessary to maximise your solid product or mass yield.From figures 3.20 and 3.21, we can observe that while moving towards higher torrefaction temperature and residence time, the mass of the final product decreases with more volatiles formation which is undesirable. Hence the torrefaction temperature of 250 °C and residence time of 30 min has been selected within the current work for obtaining the optimum amount torrefied RDF. The procedure for determining the HHV of the final torrefied product and results obtained from the simulation of the torrefaction process through Aspen plus is discussed in chapter 4.

3.3.2 Volatile modelling

As mentioned in the previous section,in order to understand the effects of torrefaction on the elemental composition changes of the products we need to obtain the instantaneous fraction yields. The fractional yields of the volatiles $V_1(\vartheta)$ and $V_2(\xi)$ are dependent on the actual gaseous species that are present within them having compositions C_x, H_x and O_x. It is then necessary to characterise the gaseous species present and to determine their variation with respect to the torrefaction temperature.

There are a total of nine gaseous compounds that are significant and present in quantifiable amounts, they are reported within the works of Bates et al.[13] and Tumuluru et al.[84],and are show in the table 3.6. As there is a gap in literature with regards to the characterisation of volatiles released during the torrefaction of RDF, the selected compounds are for the case of biomass.However this assumption can be considered valid to an extent, since the RDF as mentioned previously is considered to similar to biomass.

Table 3.6: Volatile species evolved during torrefaction of RDF.

Volatile Components	Chemical Formula
Carbon dioxide	CO_2
Carbon monoxide	CO
Methane	CH_4
Ethylene	C_2H_4 CH_4
Formaldehyde	CH_2O
Formic acid	CH_2O_2
Furfural	$C_5H_4O_2$
Methanol	CH_3OH
Acetic acid	CH_3COOH
Water	H_2O

The determination of the coefficients of these species present within the volatile streams V_1 and V_2 are carried by the formulation of an inverse problem show in equation 3.3.19.

$$\begin{bmatrix} Y_{V1}^{1} & Y_{V2}^{1} \\ Y_{V1}^{2} & Y_{V2}^{2} \\ Y_{V1}^{3} & Y_{V2}^{3} \end{bmatrix} \begin{bmatrix} Y_{a,V1} & Y_{b,V1} & \cdots\cdots & Y_{i,V1} \\ Y_{b,V2} & Y_{b,V2} & \cdots\cdots & Y_{i,V2} \end{bmatrix} = \begin{bmatrix} Y_{a}^{1} & Y_{b}^{1} & \cdot & \cdot & \cdot & Y_{i}^{1} \\ Y_{a}^{2} & Y_{b}^{2} & \cdot & \cdot & \cdot & Y_{i}^{2} \\ Y_{a}^{3} & Y_{b}^{3} & \cdot & \cdot & \cdot & Y_{i}^{3} \end{bmatrix} \tag{3.3.19}$$

Y_x^n in the above problem definition is the measured total yield of volatiles(x = a,b,c) expressed as mass fraction of the initial solid, from experiments (n = 1,2,3) of torrefaction temperatures 250°C , 270°C and 300°C. The calculated volatile yields based on the rate constants obtained is expressed as, Y_{VN}^n, where VN = V1,V2 and n = 1, 2, 3 denoting the torrefaction temperatures.

The above problem is solved through the function Liner Least Squares fitting in MATLAB environment subject to four additional constraints as shown below,to ensure consistent values are obtained.

$$Y_{V1}^{n} * Y_{x,V1} + Y_{V2}^{n} * Y_{x,V2} = Y_{x}^{n} \tag{3.3.20}$$

$$\sum_{a}^{i} Y_{x,V1} = 1 \tag{3.3.21}$$

$$\sum_{a}^{i} Y_{x,V2} = 1 \tag{3.3.22}$$

$$Y_{x,V1}, Y_{x,V2} \geq 0 \tag{3.3.23}$$

The variation in the concentration of gaseous species present in V_1 and V_2 with respect to temperatures is shown in figures 3.22 and 3.23. General linear equations dependent on the torrefaction temperatures were subsequently developed as reported in table 3.7. Due to the lack of data for the evolution of volatiles with residence times in literature, the modelling is carried for a residence time 30 min for the three selected torrefaction temperatures(250 °C, 270 °C and 300 °C).

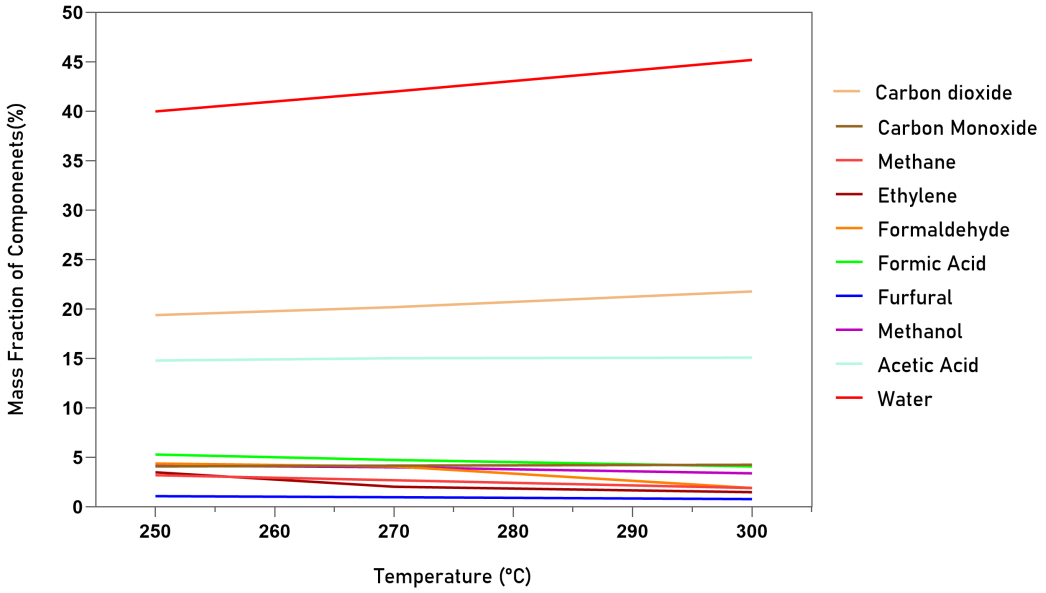

Figure 3.22: Influence of torrefaction temperature on mass fraction of gaseous species in V1 (t = 30 min).

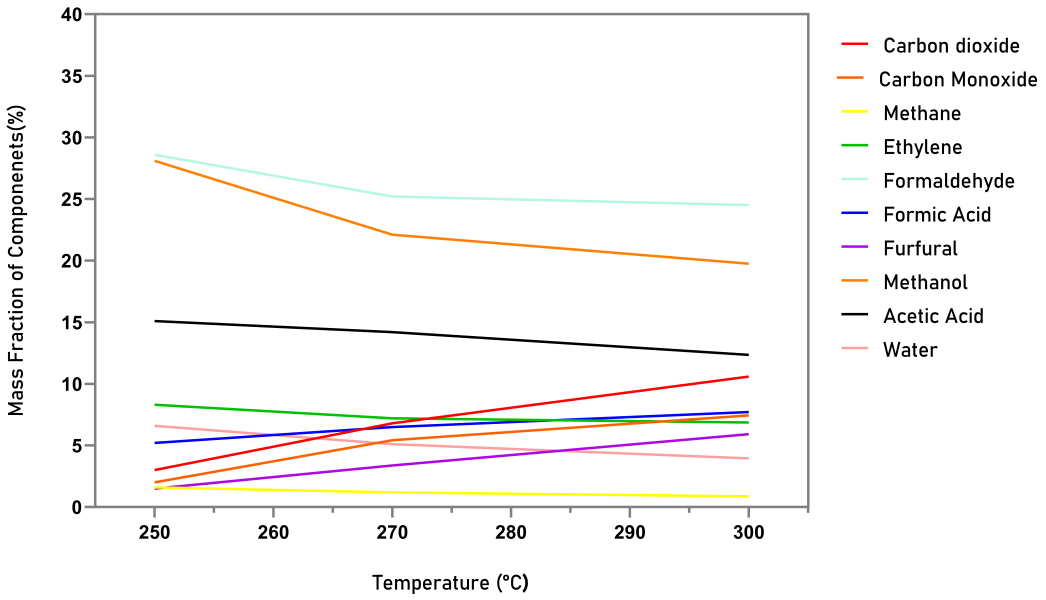

Figure 3.23: Influence of torrefaction temperature on mass fraction of gaseous species in V2 (t = 30 min).

Table 3.7: General equations for volatiles concentration variation with torrefaction temperature (T, °C).

Volatiles	V1	V2
Carbon dioxide	0.0482T - 5.987	0.1498T - 75.04
Carbon monoxide	0.00368T + 2.434	0.1057T - 52.81
Methane	-0.025618T + 16.59	-0.01432T + 9.045
Ethylene	-0.03829T + 23.27	-0.02721T + 22.2
Formaldehyde	-0.05163T + 31.68	-0.05163T + 31.68
Formic Acid	-0.02382T + 17.73	-0.04963T - 20.64
Methanol	-0.01637T + 12.82	-0.1589T + 110.6
Acetic Acid	0.0005711T + 11.86	-0.05553T + 44.22
Furfural	-0.006T + 4.238	-0.08811T - 44.53
Water	0.1402T - 142.53	-0.05184T + 33.54

From the weight loss and volatiles modelling, it was possible to determine the optimum torrefaction temperature and residence time. On the basis of the extracted data, the design of the torrefaction reactor was done, which shall be discussed in the following section.

3.3.3 Reactor design

In order to adequately carry out the simulation in Aspen Plus, certain parameters such as the length of the reactor and heat-transfer coefficients needs to be specified along with the kinetics which was previously discussed. The reactor selected to carry out torrefaction of RDF, is the indirectly heated rotary drum reactor. The decision criteria for choosing this particular system and its operational description has been detailed in section 2.5. Figure 3.24 shows the elements that are integrated to obtain an optimum design of the indirectly heated rotary drum dryer. The mass transport mechanism was not considered within the model as only the kinetics and heat transfer are the main inputs required by Aspen Plus.

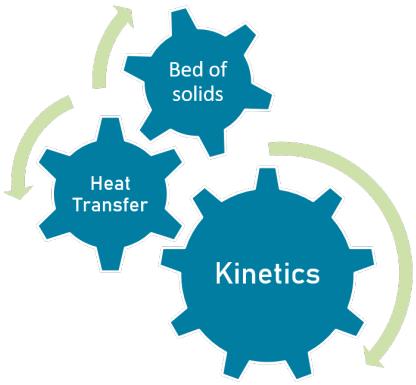

Figure 3.24: Design elements of reactor

Bed of solids

In order to determine the length of the reactor needed, it is first essential to understand the behaviour or motion of the solids within the rotating drum. The representation of the different motions encountered is shown in figure 3.25. The slipping and centrifuging motion are not used within the industry and cataracting occurs when dealing with ball milling. Only slumping, rolling and cascading motion are relevant in the case of rotary reactors and mixing equipment[52]. A brief description of these is given below.

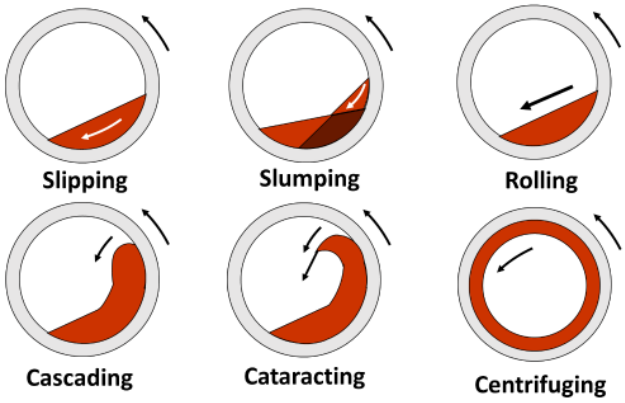

Figure 3.25: Motion of solids within the drum[52]

Slumping behaviour occurs when the rotational speed of the reactor is low and there is relatively less motion with solids. The angle of inclination of the rises until it reaches a constant static angle of repose, after which the solids detach and fall from the walls.

Rolling is characterised by the continuous movement of the solids layer, where the solids that are fed move up to the surface assisted by the rotation of the cylinder. It has a slightly higher rotational speed than slumping.

Cascading occurs by increasing the rotational speed from a rolling regime. Within this motion, the solids are dragged by the wall to higher height than in the case of the previously described motions.During this motion, bed of solids do not have a defined shape.

Each of the above described motions are characterised by various parameters such as the the filling degree (f) which is defined as the fraction of cross-sectional area of bed filled with solids[18] and Froude number (Fr) given by equation 3.3.24 represents the balance between the centrifugal, inertial and gravitation force and is used to determine the radius of rotary drum. The different conditions under which the above motion occurs is illustrated by the figure 3.26.

$$Fr = \frac{\omega^2 \cdot R}{g} \tag{3.3.24}$$

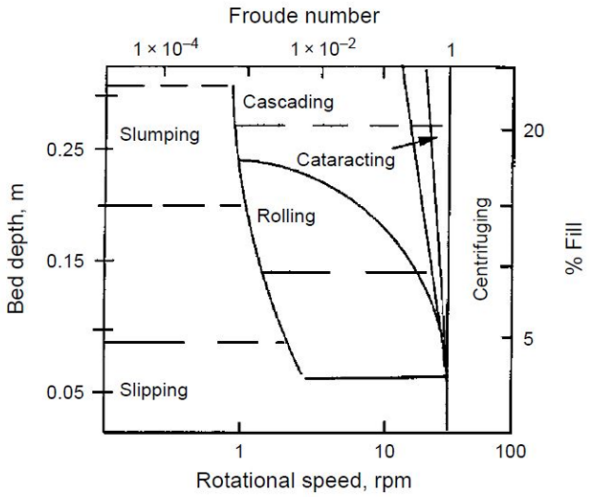

Figure 3.26: Operational parameters for different solids motion[18]

Out of the described solids motion, the rolling motion is the most commonly within the industry as it offers a good balance between mixing and maintaining the bulk properties of the solid [52][18]. In order to determine the radius of the drum the main operational parameters that needed to be considered are the Froude number and the RPM. From figure 3.26, a constant Froude number of 10^{-03} was selected since it is the logarithmic mid point between the corresponding upper and lower limits of 10^{-02} and 10^{-04} respectively for rolling motion, within the given range a RPM of 3 was taken. Theses values were substituted to the equation 3.3.24 to obtain the radius of the drum as 4 m.

The next step was to determine the length of the rector, this was done on the basis of the Saeman's model given by equations 3.3.25 and 3.3.30, which calculates the length of the rotating drum by into account the filling degree or fill % and the bed depth (H) based on the selected motion of solids within the rotating drum. As the specified motion is rolling, it can bee seen from 3.26 that fill% should be in the range of 10-15%. The corresponding variation in the bed depth can be calculated based on the equation 3.3.27 developed by Lopez[52] which relates the fill% and radius of the drum to the bed depth.

$$\frac{dH}{dz} = -\frac{3\tan\Theta}{4\pi n}\frac{m_s}{\rho_s}[R^2-(R^2-H)^2]^{-3/2} + \frac{\tan\beta}{\cos\Theta} \tag{3.3.25}$$

$$\int_0^L dz = \int_{Hi}^{Hf} \frac{dH}{-\frac{3\tan\Theta}{4\pi n}\frac{m_s}{\rho_s}[R^2-(R^2-H)^2]^{-3/2} + \frac{\tan\beta}{\cos\Theta}} \tag{3.3.26}$$

$$\frac{H}{R} = 1.698\cdot f + 0.151 \tag{3.3.27}$$

where θ is the dynamic angle of repose, β is the inclination angle of the cylindrical drum, n is the rotational speed (rad/s), R is radius of drum (m), ms is mass flow rate of solids (kg/s) and H is the bed depth.

The above integration was carried out by the Simpson's integration rule in MATLAB and the length was determined to be 12 m, which was in accordance with values reported in literature where the standard sizes of the rotary drum reactors were 2-4 m diameter and 12-15 m length[52][54].

Heat-transfer coefficients

As mentioned previously Aspen Plus requires the heat transfer coefficients as inputs in order to simulate the reactor. The two main modes of heat transfer are conduction and convection. The covered wall transfers heat to the solid bed through conduction and the governing equation as reported by Li et al[50] is shown below.

$$h_{ws}^{cd} = \frac{1}{(\chi l_p/k_g) + (2\sqrt{2k_b\rho_b c_{pb} n\phi_0}^{-1})} \tag{3.3.28}$$

Where l_p is length of the particles (m),χ is the gas film thickness(mm), k_g is thermal conductivity of the gas film (W/m.K) , k_b thermal conductivity of bed (W/m.K), n is rotational speed and ϕ is half central angle of sectional solid bed .
The convective heat transfer in rotary reactors occurs between the heating gas and wall ($h_{gw}{}^{c}$) and solid bed ($h_{gs}{}^{gw}$). The equations for these parameters were obtained from Tscheng and Watkinson[83] and are shown below.

$$h_{gw}^{c} D_e/k_g = 1.54 Re_g^{0.575} Re_w^{-0.292} \tag{3.3.29}$$

$$h_{gs}^{c} D_e/k_g = 0.46 Re_g^{0.535} Re^{0.104}\eta^{-0.341} \tag{3.3.30}$$

Where R_{eg} and R_{ew} are the flow and rotational Reynolds numbers, η is the fill percentage and D_e is the equivalent diameter.

The above equations are then implemented into Aspen Plus through the calculator block in order to simulate the torrefaction of refuse derived fuel.

3.4 Grinding and pelletization

After the torrefaction process, the torrefied RDF exiting the reactor is cooled to room temperature. The material is then subject to a grinding and pelletization (densification) process in order to improve its physical properties for transport and storage. The modelling of these two process was done solely to determine their energy consumption and it was assumed that there was no mass loss during these processes. For the simulation of the grinding unit in Aspen plus, a parameter knows as the Hardgrove Grindability Index (HGI) needs to specified for the char that is obtained from each of the three torrefaction temperatures. These values were not available in literature specifically for RDF, hence the HGI that was experimentally determined and modelled by Manouchehrinejad et al[54] after the torrefaction of biomass was extended to the current case and their variation with torrefaction temperature is shown in figure 3.27. The same assumption was extended to the energy required for pellitization which was determined by Järvinen et al.[45] and was found to be in the range of 70-80 kW/ton of feed.

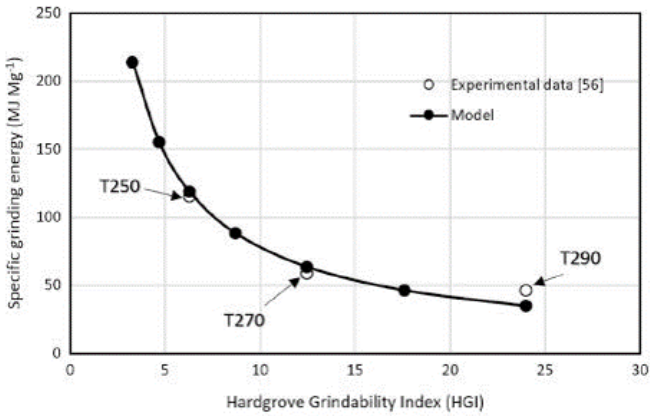

Figure 3.27: Hardgrove Grindability Index for the torrefied biomass at different temperatures[54]

3.5 Aspen Plus simulation model

Figure 3.28 shows the main flowsheet for the base processing capacity of 100 ton/day raw RDF torrefaction and pelletization plant that was developed in Aspen Plus simulation platform. The main unit operations as discussed above were drying, torrefaction, grinding and pelletization. The assumptions that were made to carry out the simulations are as follows:

- RDF needs to be specified as non-conventional solid with its ultimate and proximate analysis data as shown in table 2.2. The properly methods of HCOALGEN and DCOALIGT which was used for coal were selected for the enthalpy and density calculations of the RDF material.
- The stream class distribution selected was MCINCPSD.
- The Peng-Robinson equation with Boston-Mathias modifications (PR-BM) property model was selected for the properties estimation of convectional components (liquids and gases).
- The systems were all considered to be operating at atmospheric pressure.

3.5.1 Dryer

As discussed in previous sections, the dryer selected was a single-pass directly heated rotary dryer. For this, the pre-set convective dryer model was selected within Aspen plus. The assumptions that were made are :

- Uniform moisture content and temperature was considered for the RDF particles.
- The behaviour of solid and gas within dryer was considered as plug flow.

- The specific drying kinetics and heat and mass transfer were considered.
- No mechanical aspects such as rotational speed was included within the calculations of the model.

The moisture rich raw RDF (W-RDF) and the hot air (AIRDRY) is sent into the dryer in co-current operation. The the hot air is heated from ambient conditions to the required drying temperature through the flue gases from the torrefaction reactor. The flow rate of the hot air is adjusted using the design specification block to obtain the outlet moisture of RDF to 10% (d.b). The main inputs to the dryer model are summarised in table 3.8, the FORTRAN code implemented can be seen in Appendix A. The main outputs from the dryer model were the dryer profiles, residence time and dryer duty which is discussed in chapter 4.

Table 3.8: Main inputs for convective dryer block.

Parameter	Unit	Value
Feed (wet RDF)	ton/day	100
Inlet Moisture	w.b%	45.8
Outlet/Target Moisture	d.b%	10
Particle Size	mm	15
Diameter	m	3.2
Length	m	12
Fill grade	%	0.4
Porosity	-	0.4
NTU	-	2.5
Air inlet temperature	°C	110

3.5.2 Torrefaction

The torrefaction process based on the kinetics discussed in the above section has been implemented in Aspen Plus. The main assumptions that were considered are as follows :

- The indirectly heated co-current rotary reactor was selected and simulated through a series of RStoic and RPlug reactors.
- No radial dispersion along the reactor.
- Reactions were considered only with in the solid bed.
- The mechanical motions were only considered for the calculation of the length and does not effect the reactions taking place.
- The heat transfer through radiation was considered to be negligible due to the operating temperature ranges (200-300 °C).
- Mass transport mechanisms were not considered within the current model.

The RPlugs(TORPLUG1 and TORPLUG2) were chosen as it considers the dimensions of the reactor such as radius and length along with the heat transfer coefficients. As the kinetics discussed above are for dry RDF it necessary to vaporize the remaining moisture,therefore the RStoic reactor (TORV) was used. The moisture present was converted to waster and this mixture of RDF and moisture serves as inputs to the RPlugs.However, on carrying out various trial simulations it was found that a single RPlug reactor did not produce satisfactory results and failed to converge. The reason behind it could be attributed to the fact that the RPlugs in Aspen Plus were originally made for liquid and vapour phases and have low flexibility with regards to dealing with solids. The solution for obtaining the desired results was found by splitting the length of the rotary reactor by half with each half representing a RPlug reactor. Hence two RPLugs in series were used to represent the rotary reactor. The heating gas temperature was adjusted to 350°C in order obtain the desired torrefaction temperature. The volatiles evolved during torrefaction, exit the reactor and is combusted to serve as provide heating medium for the air entering dryer and heating gas entering the RPlugs. The main inputs to the torrefaction reactor are show in table 3.9 and the equations 3.3.9 and 3.3.10 with the rate constants shown in table 3.5 were included as reaction sets within the model. The results of torrefaction are discussed in chapter 4.

Table 3.9: Main inputs to RPlug reactors.

Parameter	Unit	Value
Diameter	m	4
Length	m	12
Heat transfer coefficient (conduction)	$W/m^2.K$	53.37
Heat transfer coefficient (convection)	$W/m^2.K$	12.55

3.5.3 Grinding and pellitization

The solids exiting the torrefaction reactor are cooled to room temperature and undergoes grinding and pelletiziation process. As mentioned within section 3.4 these unit operations were simulated for determining their energy consumption and no mass loss was assumed. The HG index was used as the input to the grinding model depending on the torrefaction temperature as show in figure 3.27.

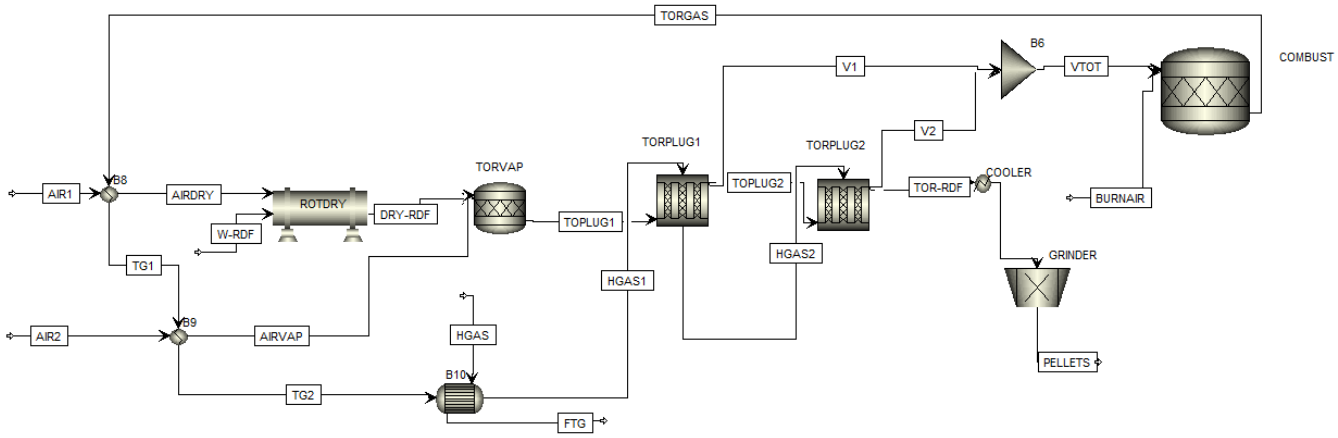

Figure 3.28: Aspen Plus simulation flowsheet.

3.6 Economic Evaluation

In order to determine the feasibility of the torrefaction project, an economic analysis needs to be done by evaluating the capital expenditures (CAPEX) and operational expenditures (OPEX) associated with the process.Based on these two cost considerations, the profitability of the project is then determined by certain economic indicators such as net present value (NPV) and payback period (PBP). The overall methodology of the economic evaluation is shown in figure 3.29.

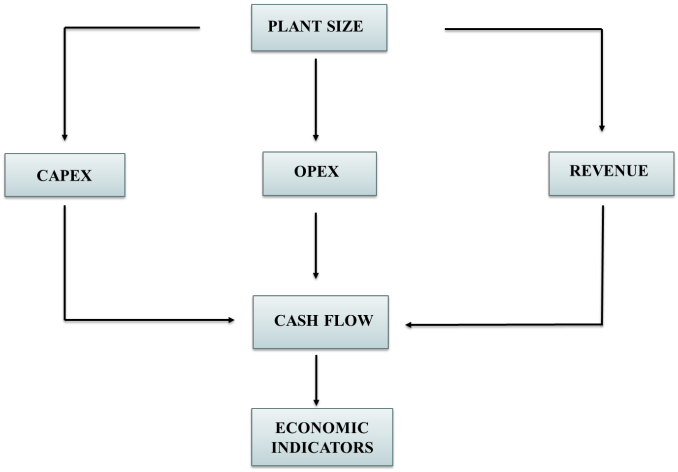

Figure 3.29: Economic evaluation methodology.

3.6.1 Capital expenditure (CAPEX)

The CAPEX of any process plant in general is determined on the basis of the total costs of the purchased equipment.The split up of the CAPEX is show in the figure 3.30 below.

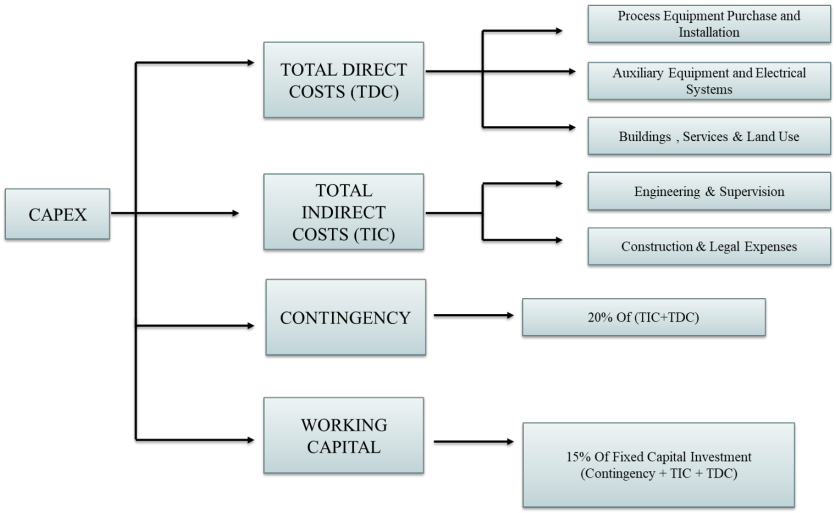

Figure 3.30: Costs considered within CAPEX.

Aspen plus was used to obtained the prices of general equipment such as heat exchangers,coolers and separators. The more process specific equipment like rotary dryer, reactor, grinder and pelletizer were calculated on the basis of the scale-up formula given by equation3.6.1 shown below, which was provided within the book for Plant Design and Economics by Timmerhaus and Peters[66].

$$Price\,2 = Price\,1\left(\frac{Size\,2}{Size\,1}\right)^{m} \tag{3.6.1}$$

Where Price 1, Size 1 an are the cost and capacity of the equipment for which the data was known, while Size 2 is the capacity of equipment that is currently being used for which the price (Price 2) needs to be obtained, m is a scale factor which is dependent on the process equipment, the scale factors of the different equipment is show in table 3.10.

Table 3.10: Scale factor for process equipment from ref [66].

Equipment	Scale Factor
Dryer	0.4
Reactors (stainless steel)	0.6
Grinder	0.4
Pelletizer	0.4

To adjust the prices obtained for the current year in which the project is being carried a price index needs to applied. Common chemical engineering price index are the Marshall&Swift index and Nelson Farrer Index. In this study the MarshalSwift Index for the year 2021 was used which is 2171.6[23]. The price of the equipment was subsequently adjusted based on the equation 3.6.2 given below.

$$Price\,2 = Price\,1 \cdot \left(\frac{Index\,2}{Index\,1}\right) \tag{3.6.2}$$

As mentioned previously the total CAPEX, was determined on the basis of the purchased equipment costs. The table 3.11 below shows the different costs as percentages of the total purchased equipment costs.The values provided were taken from Timmerhaus and Peters[66].

Table 3.11: CAPEX cost percentages[66].

Parameter	%
Equipment costs	Total purchased equipment cost (TPEC)
Purchased equipment installation cost	39%
Instrumentation and controls	28%
Piping	10%
Electrical systems	8%
Buildings (including services)	5%
Yard improvements	3%
Service facilities	4%
Land use	3%
Total indirect cost	25% of Total direct costs

3.6.2 Operational expenditure (OPEX)

The OPEX of a process plant is estimated by determine the several factors such as,utilities cost (electricity,cooling water etc), maintenance costs and labour costs among other things. An advantage in the case of WtE facilities in the case a torrefaction plant for RDF, the cost of feedstock is not present, alternatively there exists a tipping fee, which is an additional amount or revenue given to the WtE facility by the local government for carrying out the conversion and disposal of waste which otherwise would end up in landfills, they are are usually in the range of 70-90 $/ton of waste given to the WtE facility [87]. The split up of the total OPEX is shown in figure 3.31.

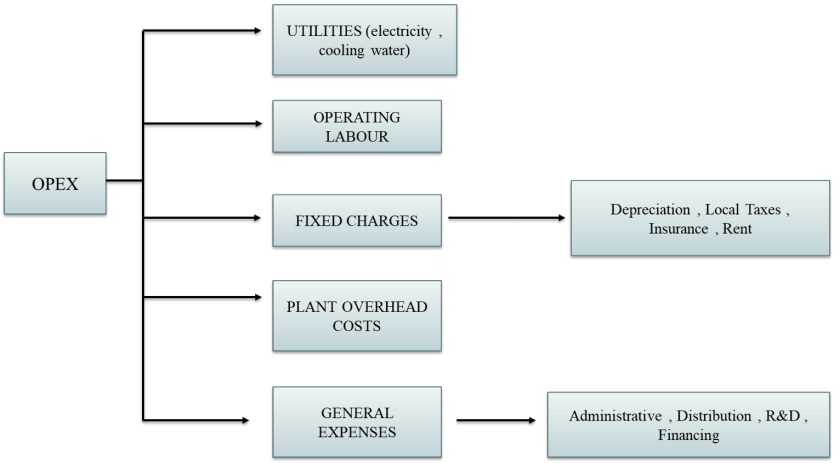

Figure 3.31: Costs considered within OPEX

Utilities

The prices of electricity and cooling water, identified as the utilities within the plant is shown in table 3.12 below. Electricity is used for all the process systems with in the plant and cooling water for the to cool down the torrefied RDF pellets.

Table 3.12: Utility prices.

Utility	Price	Unit	Source
Electricity	10.48	$ cent/kWh	[8]
Cooling water	0.0078	$/m^3	Aspen Plus

Operating labour

The total cost of operating labour was determined on the basis of personnel needed withing the plant and a round figure of the salaries they command. The work force needed was taken from a case study that was done by Bergman et al.[15] for a torrefaction plant and the salaries were adjusted based on the Labour Index of the year 2021. This procedure was similar to the one explained by Bergman et al[15]. The operating labour and the expected salaries are shown in table 3.13 below.

Table 3.13: Cost associated with OPEX[66].

Operating labor	Positions	Annual salary ($/yr)
Plant manager	1	468060
Plant engineer	1	222720
Maintenance supervisor	1	181540
Lab manager	1	178350
Shift supervisor	5	764150
Lab technician	3	381930
Maintenance technician	12	1527720
Shift operators	20	3056600
Yard employees	8	712240
Clerk and secretaries	3	343650

The remaining operating costs incurred are taken as percentages of the fixed capital investment (FCI), operating labour and total capital investment (TCI). The split of the remaining costs are shown in table 3.14.

Table 3.14: Costs associated with OPEX

Parameter	Value
Direct supervisory and clerical labour	10% of Operating labour
Laboratory charges	10% of Operating labour
Local Taxes	3% of Fixed capital investment (FCI)
Plant overhead costs	30% of Operating labour
Administrative costs	10% of Operating labour
Financing	5% of Total capital investment (TCI)

3.6.3 Economic Indicators

Economic indicators are used to determine the feasibility or profitability of the project. The commonly used indicators are net present value (NPV) and payback period (PBP). A brief description of these two methods are provided below.

Net present value (NPV)

The net present value is calculated on the basis of equation 3.6.3 shown below. It is used to evaluate the profitability of an investment or project. An NPV that is positive or equal to zero implies the project is attractive to the investors.The minimum selling price of your product can be determined through the NPV, at the point NPV is equal to zero.

$$NPV = \sum_{t}^{lifetime} \frac{Cash\,flow}{(1+r)^t} - CAPEX \tag{3.6.3}$$

Where, t is the plant life set to 15 years, r is the internal rate of return (IRR) selected as 12%, cash flow is the difference in revenue obtained through product sales (RDF pellets) and tipping fee and OPEX. A straight line depreciation was considered on the cash flow with a salvage value of 10% on the equipment at the end of their life.

Payback Period (PBP)

The payback period is interpreted as the time period (years) within which the total capital investment or CAPEX can be recovered or in other words it is the time required to break even. It is estimated on the basis of equation 3.6.4 given below. A small payback period is desirable for a new project.

$$PBP = \frac{CAPEX}{Annual\,Cash\,flow} \tag{3.6.4}$$

Chapter 4

Results and Discussion

This chapter presents the results of the modelling and simulation carried out in Aspen Plus for the base processing capacity of 100 ton/day raw RDF torrefaction, based on the methodology discussed in chapter 3. Firstly the results obtained from the simulation of the dryer is presented along with with temperature and moisture profiles. Secondly, the results from the torrefaction simulation is shown based on which the optimum process conditions were analysed and selected, along with a heat integration model. Thirdly, based on the selected operating conditions an economic evaluation was carried out for the base capacity plant as well as two more additional processing capacities of 50 and 200 ton/day, the results of which are presented below. Finally, the effect of RDF substitution within a typical cement plant is discussed and the savings that can be achieved is also provided.

4.1 Dryer Profiles

The rotary dryer was modelled in Aspen Plus based on the methodology described in section 3.2. Based on the above inputs specified in table 3.8, the dryer was simulated. The main output variables of the model such as the residence time and energy required for the dryer operation are given in the below table 4.1. The variation in moisture content and temperature of the drying medium and solids along the length of were generated in order to determine if the dimensions of the dryer that were specified was able to achieve the target moisture constant of 10% (d.b). These different profiles are shown in figures 4.1 and 4.2 given below.

Table 4.1: Dryer output variables

Parameter	Unit	Value
Mass flow of air required	kg/hr	$5.77x10^{04}$
Residence time	min	18
Duty	kW	1884.28

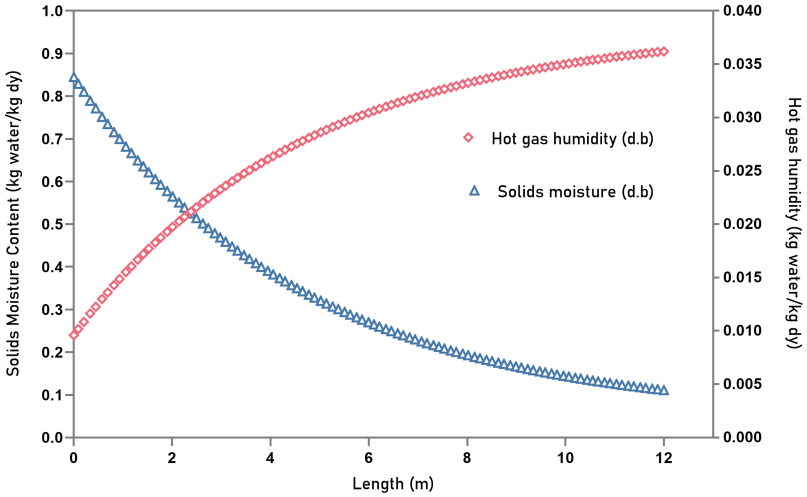

Figure 4.1: Moisture content profile along dryer length

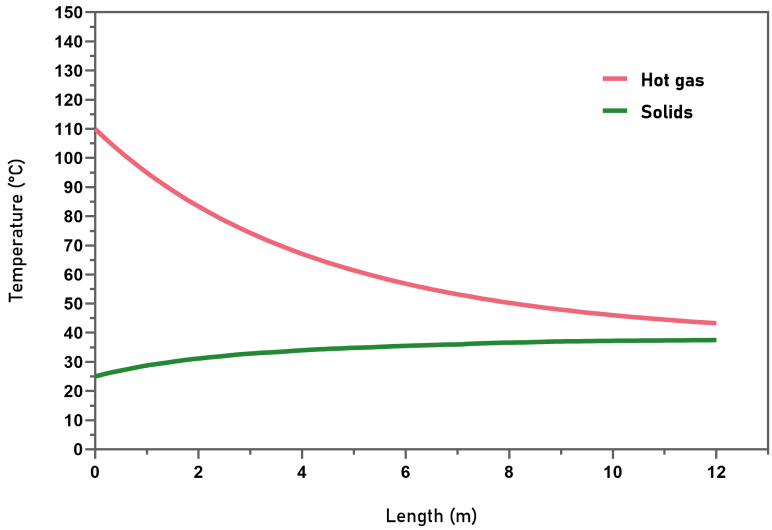

Figure 4.2: Temperature profile along dryer length

As mentioned previously the selection of dryer dimensions was done based on a sensitivity analysis at different,drying temperatures and mass flow rate of hot gas to achieve the the target moisture content of 10% (d.b). However to narrow down the range the temperature of the drying was selected to be 110 °C to avoid variability in experimental data while moving to higher temperatures as mentioned in 3.2 and an additonal constraint that the approach temperature of the outlet gas and dry solids should not exceed a difference of 10 °C. Based on these conditions the optimum dryer dimensions selected were 3x12 m (DxL), the validity of this selection is shown by the above figures. From figure 4.1, we can observe the decrease in the moisture content of the solids (RDF) from 81.1% (d.b) to the target MC of 10% and an increase in the temperature solids contrary to the decrease in temperature of the hot gas within the selected dryer length as seen from figure 4.2. The solids and gas stream exit the dryer at 35 °C and 48 °C respectively. The duty of the dryer was estimated to be 1884 kW of evaporated water, the residence time within the dryer was around 18 min which was determined on the basis of the mathematical model which is in the range reported in literature[54][11].

4.2 Torrefaction

The torrefaction reactor was simulated successfully in Aspen Plus through RStoic and a series of RPlug reactors, representing the rotary drum on the basis of work carried out by Manouchehrinejad et al.[54]. The variation in the mass concentrations of the solid products (A, B and C) with the torrefaction temperature(250°C ,270 °C and 300°C) and residence times are show in figure 4.3 below.

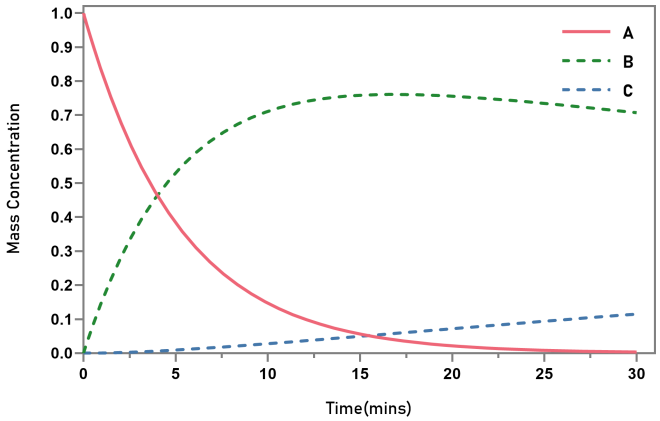

(a)

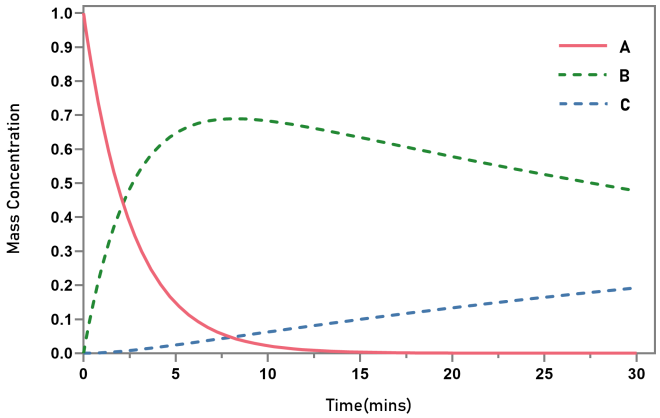

(b)

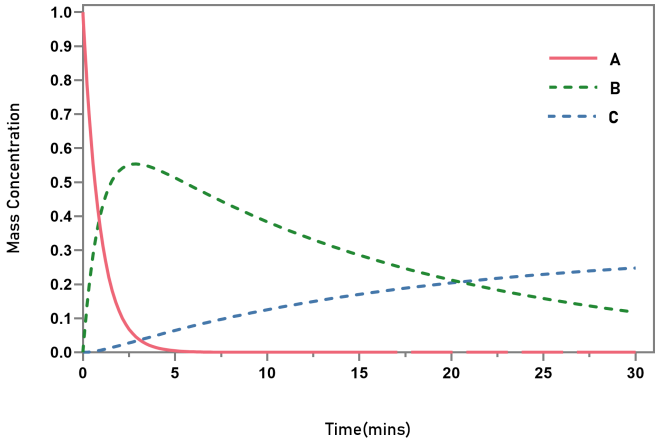

(c)

Figure 4.3: Variation in mass concentration with residence time for temperatures (a) 250°C (b) 270 °C and 300 °(C).

From the above figures, it is clear that while moving towards higher torrefaction temperatures the total mas yield decreases due to increased devolatilization. The total mass yield variation with respect to torrefaction temperatures and a residence time of 30 min is seen in figure 4.4.

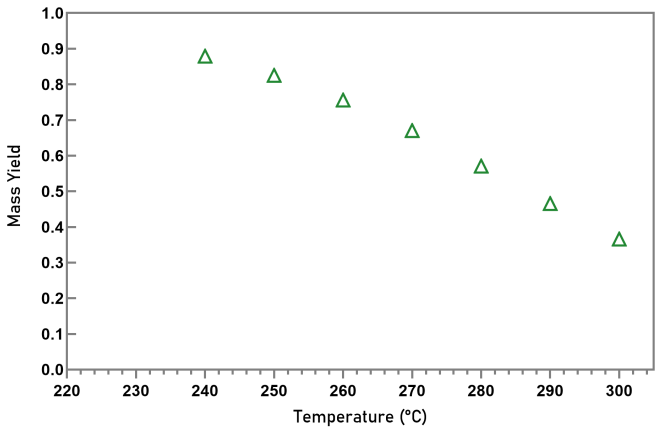

Figure 4.4: Effect of torrefaction temperature on mass yield (t = 30mins).

The calculation of the energy yield is not quite straightforward. In order to determine the HHV of the final torrefied RDF it is necessary to find the variation in the elemental compositions (C,H,O) with degree of torrefaction. This is estimated on the basis of the instantaneous fractional yields of the solids B and C and volatiles V1 and V2, the detailed explanation is provided in section 3.3. The effect of torrefaction temperature on the instantaneous fractional yields of each of the products are shown in figure 4.5 below.

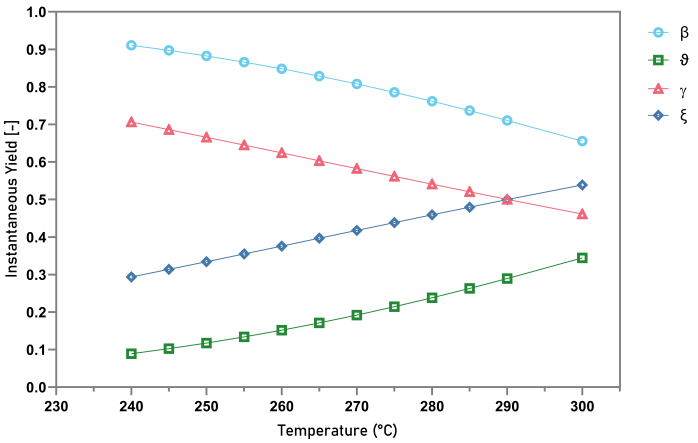

Figure 4.5: Instantaneous product yields of B, C, V1 and V2.

Based on the instantaneous yield it is possible to view the changes in the elemental composition of the products B and C, which is shown by figures 4.6 and 4.7 below. The remaining fraction in the solids is of nitrogen and ash. However, their variation with respect to temperature cannot be determined through the current modelling since they do not take part in the reactions, as reported by Bates et al[13]. In the subsequent calculation of the HHV it was assumed that nitrogen content is the same as the initially reported value in table 2.2.

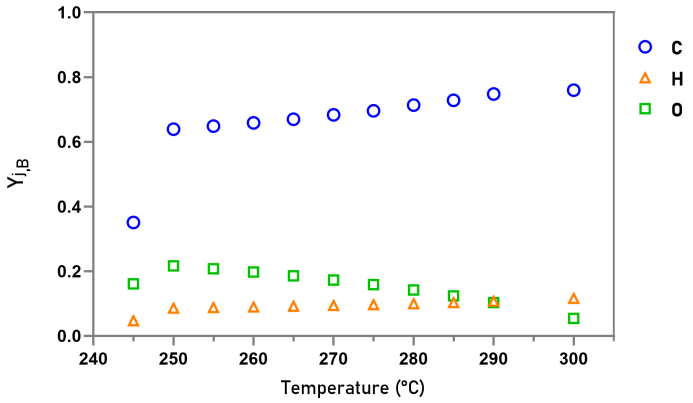

Figure 4.6: Change in elemental compositions with torrefaction temperature for solid B (j = C,H,O).

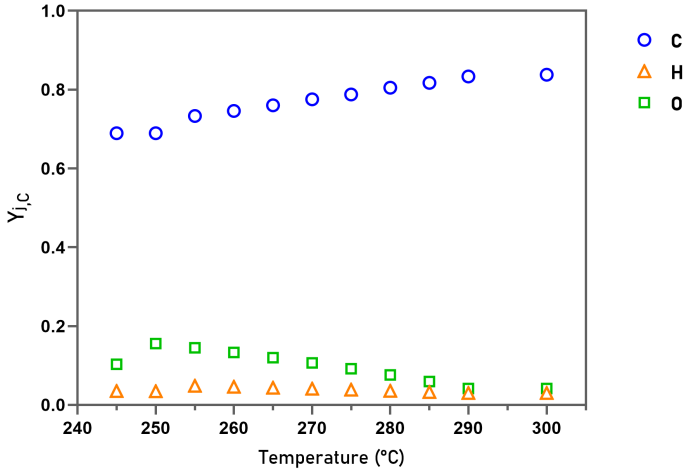

Figure 4.7: Change in elemental compositions with torrefaction temperature for solid C (j = C,H,O).

From the above figures we can observe that the increase in severity of torrefaction results in an increase in the carbon content, while the hydrogen and oxygen contents decreases. In order visualise these changes a Van-Krevelen diagram is used which plots the atomic ratio of H/C to O/C ratio. The position of the final solid product (C) on the Van-Krevelan diagram for the selected temperatures of 250°C, 270°C and 300 °C is shown in figure 4.8 below.

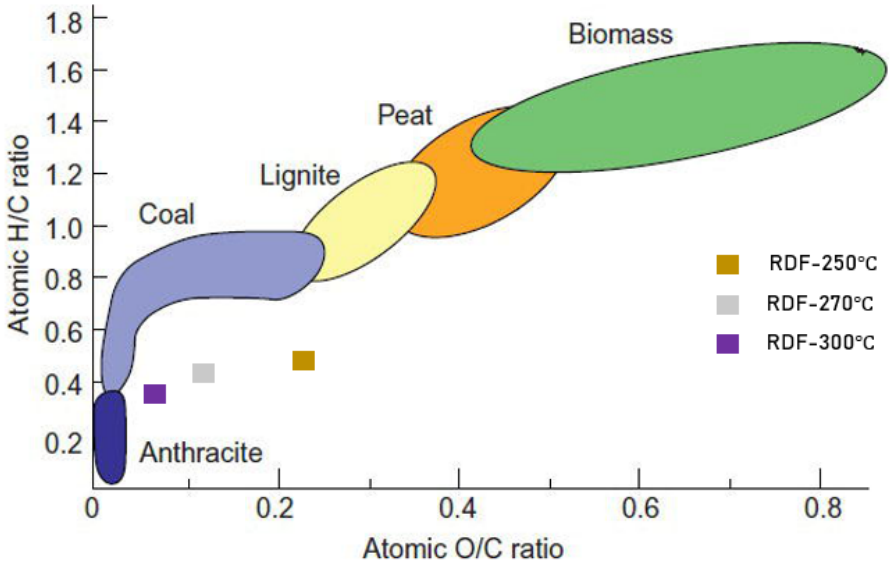

Figure 4.8: Position of torrefied RDF on the Van Krevelen diagram

The expected change in these elemental compositions helps to determine the HHV on the basis of the Boie correlation, which relates the carbon (C), hydrogen (H), oxygen (O), nitrogen (N) contents to the calorific value of the product, on the basis of the similar work done by Bates et al.[13] the nitrogen and ash content are assumed to be unchanged. Abidoye et al[7], obtained a correlation for torrefaction of MSW and the same has been extended to the current study, given by equation 4.2.1. The calorific values for obtained for the analysed torrefaction temperatures are shown in table 4.2.

$$HHV = 351.69 * [\%C] + 1162.46 * [\%H] - 110.95 * [\%O] + 104.67 * [\%S] - 62.8 * [\%N] \, (kcal/kg) \tag{4.2.1}$$

Table 4.2: Estimated higher heating values from Boie correlation

Temperature (°C)	HHV (kcal/kg)	HHV (MJ/kg)
250	4895.26	20.48
270	5781.97	24.19
300	6255.51	26.17

However, from the above values of HHV , on calculating the energy yield,we obtain values which are greater than 1, which cannot be possible. This is the shortcoming of modelling the elemental variation of the solids, as it has a tendency to greatly over-predict or under predict the carbon, hydrogen and oxygen content, this disadvantage was mentioned in the similar modelling work carried out Bates et al[13]. In order to overcome this problem encountered, a database involving the mass yields, torrefaction temperature and HHV that were reported in literature for a few feeds such as yard, food and other green wastes based on experiments conducted were sourced, which are shown in Appendix B. An equation relating these three variables (temperature, mass yield and HHV) were obtained on the basis of Curve fitting done in MATLAB, the fitted surface plot (figure 4.9) along with the corresponding equation 4.2.2 is shown below.

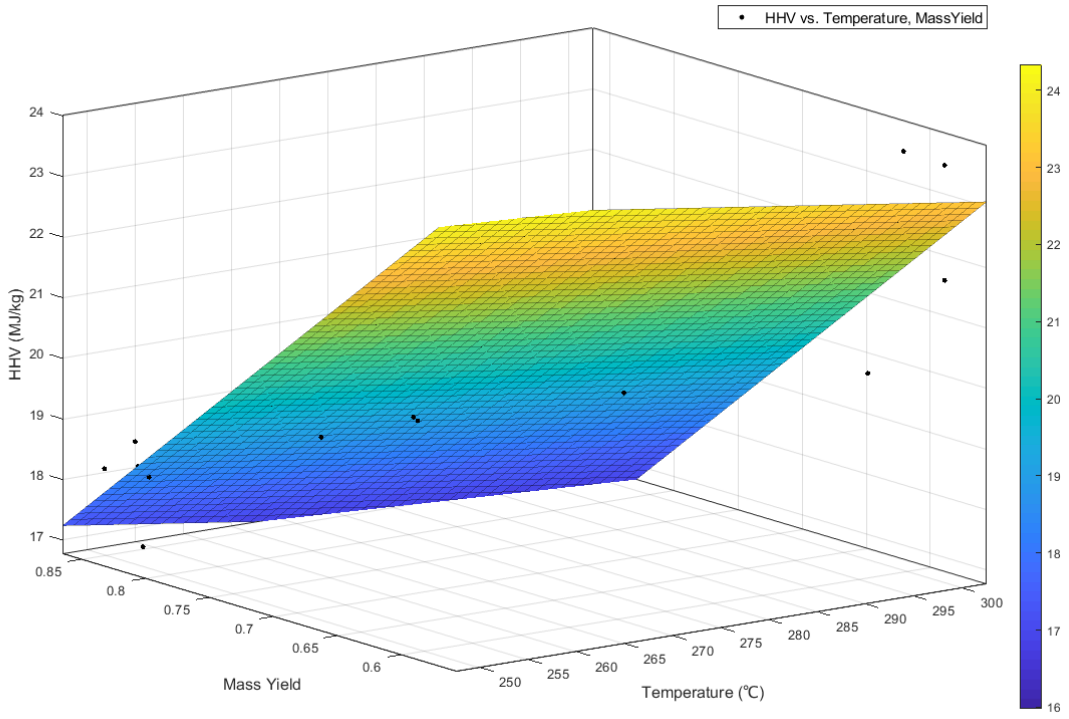

Figure 4.9: Surface plot for HHV estimation

$$f(x,y) = (36.781 - 0.005394 \times x - 20.05 \times y) \tag{4.2.2}$$

Where the x-axis is the temperature (°C), y-axis the reported mass yields and z-axis the reported HHV (MJ/kg). On the basis of this equation the corrected HHV and energy yields for the mass yields obtained in this work were determined and their variation with temperature can be seen in figure 4.10

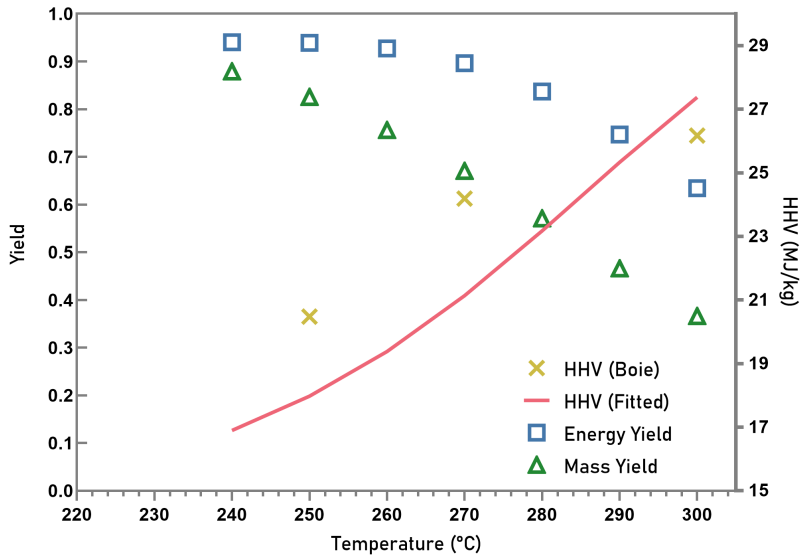

Figure 4.10: Torrefaction mass and energy yields for different temperatures with residence time o 30 mins.

From the above figure we can analyse that with an increase in the temperature of torrefaction, the devolatil-

isation of the solid product increases which causes the mass yield to decrease progressively. An increase in the temperature from 240 °C to 270 °C caused a decreases in the mass yield of about 23.7 % and about 54% when increased to 300°C. The same can be extended for the energy yields as well, where it showed a decrease with torrefaction temperature. The higher heating value increases with torrefaction temperature.The energy yield is used as a parameter to determine the trade off between loss of mass and gain in HHV. Since the aim of the current work is production of torrefied RDF pellets, it is essential to have a high mass yield.Apart from this consideration, it would be optimum to select a temperature for which kinetic data is obtained in order to avoid large variability in results. Hence on the basis of all the above results it can be concluded that the optimum torrefaction temperature is 250 °C with a residence time of 30 min for the production of torrefied RDF.

4.2.1 Heat integration

As mentioned within section 3.5, the energy of the volatiles or torgas that are evolved are used to meet the heat demands within the overall process. Aspen Energy Analyzer was used to determine the optimum stream connections through which this heat integration can be achieved. Based on the results reported in the section above, it was concluded that the optimum torrefaction parameters were 250 °C temperature and residence time of 30 min. Carrying out the simulation under the said conditions in Aspen Plus gives rise to the torgas with a temperature of 800 °C, which is the HOT Stream and is represented by the red line in the below figures. Three COLD streams are present, to which the heat from the torgas needs to be supplied, they are:

- AIR_to_AIRDRY : Air that is sent to the rotary dryer which serves as the drying medium.
- AIR2 : Air sent to RStoic reactor to vaporize remaining moisture.
- THFLUID : The thermal fluid that is sent to the rotary reactor (RPlug) which serves as the heating medium.

Figures 4.11 and 4.12 represents the unresolved and resolved stream connections. Based on the optimum connection that was made, the composite and grand composite curves were generated with a specified minimum approach temperature of 10 degree C between the hot and cold stream. These are show in figures 4.13 and 4.14. It can be seen from these figures that the hot torgas stream is able to sufficiently meet the process heat demands without the violation of the minimum approach temperature and the need of additonal heating utilities.

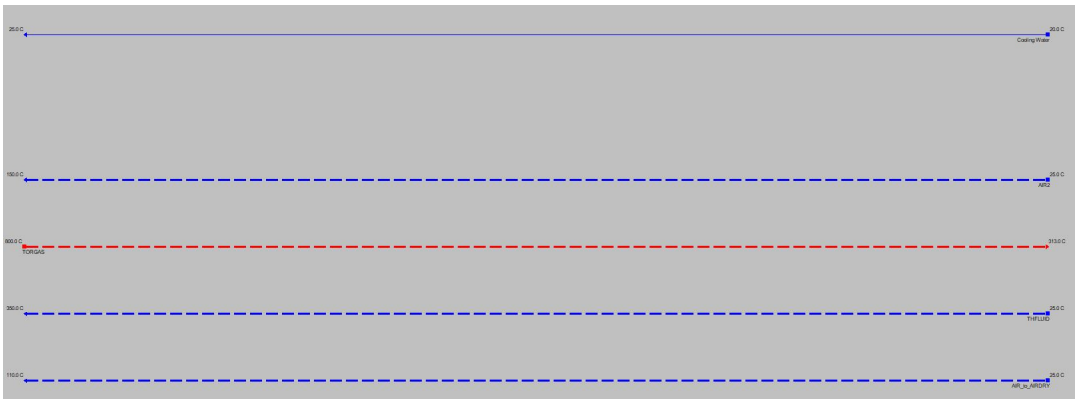

Figure 4.11: Unresolved hot and cold streams connections

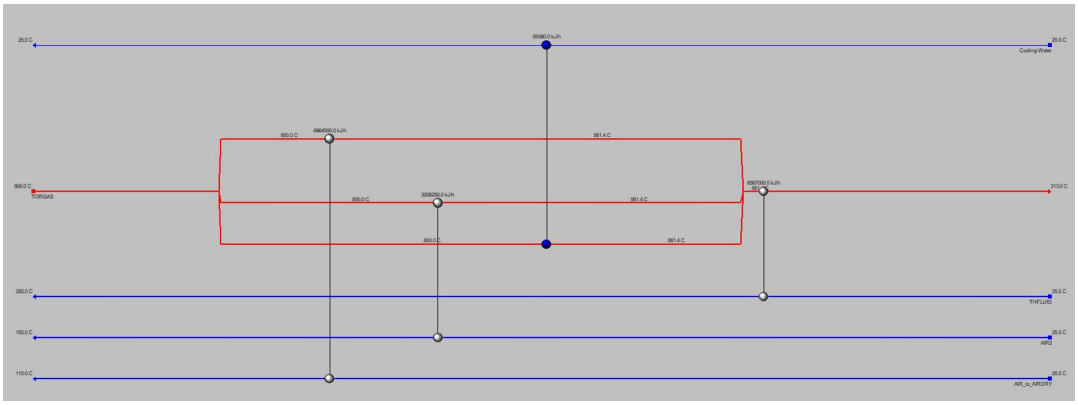

Figure 4.12: Resolved hot and cold stream connections

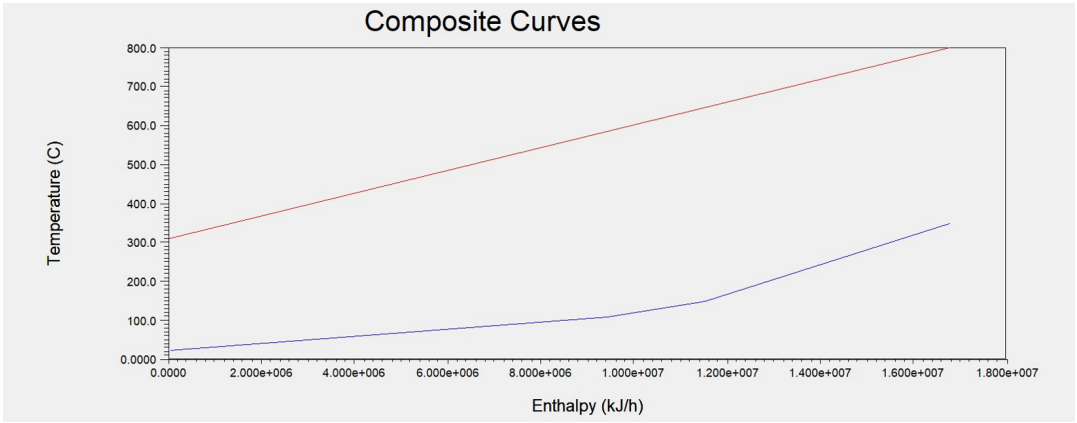

Figure 4.13: Composite curve

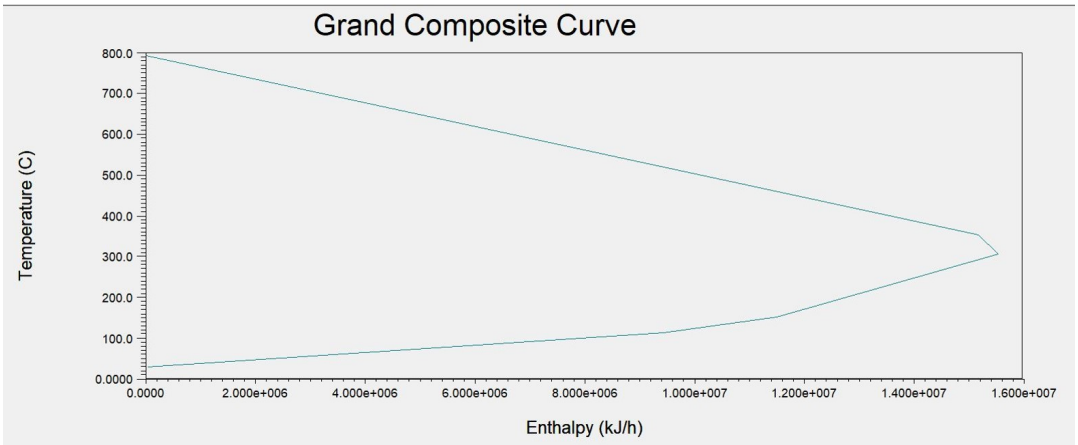

Figure 4.14: Grand composite curve

4.3 Economic Analysis

As mentioned in the previous chapter, the economic evaluation or analysis of the project is done in order to determine its profitability, which is an indicator of how attractive the investment is. Certain economic indicators such as net present value (NPV) and payback period (PBP) are used within this study to see if the

project is feasible.

In order to get a better understanding on the variation in investment required three different cases based on processing capacities or size of the torrefaction plant is used and is shown in table 4.3. The lower and upper limit of plant size was set to 50 and 200 ton/day respectively because it is possible that there could a large variability in the waste generated on a day-to-day basis, where it may have a higher or lower % fraction of recyclable materials in which the production of the raw RDF is decreased or increased respectively[87].

Table 4.3: Processing capacities selected for economic analysis

Case	Size (ton/day)
Low capacity	50
Base capacity	100
High capacity	200

4.3.1 CAPEX

The capital expenditures obtained on the basis of purchased equipment costs as discussed in section 3.6 for the three processing capacities is shown below in figure 4.15. It can be seen that the CAPEX increases with the plant size, as the equipment sizes required to process the amount of feed increases, this scale up causes the increase in CAPEX. The capital costs for the three plant size are given in table 4.4.

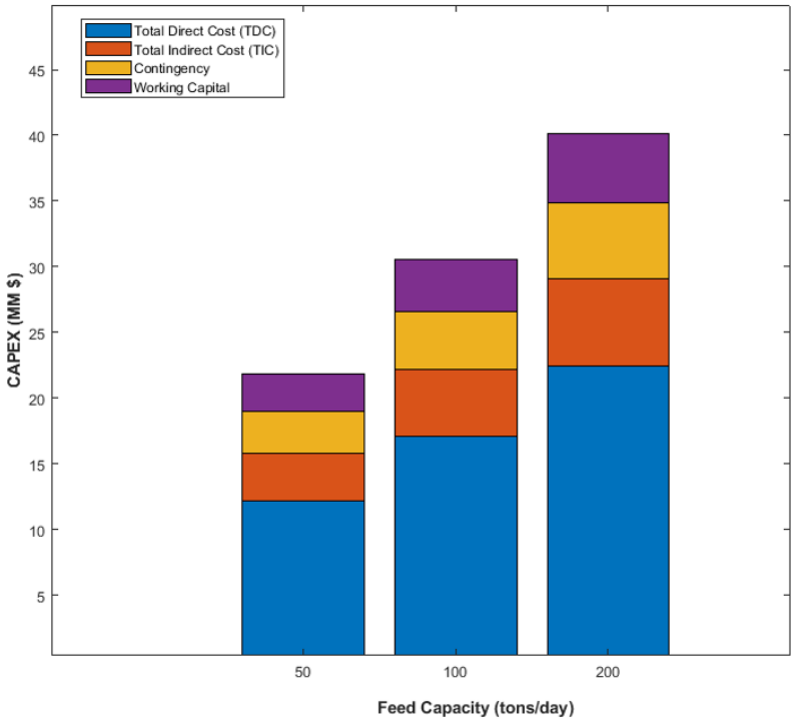

Figure 4.15: CAPEX for selected plant capacities.

Table 4.4: CAPEX of RDF torrefaction plants

Case	Size (ton/day)	CAPEX (MM $)
Low capacity	50	22
Base capacity	100	30
High capacity	200	40

4.3.2 OPEX

The methodology for determining the operating expenditure was discussed in section 3.6. The operating labour and utilities influence the operating costs the most. In order to determine the overall utility costs, the energy consumption for the different unit operations within in the plant needs to analysed and for this the energy demand for the drying, torrefaction, grinding and pellitization process was extracted from Aspen Plus and is shown in figure below 4.16

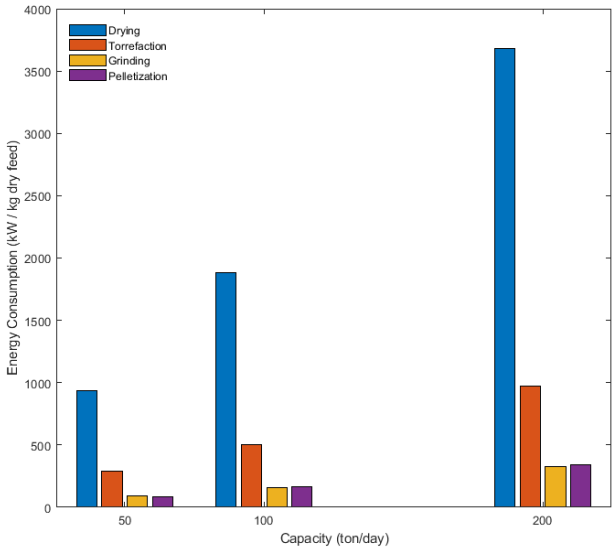

Figure 4.16: Energy consumption of different unit operations with varying capacity.

From the above figure we can observe that the energy required for the drying operation is comparatively very high with respect to the other operations within the plant,this finding is in accordance with other literature sources which have reported similar high energy consumption of the drying operation[54][15][61]. The OPEX was subsequently obtained for the different capacities and is shown in figure 4.17. Similar to the CAPEX, the OPEX is also expected to rise with increase in the processing capacities due to higher overall energy consumption. The different OPEX values are given in table 4.5 below.

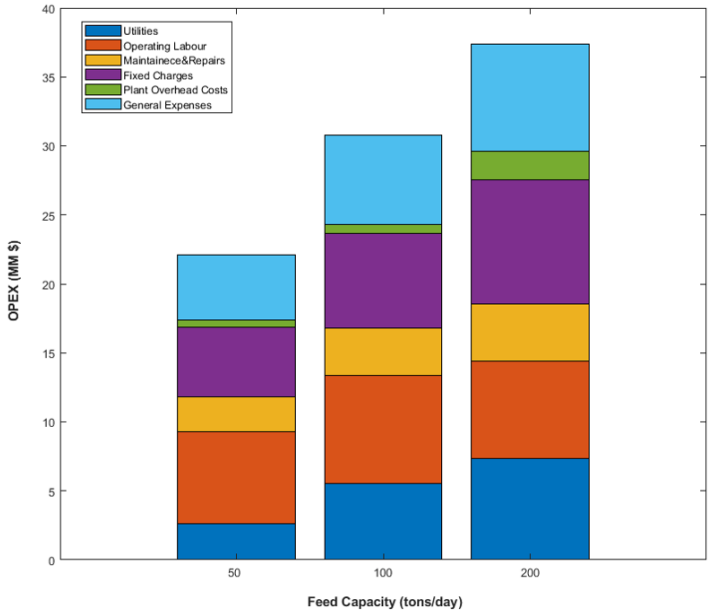

Figure 4.17: OPEX variation for selected plant capacities.

Table 4.5: OPEX of RDF torrefaction plants

Case	Size (ton/day)	OPEX (MM $)
Low capacity	50	23
Base capacity	100	30
High capacity	200	49

4.3.3 Net present value (NPV)

The net present value is an economic indicator used to analyse the profitability of an investment. The conditions of NPV under which a project is attractive is shown below.

$$NPV \geq 0 \;\; Invest\, in\, project \tag{4.3.1}$$

$$NPV < 0 \;\; Reject\, project \tag{4.3.2}$$

In order to obtain the NPV, the cash flows from the product sales as well as an additional revenue in the form of a 'tipping fee' needs to quantified. The depreciation may or may not be considered, in the current work a straight line depreciation has been included with in the calculations of the NPV. The NPV obtained for the three plant capacities are show in figures 4.18 to 4.20

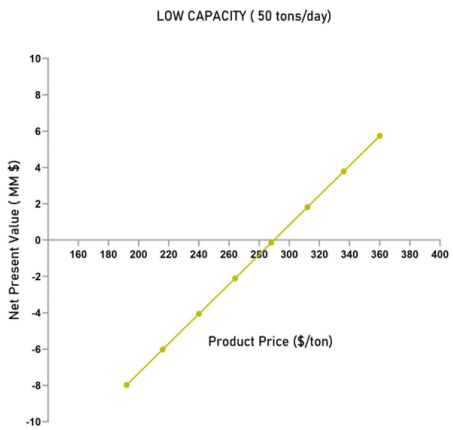

Figure 4.18: NPV of low capacity plant.

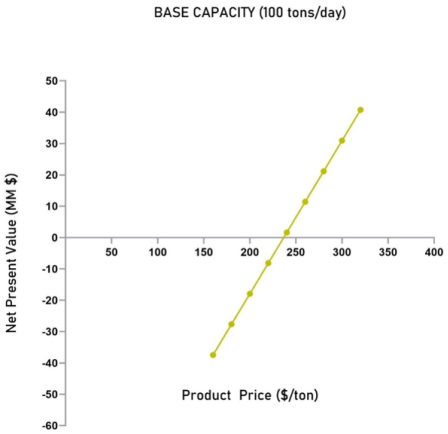

Figure 4.19: NPV of base capacity plant.

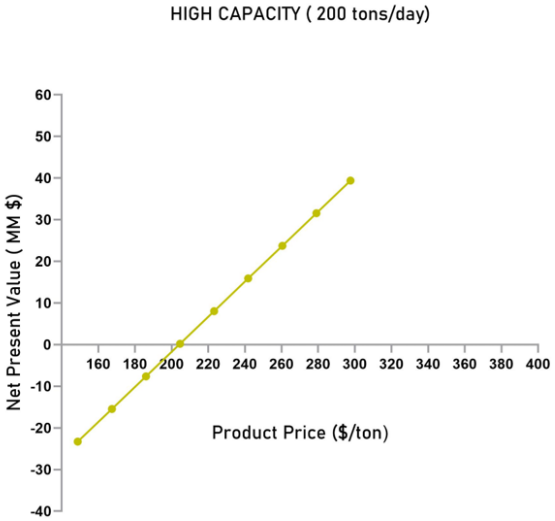

Figure 4.20: NPV of high capacity plant.

From the NPV analysis it is possible to determine the minimum selling price of the RDF pellets. The cost of torrefied pellets range from 160 to 320 $/ton hence the NPV was determined with cash flows expected within this range with a constant tipping fee of 90 $/ton of RDF[87]. The selling price of the pellets at which the NPV is just positive or close to zero is the minimum selling price for which the investment is attractive. The minimum selling price for the three different plant capacities is shown in table 4.6. Based on these values we can gather that, the low capacity plant would require a higher product selling price in order to break even on the operating costs, this mainly due to the less output obtained from the plant. Apart from this the coal prices are usually in the range of 240 $/ton - 255 $/ton, hence it would not be attractive to operate the plant at this capacity due to very less competitive prices. In the case of the base and high capacity plants the minimum selling price of the product is close to and lesser than the prices of coal respectively hence these projects offer to be quite attractive to investment.

Table 4.6: Minimum selling price needed for different plant capacities

Case	Size (ton/day)	Minimum Selling Price ($/ton)
Low capacity	50	280-290
Base capacity	100	235-250
High capacity	200	200-215

4.3.4 Payback Period

The payback period is used to determine the amount of time within with which the CAPEX can be recovered based on the revenue generated, a low payback period is desirable for a project to be attractive for investment. The payback period for the there plant capacities was calculated based on the methodologies shown in section 3.6 and results obtained are given in figure 4.21.

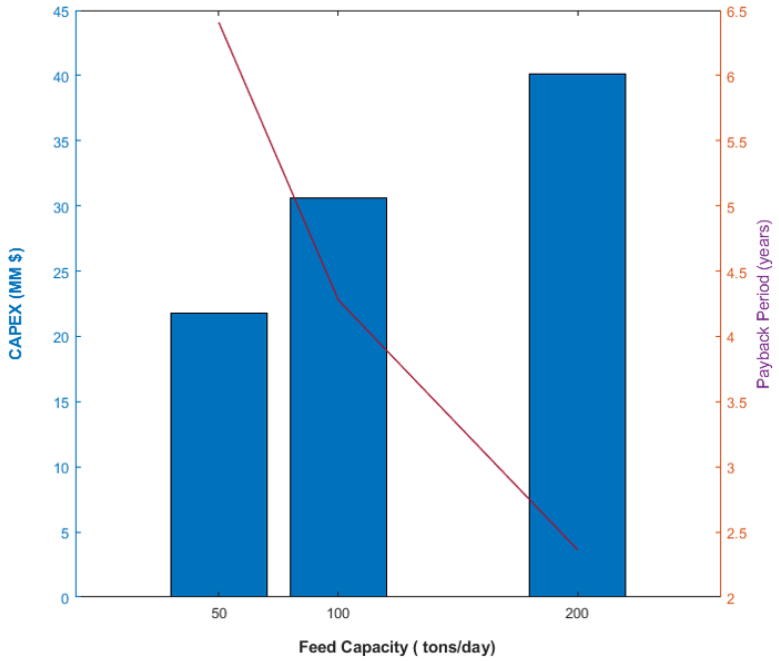

Figure 4.21: Payback for the different RDF torrefaction plants.

Based on the above figure we can gather that the low capacity plant has high payback period of 6 years, mainly owing to the low production capacity and product sales contrary the base and high capacity plants having better cash flow.

To summarise, based on the economic analysis it was found that the minimum selling price of the torrefied RDF was competitive with the prices for coal in the case of the base and high capacity plants, owing to their higher production capabilities, which in turn results in more cash flowing leading to a better NPV and payback period. However as mentioned in the beginning of this section, it is necessary to analyse the variability in the day-to-day waste generation on the fractions that are being recycled and being sent to treatment centers for obtaining RDF in order to fix more accurately on an operating range. This would require a more in depth investigation into the waste generation patterns of the region where the plant is likely to be set up.

4.4 RDF substitution

Refuse derived fuel currently finds major applications within the cement manufacturing industry as a substitute feedstock. One of them main characteristics of cement production is the CO_2 emissions accompanying the process, generally 0.65-0.95 tonnes of CO_2 is released with 1 ton of cement production[46]. The efficiency of the process, fuels used and the specific type cement type produced also plays a role in quantifying the emissions [46]. The two main sites of major CO_2 release within the production process is linked with the energy released by fuel combustion for burning clinker and other operations while the second source is from the natural release of CO_2 due to de-carbonation of limestone producing calcium silicates and aluminates in the clinker process when subject to intense heat[10].

In convectional cement manufacturing process, fossil fuels such as coal, petroleum coke or petcoke, natural gas or diesel are used to produce the high temperatures needed within the process via their combustion. It is estimated that approximately 40% of the GHG released during the production process is generated at this stage, as reported by the World Business Council for Sustainable Development[10]. On considering the annual global manufacturing of cement, a significant reduction in CO_2 emissions can be achieved with just a slight decrease in the amount of fossil fuels used,a decrease of at-least 10% of the CO_2 intensity within the production process can save close to 0.4 Gt of CO_2[46]. Considering the emissions as well as the increasing fossil fuel prices to decrease their usage,RDF emerges as a very attractive and feasible option as an alternative fuel.By substituting a part of the total fuel requirement within the process by a percentage amount of RDF, it is possible to reduce the costs associated with fossil fuel usage as well as a reduction in CO_2 emissions, without comprising on the energy requirements. Since RDF consists of materials that has certain challenges to their recycling,they most often than not end up in landfills, which is again environmentally undesirable as the result in further harmful leachates and evolution of methane, another greenhouse gas. The unique characteristics associated with cement kilns, where flame temperatures in an excess of 2000 °C are present, can aid in these materials being destroyed without producing additional waste ash or harmful emissions [46].

The major challenge that is being faced by the use of RDF in cement kilns is the chlorine content. If a high chlorine content is present, it results in the weakening of the concrete's compressive strength through the generation of micro cracks which forms as a result of reactions between chlorine compounds creating salts[10]. But the cement industry reports that up to 20% of RDF can be substituted to meet the energy requirements in cement kilns without any negative effects to the final product. Also other waste materials could also be burnt such as end of life tyres, which can aide in bringing down the requirement of fossil fuels[46].

In order to analyse what effects the amount of RDF being substituted has on the annual costs associated with fossil fuel consumption and CO_2 release, a basic economic model has been developed that takes into account four cases of substitution percentage. The model was developed based on the methodology and data that was available for a typical cement factory that was reported within a similar study carried out by[38]. Table 4.7 below shows the input data needed to carry out the evaluation along with their sources. The calorific value of the RDF was taken from the current study, based on the torrefaction carried out 250 °C and its corresponding mass yield which were inputs to the curve fit equation as mentioned in section 4.2. The cost of 1 ton RDF was taken on the basis of the economic analysis that was carried out in the previous section where the minimum selling price that was feasible for RDF was determined.

Table 4.7: Data sourced for economic model

Data	Value	Source
Daily kiln production (tons/day)	4000	[38]
Daily petcoke consumption (Tons/day)	381	[38]
Total energy consumption (MJ/kg.cl)	3.01	[38]
Calorific value of petcoke (MJ/kg)	33.49	[1]
Cost of 1 ton petcoke (USD)	350	[1]
Production cost of 1 ton RDF (USD)	200	Current Work
Calorific value of RDF (MJ/kg)	19.0	Current Work
1 kg petcoke is released as CO_2	70 %	[46]
Emission cost of 1 ton CO_2 (USD)	51	[25]

The section below details the basic calculations that were done to determine the savings expected through reduction in petcoke consumption and CO_2 emissions, by taking the case of 15% substitution of RDF.

1. Energy needed by kiln to meet production capacity of 4000 tons/day :

$$4000\, ton/day \times 1000 \times 2.9\, MJ/kg.cl = 11.6 \times 10^6\, MJ/day$$

2. On substitution of 15% RDF, energy saving of petcoke achieved is :

$$11.6 \times 10^6\, MJ/day \times 0.15 = 17.4 \times 10^5 MJ/day$$

3. Amount of RDF needed per hour to compensate energy saved in (2) :

$$17.4 \times 10^5 MJ/day/19.01 MJ/kg/1000/24\,h\,per\,day = 3.81\,ton/h$$

4. Amount of petcoke needed to supply remaining 80% of energy :

$$(11.6 \times 10^6 - 17.4 \times 10^5)\,MJ/day/33.47\,MJ/kg/1000/24\,h\,per\,day = 12.27\,ton/h$$

5. Annual savings of petcoke is :

$$(15.9 - 12.27)\,tons/h \times 24\,h/day \times 300\,days/year = 26,107.62\,ton/year$$

6. Total amount saved for petcoke by 15% substitution of RDF :

$$26,107.62\,ton/year \times 350\,USD/ton = 9,137,670\,USD/year$$

7. Annual consumption of RDF :

$$3.81\,ton/h \times 24\,h/day \times 300\,days/year = 27,459.23\,ton/year$$

8. Total costs incurred by the use of RDF :

$$27,459.23\,ton/year \times 200\,USD/ton = 5,491,846\,USD/year$$

9. The actual financial savings is expected to be :

$$9,137,670\,USD/year - 5,491,846\,USD/year = 3,645,823\,USD/year$$

   The amount of CO_2 emissions and the associated costs that can be saved through the substitution of RDF can be determined in a similar. It has been estimated that 70% of 1 kg petcoke is released as CO_2 and the cost of emission of 1 ton carbon dioxide or the social cost of carbon is around 51 USD[25][27].

10. Annual CO_2 savings by reduction in petcoke amount :

$$12.27\,ton/h \times 0.70 \times 24\,h\,per\,day \times 300\,days/year = 18,275\,ton/year$$

11. Annual CO_2 savings by in petcoke (cost) :

$$18,275\,ton/year \times 51\,USD/ton = 932,042\,USD/year \tag{4.4.1}$$

12. Efficiency loss by the use of RDF substitution :

$$20\% \times RDF\%\,addition \times 100 = (0.20 \times 0.15) \times 100 = 3\% \tag{4.4.2}$$

13. The net savings achieved through the substitution of RDF is :

$$((petcoke\,saving + CO_2\,emission\,savings\,in\,petcoke(cost) - RDF\,production\,cost) \times (100 - efficiency loss))/100 \tag{4.4.3}$$

$$((9,137,670\,USD/year + 932,042\,USD/year - 5,491,846\,USD/year) \times (100-3))/100 = 4,440,530\,USD/year \tag{4.4.4}$$

Table 4.8 below summarises the findings for the remaining cases of substitution percentage. On the basis of the above calculations carried out, it is evident that the substitution of RDF within a cement kiln as an alternative fuel has a positive effect on of the savings associated reduction in fossil fuel consumption and carbon dioxide emissions.

Table 4.8: Model summary for the use and savings associated with RDF and petcoke

Parameter	Unit	Case 0	Case 1	Case 2	Case 3	Case 4
Petoke consumption percentage	%	100	95	90	85	80
RDF substitution percentage	%	0	5	10	15	20
Petcoke consumption rate	ton/h	15.90	13.71	12.99	12.27	11.55
RDF consumption rate	ton/h	0	1.27	2.54	3.81	5.09
Petcoke savings	ton/year	0	15,710	20,909	26,107	31,306
Petcoke savings	USD/year	0	5,498,807	7,318,239	9,137,670	10,957,101
CO2 emissions savings in petcoke	ton/year	0	10,997	14,636	18,275.	21,914
CO2 emissions savings in petcoke	USD/year	0	560,878	746,460	932,042	1,117,624
RDF procurement cost	USD/year	0	1,830,615.	3,661,230	5,491,846	7,322,461
Net savings	USD/year	0	4,186,780	4,315,399	4,440,530	4,562,173

Chapter 5

Conclusion and recommendations

5.1 Conclusion

The current thesis was carried out to fill the gap in literature with regards to the process design and economics associated with the torrefaction of RDF. The unit operations that were modelled within the current study for a 100 ton/day RDF torrefaction plant were a dryer, torrefaction reactor, grinder and pelletization. Simulation of the dryer and torrefaction units were carried out on the basis of experimental data that was available in literature. From curve fitting analysis that were carried out the Henderson-Pabis model was concluded to have shown better correlations with the experimental drying data of RDF with $R^2 > 0.98$. The equation was then modified in order to understand the variability in residence time of RDF in the dryer with particle size. The developed equations were implemented into the Aspen Plus model for the convective dryer in order to provide a greater flexibility to the operation in terms of controlling the temperature of drying as well as the particle sizes and to view their effects on the residence time. A residence time of 19 mins was obtained within the dryer for the base processing capacity of 100 ton/day of raw RDF at a drying temperature of 110°C and particle size of 15 mm.

The torrefaction reactor was modelled on the basis of kinetic equations where the rate constants were obtained from weight loss vs time data reported within literature for torrefaction experiments. As mentioned within the previous sectioned an assumption had to made at this point in order to proceed further due to the lack of reported weight loss data in literature for pure RDF. It was considered that the feed is primarily composed of organic or green waste which constitutes of yard as well as traces of food waste. Torrefaction temperatures of 250°C, 270°C and 300 °C with residence time of 30 min were analysed to determine the optimum condition for maximising the mass and energy yield of the final product. It was concluded that the optimum torrefaction conditions were 250°C and residence time of 30 min since the final aim is to maximise the output of torrefied pellets to be used as an alternative fuel. The higher heating value (HHV) of the final product showed a significant increase in its HHV from 15.6 MJ/kg of the initial material to 19 MJ/kg under the specified conditions of torrefaction at 250 °and residence time of 30 min. A heat integration analysis carried out by combusting the evolved volatiles further reinforces the selection of these torrefaction parameters as the amount of energy present within these volatiles is sufficient to meet the heat requirements within 100 ton/day processing capacity plant. This energy could be used for heating up the air used for drying and the thermal fluid within the rotary drum reactor.

The economic feasibility of implementing the torrefaction process on a large scale was analysed on the basis of the CAPEX and OPEX which were calculated as per the selected process conditions of torrefaction at 250 °and residence time of 30 min. Apart from the base case of 100 ton/day, two additional plant sizes of 50 ton/day and 200 ton/day for processing the raw RDF was selected for the economic analysis. For the CAPEX and OPEX it was observed that with an increase in the processing capacity there is an increase in the costs incurred due to larger equipment sizes required as well more utilities consumption. The results from the NPV analysis showed that the minimum selling price that needs to be set for the final product obtained from each of the three plant sizes of 50 ton/day, 100 ton/day and 200 ton/day were 280 $/ton, 235 $/ton and 200 $/ton respectively for an internal rate of return of 12%. The revenue was calculated based on the minimum selling price that was obtained from the NPV analysis and the payback period determined were approximately

6.5 years, 4 and 2 years for the 50 ton/day, 100 ton/day and 200 ton/day plants respectively. In order to fix upon the optimum operational capacity of the torrefaction plant, the minimum selling price needs to be as competitive as the price of coal and petcoke which are commonly used fuels within the cement industry and their prices range from 240$ton to 350$/ton depending on the quality. Based on this constraint it is evident that the optimum plant sizes should be in the range of 100 to 200 ton/day and they also have a good payback period. However an additional challenge that is posed when moving to higher processing capacities is the availability of the raw RDF itself. As the waste generation patterns are subject to daily, monthly and seasonal variations there may be instances where a higher fraction of recyclable material could be present in which a sufficient amount of raw RDF cannot not be sourced from the mechanical treatment plants.

An additional economic analysis was carried out to determine the savings that could be made within a typical cement that substitutes RDF along with a conventional fuel such as petcoke. Four cases considering RDF substitution percentages of 5%,10%,15% ad 20% were analysed and it was found that overall a positive net savings of 4-4.5 MM$ which is inclusive of the reduction in costs incurred from fossil fuel consumption as well the emission costs of carbon dioxide.

Based on the results obtained from the current work it can be concluded that the torrefaction of RDF is indeed attractive and feasible on a large scale, and the final product obtained shows improved physical and chemical properties which makes it a suitable alternative fuel within an energy intensive industry such as cement manufacturing which currently relies on fossil fuels. From an economic perspective, as the prices of these fossil fuels are only expected to increase, the torrefied RDF could serve as a cheaper alternative and significant savings could be achieved through their use.

5.2 Recommendations

The main challenge that was faced during this thesis was the availability of experimental data for the drying and torrefaction operations. Since the usage of refuse derived fuel as an alternative fuel is a relatively new area of study there is quite a large gap present in literature. Given below are certain recommendations that can aid in taking the current work forward.

- The initial raw RDF is subject to a large variability in its composition based on the location and day-to-day waste generation patterns of the region. As such the operational conditions needs to be adjusted to account for this variability and the system boundaries needs to be determined. This can only be carried out through a more in extensive literature survey of the region where the plant is proposed to be set up. The effect of additional pre-conditioning steps such as screening should also be explored and evaluated.
- Further drying experiments for RDF with various compositions, moisture contents and higher temperatures need to be carried out in order to reduce the energy consumption as well the drying times. An analysis into the demand of RDF with respect to its end users needs to be explored, in which case the feasibility of alternative options such as bio-drying and solar drying can be evaluated when moving towards a batch wise operation.
- Torrefaction experiments also needs to be carried out for varying composition of RDF with the accurate reporting of their weight loss data in order to carry out similar modelling and simulation studies. A large gap exits in literature with respect to the characterisation of the components present within the volatiles released during the torrefaction of RDF. It would be highly beneficial if these compounds could be accurately identified and quantified such that the potential for their valorization could be explored through chemical looping combustion or oxy-fuel combustion to improve the process integration.
- The HGI index for the grindability of RDF and the enery need for its pelletization for various torrefaction conditions as well as initial particle sizes needs to be experimentally determined.
- If sufficient data for the above mentioned unit operations become available, the flexibility of the model could be further increased through the implementations of artificial neural networking (ANN). The ANN model could take the material compositions of the raw RDF as its inputs and can return an estimate of the proximate and ultimate analysis. The simulation model can then run for wide range of the raw RDF compositions provided a large database is created to have good degree of accuracy.

Bibliography

[1] Petcoke prices 2021. URL https://nxhuiheng.en.made-in-china.com/product/wCQEsmzOAHhW/China-0-3mm-Calcined-Pet-Coke-Hard-Coke-with-Good-Price.html.

[2] bp statistical review of world energy 2020.

[3] Technologies for Converting Biomass to Useful Energy. 2013. doi: 10.1201/b14561.

[4] Stastica (2018). Generation of municipal solid waste worldwide in 2017, by select country (in million metric tons). https://www.statista.com/statistics/916749/global-generation-of-municipal-solid-waste-bycountry/, 2018. [Online; accessed 03-November-2021].

[5] Stastica (2020). Projected generation of municipal solid waste worldwide from 2016 to 2050. https://www.statista.com/statistics/916625/global-generation-of-municipal-solid-waste-forecast/, 2020. [Online; accessed 03-November-2021].

[6] Noor Asma Fazli Abdul Samad, Nur Ashikin Jamin, and Suriyati Saleh. Torrefaction of Municipal Solid Waste in Malaysia. In Energy Procedia, volume 138, 2017. doi: 10.1016/j.egypro.2017.10.106.

[7] Luqman Abidoye and Faiz Mahdi. Novel linear and nonlinear equations for the higher heating values of municipal solid wastes and the implications of carbon to energy ratios. Journal of Energy Technologies and Policy, 4:14–27, 05 2014.

[8] U.S. Energy Information Administration. Electric Power Monthly. https://www.eia.gov/electricity/monthly/epm_table_grapher.php?t=epmt_5_6_a, 2020. [Online; accessed 19-November-2021].

[9] N. Agon, M. Hrabovský, O. Chumak, M. Hlína, V. Kopecký, A. Mašláni, A. Bosmans, L. Helsen, S. Skoblja, G. Van Oost, and J. Vierendeels. Plasma gasification of refuse derived fuel in a single-stage system using different gasifying agents. Waste Management, 47, 2016. ISSN 18792456. doi: 10.1016/j.wasman.2015.07.014.

[10] Alfonso Aranda Usón, Ana M. López-Sabirón, Germán Ferreira, and Eva Llera Sastresa. Uses of alternative fuels and raw materials in the cement industry as sustainable waste management options, 2013. ISSN 13640321.

[11] Fatemeh Asadi. Drying of refuse-derived fuel (rdf). 2016.

[12] C.L.Law A.S.Mujumdar S.V.Jangam. Drying of foods, vegetables and fruits volume 1. 2010.

[13] Richard B. Bates and Ahmed F. Ghoniem. Biomass torrefaction: Modeling of volatile and solid product evolution kinetics. Bioresource Technology, 124, 2012. ISSN 18732976. doi: 10.1016/j.biortech.2012.07.018.

[14] B. Batidzirai, A. P.R. Mignot, W. B. Schakel, H. M. Junginger, and A. P.C. Faaij. Biomass torrefaction technology: Techno-economic status and future prospects. Energy, 62, 2013. ISSN 03605442. doi: 10.1016/j.energy.2013.09.035.

[15] P. Bergman, Arjen Boersma, Robin Zwart, and Kiel. Torrefaction for biomass co-firing in existing coal-fired power stations. Energy research Centre of the Netherlands, 01 2005.

[16] Andrzej Białowiec, Jakub Pulka, Paweł Stępień, Piotr Manczarski, and Janusz Gołaszewski. The RDF/SRF torrefaction: An effect of temperature on characterization of the product – Carbonized Refuse Derived Fuel. Waste Management, 70, 2017. ISSN 18792456. doi: 10.1016/j.wasman.2017.09.020.

[17] Colomba Di Blasi and Mario Lanzetta. Intrinsic kinetics of isothermal xylan degradation in inert atmosphere. Journal of Analytical and Applied Pyrolysis, 40-41, 1997. ISSN 01652370. doi: 10.1016/S0165-2370(97)00028-4.

[18] A. A Boateng. Basic description of rotary kiln operation. Rotary Kilns, 2016. doi: 10.1016/b978-0-12-803780-5.00002-2.

[19] A. Bosmans, I. Vanderreydt, D. Geysen, and L. Helsen. The crucial role of Waste-to-Energy technologies in enhanced landfill mining: a technology review. Journal of Cleaner Production, 55:10–23, sep 2013. ISSN 0959-6526. doi: 10.1016/J.JCLEPRO.2012.05.032.

[20] J. G. Brammer and A. V. Bridgwater. The influence of feedstock drying on the performance and economics of a biomass gasifier - Engine CHP system. Biomass and Bioenergy, 22(4), 2002. ISSN 09619534. doi: 10.1016/S0961-9534(02)00003-X.

[21] V. V. Bukhmirov, O. B. Kolibaba, and R. N. Gabitov. Experimental research of solid waste drying in the process of thermal processing. volume 93, 2015. doi: 10.1088/1757-899X/93/1/012006.

[22] Margareta Novian Cahyanti, Tharaka Rama Krishna C. Doddapaneni, Marten Madissoo, Linnar Pärn, Indrek Virro, and Timo Kikas. Torrefaction of agricultural and wood waste: Comparative analysis of selected fuel characteristics. Energies, 14, 2021. ISSN 19961073. doi: 10.3390/en14102774.

[23] Yanán Camaraza-Medina, Andres A. Sánchez-Escalona, Yoalbys Retirado-Mediaceja, and Osvaldo F. García-Morales. Use of air cooled condenser in biomass power plants: A case study in cuba. International Journal of Heat and Technology, 38, 2020. ISSN 03928764. doi: 10.18280/ijht.380218.

[24] Antonio C. Caputo and Pacifico M. Pelagagge. RDF production plants: I Design and costs. Applied Thermal Engineering, 22(4):423–437, mar 2002. ISSN 1359-4311. doi: 10.1016/S1359-4311(01)00100-4.

[25] Jean Chemnik. Cost of carbon pollution pegged at $51 a ton. Scientific American, 2021. URL `https://www.scientificamerican.com/article/cost-of-carbon-pollution-pegged-at-51-a-ton/`.

[26] Ciprian Cimpan and Henrik Wenzel. Energy implications of mechanical and mechanical-biological treatment compared to direct waste-to-energy. Waste Management, 33, 2013. ISSN 0956053X. doi: 10.1016/j.wasman.2013.03.026.

[27] European Commission. Guidelines on the interpretation of the r1 efficiency formula for incineration facilities dedicated to the processing of municipal solid waste according to annex ii of directive 2008/98/ec on waste. 2008.

[28] European Commission. Directive (EU) 2018/851 of the European Parliament and of the Council of 30 May 2018 amending Directive 2008/98/EC on waste (Text with EEA relevance). Official Journal of the European Union, 2018.

[29] S. Consonni, M. Giugliano, and M. Grosso. Alternative strategies for energy recovery from municipal solid waste: Part A: Mass and energy balances. Waste Management, 25(2):123–135, jan 2005. ISSN 0956-053X. doi: 10.1016/J.WASMAN.2004.09.007.

[30] Ed Cook, Stuart Wagland, and Frédéric Coulon. Investigation into the non-biological outputs of mechanical-biological treatment facilities. Waste Management, 46, 2015. ISSN 18792456. doi: 10.1016/j.wasman.2015.09.014.

[31] Alok Dhungana, Prabir Basu, and Animesh Dutta. Effects of reactor design on the torrefaction of biomass. Journal of Energy Resources Technology, 134, 2012. ISSN 0195-0738. doi: 10.1115/1.4007484.

[32] Mar Edo, Nils Skoglund, Qiuju Gao, Per Erik Persson, and Stina Jansson. Fate of metals and emissions of organic pollutants from torrefaction of waste wood, MSW, and RDF. Waste Management, 68, 2017. ISSN 18792456. doi: 10.1016/j.wasman.2017.06.017.

[33] Emmanuel C. Efika, Jude A. Onwudili, and Paul T. Williams. Products from the high temperature pyrolysis of rdf at slow and rapid heating rates. Journal of Analytical and Applied Pyrolysis, 112, 2015. ISSN 01652370. doi: 10.1016/j.jaap.2015.01.004.

[34] L. Fagernäs, J. Brammer, C. Wilén, M. Lauer, and F. Verhoeff. Drying of biomass for second generation synfuel production. Biomass and Bioenergy, 34, 2010. ISSN 09619534. doi: 10.1016/j.biombioe.2010.04.005.

[35] Ahsan Farooq, Piyanon Haputta, Thapat Silalertruksa, and Shabbir H. Gheewala. A Framework for the Selection of Suitable Waste to Energy Technologies for a Sustainable Municipal Solid Waste Management System. Frontiers in Sustainability, 2, 2021. doi: 10.3389/frsus.2021.681690.

[36] Tesfaldet Gebreegziabher, Adetoyese Olajire Oyedun, and Chi Wai Hui. Optimum biomass drying for combustion - A modeling approach. Energy, 53, 2013. ISSN 03605442. doi: 10.1016/j.energy.2013.03.004.

[37] Dr. Don W. Green and Dr. Marylee Z. Southard. Perry's chemical engineers' handbook, 9th edition. Perry's Chemical Engineers' Handbook, 9th Edition, 2019.

[38] Safwat Hemidat, Motasem Saidan, Salam Al-Zu'bi, Mahmoud Irshidat, Abdallah Nassour, and Michael Nelles. Potential utilization of RDF as an alternative fuel to be used in cement industry in Jordan. Sustainability (Switzerland), 11(20), 2019. ISSN 20711050. doi: 10.3390/su11205819.

[39] Francisco D. Hernandez-Atonal, Changkook Ryu, Vida N. Sharifi, and Jim Swithenbank. Combustion of refuse-derived fuel in a fluidised bed. Chemical Engineering Science, 62, 2007. ISSN 00092509. doi: 10.1016/j.ces.2006.09.025.

[40] P. Bhada-Tata D. Hoornweg. What a waste : A global review of solid waste management cb. World Bank, 15, 2014.

[41] I.E.A. Global energy co2 status report 2019. URL `https://www.iea.org/reports/global-energy-co2-status-report-2019`.

[42] Uwem Ekwere Inyang, Innocent Oseribho Oboh, and Benjamin Reuben Etuk. Kinetic models for drying techniques—food materials. Advances in Chemical Engineering and Science, 08, 2018. ISSN 2160-0392. doi: 10.4236/aces.2018.82003.

[43] Tamer M. Ismail, Khaled Ramzy, and Hisham Sherif. Drying of refuse-derived fuel (RDF) using solar tunnel dryer integrated with flat-plate solar collector: An experimental approach. Detritus, 13, 2020. ISSN 26114135. doi: 10.31025/2611-4135/2020.14028.

[44] N. A. Jamin, N. A.F.A. Samad, and S. Saleh. Anhydrous weight loss kinetics model development for torrefied green waste. volume 702, 2019. doi: 10.1088/1757-899X/702/1/012008.

[45] T. Järvinen and D. Agar. Experimentally determined storage and handling properties of fuel pellets made from torrefied whole-tree pine chips, logging residues and beech stem wood. Fuel, 129, 2014. ISSN 00162361. doi: 10.1016/j.fuel.2014.03.057.

[46] Mustafa Kara. Environmental and economic advantages associated with the use of rdf in cement kilns. Resources, Conservation and Recycling, 68, 2012. ISSN 09213449. doi: 10.1016/j.resconrec.2012.06.011.

[47] Silpa Kaza, Lisa C. Yao, Perinaz Bhada-Tata, and Frank Van Woerden. What a Waste 2.0: A Global Snapshot of Solid Waste Management to 2050. 2018. doi: 10.1596/978-1-4648-1329-0.

[48] Jaap Koppejan, Shahab Sokhansanj, Staffan Melin, and Sebnem Madrali. Status overview of torrefaction technologies. IEA Bioenergy Task 32, 2012.

[49] Laura Levaggi, Rosella Levaggi, Carmen Marchiori, and Carmine Trecroci. Waste-to-energy in the EU: The effects of plant ownership, waste mobility, and decentralization on environmental outcomes and welfare. Sustainability (Switzerland), 12(14), 2020. ISSN 20711050. doi: 10.3390/su12145743.

[50] Shui Qing Li, L. B. Ma, W. Wan, and Q. Yao. A mathematical model of heat transfer in a rotary kiln thermoreactor. Chemical Engineering and Technology, 28, 2005. ISSN 09307516. doi: 10.1002/ceat.200500241.

[51] Maria Chiara Di Lonardo, Maurizio Franzese, Giulia Costa, Renato Gavasci, and Francesco Lombardi. The application of srf vs. rdf classification and specifications to the material flows of two mechanical-biological treatment plants of rome: Comparison and implications. Waste Management, 47, 2016. ISSN 18792456. doi: 10.1016/j.wasman.2015.07.018.

[52] Jorge Lopez Ordovas, Charlotte Bryant, Katie Chong, and Tony Bridgwater. Feedstock characterisation and slow pyrolysis kinetic study for the production of char -greencarbon project. 05 2019. doi: 10.13140/RG.2.2.26565.68323.

[53] J. Malinauskaite and H. Jouhara. The trilemma of waste-to-energy: A multi-purpose solution. Energy Policy, 129, 2019. ISSN 03014215. doi: 10.1016/j.enpol.2019.02.029.

[54] Maryam Manouchehrinejad and Sudhagar Mani. Process simulation of an integrated biomass torrefaction and pelletization (iBTP) plant to produce solid biofuels. Energy Conversion and Management: X, 1, 2019. ISSN 25901745. doi: 10.1016/j.ecmx.2019.100008.

[55] Mariel Vilella and Carlos Arribas. Cement, waste and carbon markets : Problems related to waste incineration in cement kilns under the eu ets. URL `https://ec.europa.eu/clima/sites/default/files/docs/0017/organisations/global_3_en.pdf`.

[56] Felix Mayer, Ramchandra Bhandari, and Stefan Gäth. Critical review on life cycle assessment of conventional and innovative waste-to-energy technologies, 2019. ISSN 18791026.

[57] Diego Moya, Clay Aldás, Germánico López, and Prasad Kaparaju. Municipal solid waste as a valuable renewable energy resource: A worldwide opportunity of energy recovery by using Waste-To-Energy Technologies. In Energy Procedia, volume 134, 2017. doi: 10.1016/j.egypro.2017.09.618.

[58] P. Murugan, S. Dhanushkodi, K. Sudhakar, and Vincent H. Wilson. Industrial and small-scale biomass dryers: An overview. Energy Engineering: Journal of the Association of Energy Engineering, 118, 2021. ISSN 15460118. doi: 10.32604/EE.2021.013491.

[59] Albany Milena Lozano Násner, Electo Eduardo Silva Lora, José Carlos Escobar Palacio, Mateus Henrique Rocha, Julian Camilo Restrepo, Osvaldo José Venturini, and Albert Ratner. Refuse Derived Fuel (RDF) production and gasification in a pilot plant integrated with an Otto cycle ICE through Aspen plus™ modelling: Thermodynamic and economic viability. Waste Management, 69:187–201, nov 2017. ISSN 0956-053X. doi: 10.1016/J.WASMAN.2017.08.006.

[60] Muhammad Nasrullah, Pasi Vainikka, Janne Hannula, Markku Hurme, and Pekka Oinas. Elemental balance of srf production process: Solid recovered fuel produced from municipal solid waste. Waste Management and Research, 34, 2016. ISSN 10963669. doi: 10.1177/0734242X15615697.

[61] Daya Nhuchhen, Prabir Basu, and Bishnu Acharya. A comprehensive review on biomass torrefaction. International Journal of Renewable Energy Biofuels, 2014. ISSN 2333-0589. doi: 10.5171/2014.506376.

[62] Jidapa Nithikul. Potential of Refuse Derived Fuel production from Bangkok Municipal Solid Waste. PhD thesis, 2007.

[63] Catarina Nobre, Cândida Vilarinho, Octávio Alves, Benilde Mendes, and Margarida Gonçalves. Upgrading of refuse derived fuel through torrefaction and carbonization: Evaluation of rdf char fuel properties. Energy, 181, 2019. ISSN 03605442. doi: 10.1016/j.energy.2019.05.105.

[64] Shusheng Pang and Arun S. Mujumdar. Drying of woody biomass for bioenergy: Drying technologies and optimization for an integrated bioenergy plant. Drying Technology, 28(5), 2010. ISSN 07373937. doi: 10.1080/07373931003799236.

[65] Pawale, Dharmarao, and Pawar. Solar Assisted Dryer for Municipal Solid Waste Solar. Int. J. Innov. Eng. Res . . . , 2(January 2015), 2015.

[66] Max S. Peters, Klaus D. Timmerhaus, and Ronald E. West. Plant Design and Economics for Chemical Engineers 5th Edition, volume 369. 2003.

[67] A. Pinacho, P. A. García-Encina, P. Sancho, P. Ramos, and M. C. Márquez. Study of drying systems for the utilization of biodegradable municipal solid wastes as animal feed. Waste Management, 26, 2006. ISSN 0956053X. doi: 10.1016/j.wasman.2005.04.006.

[68] Mark J. Prins, Krzysztof J. Ptasinski, and Frans J.J.G. Janssen. Torrefaction of wood. part 1. weight loss kinetics. Journal of Analytical and Applied Pyrolysis, 77, 2006. ISSN 01652370. doi: 10.1016/j.jaap.2006.01.002.

[69] Elena Cristina Rada and Gianni Andreottola. Rdf/srf: Which perspective for its future in the eu. Waste Management, 32, 2012. ISSN 0956053X. doi: 10.1016/j.wasman.2012.02.017.

[70] J. Ratte, E. Fardet, D. Mateos, and J. S. Héry. Mathematical modelling of a continuous biomass torrefaction reactor: Torspyd™ column. Biomass and Bioenergy, 35, 2011. ISSN 09619534. doi: 10.1016/j.biombioe.2011.04.045.

[71] J. Recari, C. Berrueco, N. Puy, S. Alier, J. Bartrolí, and X. Farriol. Torrefaction of a solid recovered fuel (SRF) to improve the fuel properties for gasification processes. Applied Energy, 203, 2017. ISSN 03062619. doi: 10.1016/j.apenergy.2017.06.014.

[72] Walter V. Reid, Mariam K. Ali, and Christopher B. Field. The future of bioenergy. Global Change Biology, 26(1):274–286, 2020. doi: https://doi.org/10.1111/gcb.14883. URL `https://onlinelibrary.wiley.com/doi/abs/10.1111/gcb.14883`.

[73] Matthias Reuter, Martin K. Patel, and Wolfgang Eichhammer. Applying ex-post index decomposition analysis to primary energy consumption for evaluating progress towards European energy efficiency targets. Energy Efficiency, 10(6), 2017. ISSN 15706478. doi: 10.1007/s12053-017-9527-2.

[74] Fabián Robles-Martínez. Biodrying under Greenhouse Conditions as Pretreatment for Horticultural Waste. Journal of Environmental Protection, 03(04), 2012. ISSN 2152-2197. doi: 10.4236/jep.2012.34038.

[75] Vera Susanne Rotter, Thomas Kost, Joerg Winkler, and Bernd Bilitewski. Material flow analysis of RDF-production processes. Waste Management, 24(10):1005–1021, jan 2004. ISSN 0956-053X. doi: 10.1016/J.WASMAN.2004.07.015.

[76] Asma Sakri, Ali Aouabed, Abdallah Nassour, and Michael Nelles. Refuse-derived fuel potential production for co-combustion in the cement industry in algeria. Waste Management and Research, 39, 2021. ISSN 10963669. doi: 10.1177/0734242X20982277.

[77] Mehrdad Shirinbakhsh and Majid Amidpour. Design and optimization of solar-assisted conveyer-belt dryer for biomass. Energy Equipment and Systems, 06 2017.

[78] Tooran Shoulaifar. Chemical Changes in Biomass during Torrefaction. PhD thesis, 01 2016.

[79] Rita Barros Silva, Rui Fragoso, Carlos Sanches, Mario Costa, and Susete Martins-Dias. Which chlorine ions are currently being quantified as total chlorine on solid alternative fuels? Fuel Processing Technology, 128, 2014. ISSN 03783820. doi: 10.1016/j.fuproc.2014.07.003.

[80] Paweł Stępień and Andrzej Białowiec. Kinetic parameters of torrefaction process of alternative fuel produced from municipal solid waste and characteristic of carbonized refuse derived fuel. Detritus, 3(September), 2018. ISSN 26114135. doi: 10.31025/2611-4135/2018.13702.

[81] Karolina Słomka-Polonis, Bogusława Kordon-Łapczyńska, and Jarosław Frączek. Drying kinetics of rdf: Experimental investigation and modeling. BIO Web of Conferences, 10, 2018. doi: 10.1051/bioconf/20181002030.

[82] Budi Triyono, Pandji Prawisudha, Mardiyati, and Ari Darmawan Pasek. Experimental study on utilization of indonesian non-recycled organic waste as renewable solid fuel using wet torrefaction process. Engineering Journal, 22, 2018. ISSN 01258281. doi: 10.4186/ej.2018.22.6.81.

[83] S. H. Tscheng and A. P. Watkinson. Convective heat transfer in a rotary kiln. The Canadian Journal of Chemical Engineering, 57, 1979. ISSN 1939019X. doi: 10.1002/cjce.5450570405.

[84] Jaya Shankar Tumuluru, Shahab Sokhansanj, J. Richard Hess, Christopher T. Wright, and Richard D. Boardman. A review on biomass torrefaction process and product properties for energy applications. Industrial Biotechnology, 7, 2011. ISSN 15509087. doi: 10.1089/ind.2011.7.384.

[85] Maw Maw Tun and Dagmar Juchelková. Drying methods for municipal solid waste quality improvement in the developed and developing countries: A review, 2019. ISSN 2005968X.

[86] Patchimaporn Udomkun, Sebastian Romuli, Steffen Schock, Busarakorn Mahayothee, Murat Sartas, Tesfamicheal Wossen, Emmanuel Njukwe, Bernard Vanlauwe, and Joachim Müller. Review of solar dryers for agricultural products in Asia and Africa: An innovation landscape approach, 2020. ISSN 10958630.

[87] US Department of Energy . Waste-to-energy from municipal solid wastes. Technical report, August 2019.

[88] Yan Yang, Rock Keey Liew, Arularasu Muthaliar Tamothran, Shin Ying Foong, Peter Nai Yuh Yek, Poh Wai Chia, Thuan Van Tran, Wanxi Peng, and Su Shiung Lam. Gasification of refuse-derived fuel from municipal solid waste for energy production: a review. Environmental Chemistry Letters, 19, 2021. ISSN 16103661. doi: 10.1007/s10311-020-01177-5.

[89] Haoran Yuan, Yazhuo Wang, N. Kobayashi, Dandan Zhao, and Shiyou Xing. Study of fuel properties of torrefied municipal solid waste. Energy and Fuels, 29, 2015. ISSN 15205029. doi: 10.1021/ef502277u.

Appendices

Appendix A

Dryer

A.1 MATLAB Code

```
% T = 60 ; IMC = 31.1%
%
%  T = readtable('Dryingdata1.xlsx','Sheet',1, 'Range','H1:H33');
%  M = readtable('Dryingdata1.xlsx','Sheet',1, 'Range','B1:B33');
%  MR= table2array(M)
%  time= table2array(T)
%
%  [n,m] = size (MR)
%
%  for k = 1:n
%      for j = 1:m
%      lnM(k,j)= log(MR(k,j))
%  end
%  end
% %
%  figure (1)
%  p=polyfit(time,lnM,1)
%  slope = p(1);
%  y1 = polyval( p,time)
%  figure(2)
% plot (time,lnM,'o')
% hold on
%  plot ( time , y1)
%  hold off
%  title ('Ln(MR)vs t (60)')
%  xlabel ('Time(mins)')
%  ylabel (' Ln(MR)')
%  legend ('experimental' , 'Fitted')
%  L = 5*10^(-3) % Half thickness of slab (m)
%  Deff = -(-0.00133*4*L*L)*((pi)^2)
%
% %
%
% dydx = gradient(y) ./ gradient(x);
% Derivative Of Unevenly-Sampled Data
% zci = @(v) find(v(:).* circshift(v(:), [-1 0]) <= 0);
% Returns Approximate Zero-Crossing Indices Of Argument Vector
% zxidx = zci(dydx);
% Approximate Indices Where  dydx =0
```

```
% for k1 = 1:numel(zxidx)
% Loop Finds    x    &    y    For   dydx =0
%      ixrng = max(zxidx(k1)-2,1):min(zxidx(k1)+2,numel(x));
%      inflptx(k1) = interp1(dydx(ixrng), x(ixrng), 0, 'linear');
%      inflpty(k1) = interp1(x(ixrng), y(ixrng), inflptx(k1), 'linear');
% end
% figure(1)
% plot(x, y)
% hold on
% plot(x, dydx)
% plot(inflptx, inflpty, 'pg', 'MarkerFaceColor','g')
% hold off
% grid
% legend('Data', 'Derivative', 'Inflection Points')
% inflpts = sprintfc('(%5.3f, %5.3f)', [inflptx; inflpty].');
% text(inflptx, inflpty, inflpts,'FontSize',8, 'HorizontalAlignment','center', 'VerticalAlignment',
%
% %
%
% [TF,m,b] = ischange(y, 'linear', 'MaxNumChanges',2);
% chgpts = [find(TF); m(TF); b(TF)].';
% chgidx = find(chgpts(:,2)<0,1);
% figure
% plot(t,MR,'linewidth',1.5)
% hold on
% plot(t(chgpts(chgidx(:,1))), MR(chgpts(chgidx(:,1))), 'xr')
% hold off
% grid on
% xlabel('Time [s]','FontWeight','bold')
% ylabel('Moisture Ratio','FontWeight','bold')
% title('Opening angle')

% %% T = 80 IMC = 31.1%
% %
% T2 = readtable('Dryingdata1.xlsx','Sheet',2, 'Range','B1:B35');
% M2 = readtable('Dryingdata1.xlsx','Sheet',2,'Range','C1:C35');
% MT2 = table2array(M2)
% t2= table2array(T2)
% %
% [x,y] = size (MT2)
%
%  for k = 1:x
%      for j = 1:y
%      lnM1(k,j)= log(MT2(k,j))
%  end
%  end
% %
%  figure (3)
%  p=polyfit(t2,lnM1,1)
%  slope2 = p(1);
%  y1 = polyval( p,t2)
%  intercept = p(2)
%  figure(2)
% plot (t2,lnM1,'o')
% hold on
%  plot ( t2 , y1)
```

```
%  hold off
%  title ('Ln(MR)vs t (80)')
%  xlabel ('Time(mins)')
%  ylabel (' Ln(MR)')
%  legend ('experimental' , 'Fitted')
%  L = 5*10^(-3) % Half thickness of slab (m)
%  Deff2 = -(-0.002761*4*L*L)*((pi)^2)
% %% T = 100 , IMC = 31.1%
%  T3 = readtable('Dryingdata1.xlsx','Sheet',3, 'Range','B1:B27');
% M3 = readtable('Dryingdata1.xlsx','Sheet',3,'Range','C1:C27');
% MT3 = table2array(M3)
% t3= table2array(T3)
% %
% [x1,y1] = size (MT3)
%
% for k = 1:x1
%       for j = 1:y1
%       lnM2(k,j)= log(MT3(k,j))
%  end
% end
% %
% figure (4)
%  p=polyfit(t3,lnM2,1)
%  slope3 = p(1);
%  y1 = polyval( p,t3)
%  figure(2)
% plot (t3,lnM2,'o')
% hold on
%  plot ( t3 , y1)
%  hold off
%  title ('Ln(MR)vs t (100)')
%  xlabel ('Time(mins)')
%  ylabel (' Ln(MR)')
%  legend ('experimental' , 'Fitted')
%  Deff3 = -(-0.004174*4*L*L)*((pi)^2)
% %
% %  %%
%  A = [1.21 1.199 1.28];
%  K = [ 0.00133 0.002761 0.004174];
%  T = [ 60 80 100];
% %
%
% % plot(T,K,'-o')
% %
%
% % pp = spline(T,X);
%
% Deffx = [ log(1.312657385344885e-06) log(2.724997775140772e-06) log(4.119572877014698e-06) ]
% T = [-1/(273+60) -1/(273+80) -1/(2730+100)]
% plot(T , Deffx)
% figure (6)
%  p=polyfit(T,Deffx,1)
%  slope3 = p(1)*10;
%  y1 = polyval( p,T)
%  figure(2)
% plot (T,Deffx,'o')
```

```
% hold on
%  plot (T , y1)
%  hold off
%  title ('Ln(MR) vs t (100)')
%  xlabel ('Time(mins)')
%  ylabel (' Ln(MR)')
%  legend ('experimental' , 'Fitted')
%  Deff3 = -(-0.004174*4*L*L)*((pi)^2)
%
%
%  Ea = slope3*8.314
%
%%%
%
%%  T = readtable('Dryingdata1.xlsx','Sheet',3, 'Range','B2:B28');
%%  M = readtable('Dryingdata1.xlsx','Sheet',3, 'Range','D2:D28');
%%  MT = table2array(M)
%%  t= table2array(T)
%%
%%  plot (t,MT)
%%
%%  DRx = readtable('Dryingdata1.xlsx','Sheet',3, 'Range','E3:E28');
%%  Tx = readtable('Dryingdata1.xlsx','Sheet',3, 'Range','B3:B28');
%%  DR =  table2array(DRx)
%%  tx =  table2array(Tx)
%%  plot (tx,DR)
%%
%  NMx = 100*[0.010869821 0.009976713 0.009171715 0.005927202 0.004530531 0.003180285 0.002237402 0
%NDRx = [1 0.914979965 0.876650829 0.714903123 0.595059633 0.46908059 0.414566394 0.298777902 0.18
% plot (NMx,NDRx)
%%%
%
% Tx= readtable('Dryingdata2.xlsx','Sheet',7, 'Range','A1:A10');
% tx = readtable('Dryingdata2.xlsx','Sheet',7, 'Range','B1:B10');
%  ttx = table2array(tx)
%  TTx= table2array(Tx)
%
%  plot(TTx,ttx,'LineWidth',2)

%MC = 0.45;
% Volatiles = 0.49;
% Char = 0.05 ;
% Ash = 0.17 ;
% LHV = 12 ;% MJ/kg
%
%% Ultimate Analysis
% C = 0.288 ;
% H =  0.041 ;
% O = 0.204 ;
% N = (0.5/100) ;
% S = (0.2/100);
%
% RDFI = 100 ;% t/d
%
% Feed = 3779.936 ;
% Xi = 0.458;
```

```
% Xf= 0.10;
% TO = 37.3;
% TI = 25;
%
% Water = Feed*Xi;
% Solids = Feed*(1-Xi);
% DryRDF = Solids/(1-0.10) ;
% RemovedM = Feed - DryRDF ;
%
% Density = 300 ;
% Heatcap = 1.2552 ;
%
% MC1 = RemovedM;
% Cp = 4.184;
% Lv = 2260 ;
%
% Q1 = MC1*Cp*(100-TI)+MC1*Lv;
%
% Q2 = Solids * Heatcap*(37.56-TI);
%
% Q3 = (Q1+Q2)*1.5;
%
% TAIN = 110 ;
% TAO = 44.836 ;
%
% cpa =1.02199999024;
%
%  MAir = Q3 /(cpa *(TAIN-TAO)) ;
%
%
% G = 10000 ;
% Area = MAir / G;
% Dia = sqrt(4*Area/3.14);
% k= 5.25;
% n=0.67;
% Ua = k*G^(n)/(Dia) ;
% Nt = 2.5 ;
%
% Tw = (TAIN-(TAO*exp(Nt)))/(1-exp(Nt));
% TLN = ((TAIN-Tw)-(TAO-Tw))/log ((TAIN-Tw)/(TAO-Tw));
% TLK = TLN + 273 ;
%
% L = (Q3*4.187)/(Area*Ua*TLK) ;
% x = L/Dia ;
%
```

A.2 CALCULATOR BLOCK

```
%       M = 0.10;
%       A = (0.0003175*TAIR*TAIR) -( 0.04785*TAIR) + 2.995;
%       C = (0.00007725*TAIR) - 0.00338
%       Y = DLOG(A);
%       X = DLOG(M);
%       RESTIME = (Y-X)/C;
%       V1 = MAIR/ADENS/(3600*AREA);
%       Diff = 0.00000441;
```

```
%       RE = V1*SQRT(AREA/3.1415)*2/Diff;
%       Sc = 0.704;
%       Pr = 0.71;
%       SH1 = 0.664*RE**(1/2)*Sc**(1/3);
%       SH2 = 0.037*RE**(0.8)*Pr/(1+2.433*RE**(-1/10)*(Pr**(2/3)-1));
%       SH = SQRT(SH1**2+SH2**2);
%       HCAL = 1620500*4.186/3600;
%
%
```

Appendix B

Torrefaction

B.1 Two-step mechanism derivation

The reaction model is shown below.

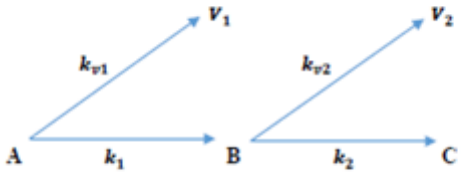

A is the initial solid, B for intermediate solid and C is the final char. V_1 and V_2 are the volatiles released from during the two conversion stages. The reaction rates are k_1, k_{v1}, k_2, k_{v2}.

A.1.1 *Mathematical modelling*

$$r_A = \frac{dA}{dt} = -(k_1 + k_{v1})A \qquad (B.1)$$

$$r_B = \frac{dB}{dt} = k_1 A - (k_2 + k_{v2})B \qquad (B.2)$$

$$r_c = \frac{dC}{dt} = k_2 B \qquad (B.3)$$

$$r_{v1} = \frac{dV_1}{dt} = k_{v1} A \qquad (B.4)$$

$$r_{v2} = \frac{dV_2}{dt} = k_{v2} B \qquad (B.5)$$

Where $r_x (X = A, B, C, V_1, V_2)$ represents the reaction rates for the solid and volatile components. The rate constant k , can be expressed in the form of the Arrhenius equation.

$$k_i = A.e^{\frac{-E_A}{RT}} \qquad (B.6)$$

Where A is the pre-exponential factor (s^{-1}), E_A is the activation energy (J mol^{-1}), R is the universal gas constant (J mol^{-1} K^{-1}) and T is temperature (K^{-1}).

A.1.2 Analytical Solution

The reactions taking place are assumed as first order. The system of differential equations (B.1) to (B.6) are solved based on the initial conditions A = A_o, B = 0 and C = 0 at t =0.

From Eq. (B.1)

$$\frac{dA}{A} = -(k_1 + k_{v1})dt \qquad (B.7)$$

Integrating both side of Eq. (B.7) with the initial condition, t=0, A = A0.

$$A = A_o e^{-(k_1 + k_{v1})t} \qquad (B.8)$$

Solve Eq. (B.3) to get B. From Eq. (B.3) and (B.9) ,

$$\frac{dB}{dt} = k_1 A_o e^{-(k_1+k_{v1})t} - (k_2 + k_{v2})B \qquad (B.9)$$

Let $K_1 = k_1 + k_{v1}$ and $K_2 = k_2 + k_{v2}$. Rewriting Eq. (B.9)

$$\frac{dB}{dt} = k_1 A_o e^{-K_1 t} - K_2 B \qquad (B.10)$$

Eq. (B.10) is a non-homogenous first order ODE whose general solution is:

$$B_h = C_1 e^{-K_2 t} \quad \text{where } C_1 \text{ is a constant.} \qquad (B.11)$$

The solution to Eq. (B.11) is $B_p = C_2 e^{-K_1 t}$ and $B'_p = -K_1 C_2 e^{-K_1 t}$.On substituting these in Eq. (B.10) we obtain,

$$-K_1 C_2 e^{-K_1 t} + K_2 C_2 e^{-K_1 t} = k_1 A_o e^{-K_1 t}$$

$$C_2 = \frac{k_1 A_o}{(K_2 - K_1)} \quad now \quad B_p = \frac{k_1 A_o}{(K_2 - K_1)} \quad e^{-K_1 t}$$

$$B = B_h + B_p = C_1 e^{-K_2 t} + \frac{k_1 A_o}{(K_2 - K_1)} e^{-K_1 t}$$

On including the initial conditions, B = 0 at t=0, we obtain C_1

$$C_1 = -\frac{k_1 A_o}{(K_2 - K_1)}$$

$$B = -\frac{k_1 A_o}{(K_2 - K_1)} e^{-K_2 t} + \frac{k_1 A_o}{(K_2 - K_1)} e^{-K_1 t}$$

$$B = \frac{k_1 A_o}{(K_1 - K_2)} (e^{-K_2 t} - e^{-K_1 t}) \qquad (B.12)$$

From Eq.(B.3) and (B.12) we get ,

$$\frac{dC}{dt} = \frac{k_1 k_2 A_o}{(K_1 - K_2)}(e^{-K_2 t} - e^{-K_1 t}) \qquad (B.13)$$

On integrating and simplifying the above Eq.(B.13) ,

$$C = \frac{k_1 k_2 A_o}{K_1 K_2 (K_1 - K_2)}(K_2 e^{-K_1 t} - K_1 e^{-K_2 t}) + C_3$$

The integration constant C_3 can be obtained by applying the initial conditions C=0 at t=0,

$$C_3 = -\frac{k_1 k_2 A_o}{K_1 K_2 (K_1 - K_2)}(K_2 - K_1)$$

$$C = \frac{k_1 k_2 A_o}{K_1 K_2 (K_1 - K_2)}(K_2 e^{-K_1 t} - K_1 e^{-K_2 t}) - \frac{k_1 k_2 A_o}{K_1 K_2 (K_1 - K_2)}(K_2 - K_1)$$

$$C = \frac{k_1 k_2 A_o}{K_1 K_2 (K_1 - K_2)}(K_1 - K_2 - K_1 e^{-K_2 t} + K_2 e^{-K_1 t}) \qquad (B.14)$$

From Eq. (B.4) and Eq. (B.8) , We obtain ,

$$\frac{dV_1}{dt} = k_{v1} A_o e^{-K_1 t}$$

$$V_1 = -\frac{k_{v1} A_o}{K_1} e^{-K_1 t} + C_4 \text{ (intergrating both side)}$$

Applying initial condition V1 =0 at t=0,

$$V_1 = \frac{k_{v1} A_o}{K_1}(1 - e^{-K_1 t}) \qquad (B.15)$$

From Eq.(B.7) and (B.12) ,

$$\frac{dV_2}{dt} = k_{v2}\frac{k_1 A_o}{(K_1 - K_2)}(e^{-K_2 t} - e^{-K_1 t})$$

$$V_2 = \frac{k_1 k_{v2} A_o}{(K_1 - K_2)}\left[\left(\frac{1}{-K_2}\right)e^{-K_2 t} + \left(\frac{1}{K_1}\right)e^{-K_1 t}\right] + C_5$$

Applying initial condition V2 =0 at t=0 to get C_5,

$$V_2 = \frac{k_1 k_{v2} A_o}{K_1 K_2 (K_1 - K_2)}(K_1 - K_2 - K_1 e^{-K_2 t} + K_2 e^{-K_1 t}) \quad (B.16)$$

On solving the initial ODE's Eq.(B.1) to (B.4) we obtain,

$$A = A_o e^{-K_1 t} \quad (B.17)$$

$$B = \frac{k_1 A_o}{(K_1 - K_2)}(e^{-K_2 t} - e^{-K_1 t}) \quad (B.18)$$

$$C = \frac{k_1 k_2 A_o}{K_1 K_2 (K_1 - K_2)}(K_1 - K_2 - K_1 e^{-K_2 t} + K_2 e^{-K_1 t}) \quad (B.19)$$

$$V_1 = \frac{k_{v1} A_o}{K_1}(1 - e^{-K_1 t}) \quad (B.20)$$

$$V_2 = \frac{k_1 k_{v2} A_o}{K_1 K_2 (K_1 - K_2)}(K_1 - K_2 - K_1 e^{-K_2 t} + K_2 e^{-K_1 t}) \quad (B.21)$$

The solid mass (M) and the volatile (V) obtained after torrefaction are, M = A+B+C and V = V1+V2.

$$M = A_o e^{-K_1 t} + \frac{k_1 A_o}{(K_1 - K_2)}(e^{-K_2 t} - e^{-K_1 t}) + \frac{k_1 k_2 A_o}{K_1 K_2 (K_1 - K_2)}(K_1 - K_2 - K_1 e^{-K_2 t} + K_2 e^{-K_1 t}) \quad (B.23)$$

$$\frac{M}{A_o} = \left(1 + \left[\frac{k_1 K_1 + k_1 k_2}{K_1 (K_2 - K_1)}\right]\right)e^{-K_1 t} + \left[\frac{-k_1 K_2 + k_1 k_2}{K_2 (K_2 - K_1)}\right]e^{-K_2 t} + \frac{k_1 k_2}{K_1 K_2}$$

M/A_o is the solid yield (Y_s), on rewriting the above equation,

$$Y_s = \left(1 + \left[\frac{k_1K_1 + k_1k_2}{K_1(K_2 - K_1)}\right]\right) e^{-K_1 t} + \left[\frac{-k_1K_2 + k_1k_2}{K_2(K_2 - K_1)}\right] e^{-K_2 t} + \frac{k_1k_2}{K_1K_2} \qquad (B.24)$$

For the volatiles,

$$V = \frac{k_{v1}A_o}{K_1}(1 - e^{-K_1 t}) + \frac{k_1k_{v2}A_o}{K_1K_2(K_1 - K_2)}(K_1 - K_2 - K_1e^{-K_2 t} + K_2e^{-K_1 t})$$

$$\frac{V}{A_o} = \left(\frac{k_1k_{v2}}{K_1(K_1 - K_2)} - \frac{k_{v1}}{K_1}\right) e^{-K_1 t} - \frac{k_1k_{v2}}{K_2(K_1 - K_2)} + \frac{k_{v1}}{K_1} + \frac{k_1k_{v2}}{K_1K_2} \qquad (B.25)$$

V/A_o is the volatile yield (Yv). On rewriting the above equation,

$$Y_v = \left(\frac{k_1k_{v2}}{K_1(K_1 - K_2)} - \frac{k_{v1}}{K_1}\right) e^{-K_1 t} - \frac{k_1k_{v2}}{K_2(K_1 - K_2)} + \frac{k_{v1}}{K_1} + \frac{k_1k_{v2}}{K_1K_2} \qquad (B.26)$$

It can also be written as , Yv = 1-Ys

B.2 Database for HHV estimation

Type	Temperature (°C)	Mass Yield	HHV (MJ/kg)	Source
MSW	250	0.82	17.1	[6]
	270	0.62	19.1	
	300	0.57	23.66	
	330	0.46	28.09	
MSW	250	0.86	18.27	[89]
	300	0.73	23.66	
RDF	250	0.82	18.24	[16]
	260	0.75	21.65	
	280	0.64	22.26	
	300	0.58	25.47	
Kitchen waste	250	0.81	18.13	[82]
	270	0.73	20.97	
	300	0.46	23.28	
Agriculture and wood waste	250	0.82	18.74	[22]
	270	0.76	19.57	
	300	0.60	23.68